Investigation of a Novel Dew Point Indirect Evaporative Air Conditioning System for Buildings

By

Zhiyin Duan

Thesis submitted to the University of Nottingham

for the degree of Doctor of Philosophy

September 2011

Abstract

This study aims to improve the performance of existing indirect evaporative coolers. A new dew point indirect evaporative cooler with counter-current heat/mass exchanger was developed in this research by optimal design, material selection, numerical simulation, experimental investigations and economic, environmental, regional acceptance analysis.

A new dew point heat/mass exchanger using a counter-current flow pattern was designed by numerical simulation in terms of material, structure, geometrical sizes and operating conditions. The numerical results indicate that under a typical cooling design condition, i.e., 35^{o}C dry-bulb/24^{o}C wet-bulb temperatures, the heat exchanger could achieve a wet-bulb effectiveness of approximately 1.4. The results of numerical simulation are consistent with some published test data. Based on the numeric results and the material selection determined from a set of related tests, a prototype dew point heat/mass exchanger and the associated air cooler was designed and constructed in laboratory. Testing was carried out to evaluate the performance of the experiment prototype. The results indicate that the wet-bulb effectiveness of the prototype ranged from 55% to 110% for all test conditions. The power consumption of the prototype ranged from 10 to 50 W with energy efficiency (or COP) rated from 3 to 12. It is also found that the water consumption of the prototype was very small which ranged from 0.2-1.3 litre/h. A comparison between the numerical and experimental results was carried out and the reasons for the discrepancy were analysed. This research also investigates the feasibility, economic and environmental potential of using a dew point cooler in buildings in Europe and China.

From the related studies in this thesis, it is concluded that the dew point cooler can achieve a higher performance (in terms of effectiveness and energy efficiency) than the typical indirect evaporative coolers without adding too much cost. It is found that the effectiveness and energy efficiency of the heat/mass exchanger in the cooler are largely dependent upon channel geometries, the intake air velocity, temperature, humidity and the working-to-intake air ratio but less on the feed water temperature. To maximise effectiveness and energy efficiency, it is suggested that 1) the channel height and the length of exchanger should be set below 6 mm and 1-1.2 m respectively; 2) the intake channel air velocity should be controlled to 0.5-1 m/s; and 3) the

working-to-intake air ratio should be adjusted to 0.4-0.5. It is also concluded that the dew point system is suitable for most regions with dry, mild and hot climate. It is, however, unsuitable for humid regions where the system is used as a stand-alone unit. Compared to the conventional mechanical compression cooling system, the dew point system has a significantly higher potential in saving energy bills and reducing carbon emission.

A project to construct an 8 kW commercial dew point cooler is currently under development with the assistance of a Chinese company. By the optimisation of material, structure and geometries, the cooler is expected to achieve a cooling output of 8 kW at the inlet air of 38^{o}C dry-bulb/ 21^{o}C wet-bulb temperatures, with a wet-bulb effectiveness of 1.02 at 1530 m^{3}/h of supply air flow and 1200 m^{3}/h of discharge air flow, whereas the power input of the unit is about 450 W and the energy efficiency (or COP) at 18.5.

Publications

Xudong Zhao, Zhiyin Duan, Changhong Zhan, 2009, *Dynamic performance of a novel dew point air conditioning for the UK buildings*, International Journal of Low-Carbon Technologies. vol. 4, pp.27-35.

Xudong Zhao, Zhiyin Duan, Changhong Zhan, Saffa B. Riffat, 2010, *A Novel Dew Point Air conditioning System*, International Patent, GB0817468.2.

Changhong Zhan, Zhiyin Duan, Xudong Zhao, Hong Jin, Saffa B. Riffat, *Comparative study of the performance of the M-cycle counter-flow and cross-flow heat exchangers for indirect evaporative cooling.* To be submitted.

Xudong Zhao, Shuang Yang, Zhiyin Duan, Saffa B. Riffat, 2009, *Feasibility study of a novel dew point air conditioning system for China building application*, Building and Environment, vol. 44, pp.1990-1999.

Zhiyin Duan, Changhong Zhan, Xudong Zhao, Saffa B. Riffat, 2009, *Performance Assessment of a Novel Dew Point Air Conditioning System in the UK Climate Conditions.* Proc. US-EU-China Thermophysics Conference-Renewable Energy, Beijing, China.

Acknowledgement

I would like to express my sincere and heartfelt gratitude to my supervisor Professor Xudong Zhao for his continuous support and guiding, for his patience, motivation, enthusiasm, immense knowledge and dedicated involvement throughout the whole process of my PhD research. From the beginning to the final level, his encouragement, guidance and assistance help me to develop a better understanding of this PhD subject. I would also like to thank my other supervisors Professor Saffa B Riffat and Dr Yuehong Su for their supports and suggestions.

I wish to thank Innovation China UK and European Commission Marie Curie action for their financial supports on this project.

I am indebted to many of my supportive colleagues in our project team. They are Dr Changhong Zhan, Mr. Lu Wang and Ms Shuang Yang. Special thanks to the knowledgeable and helpful technicians in the Department of Architecture and Built Environment within University of Nottingham including Mr. Dave Oliver, Mr. Dave Taylor, Mr. Bob Clarke, Mr. Jonathan Moss, for their cooperation during construction of my experiment prototypes.

Finally, I wish to thank and dedicate this thesis to my parents for their unselfish, endless love, care and encouragement. I could never have accomplished so much without them.

Contents

Nomenclature

A_{cross}	cross sectional area of channel, m^2
A_d	heat transfer area of dry channel, m^2
A_w	heat transfer area of wet channel, m^2
$c_{p,a}$	specific heat of dry air at constant pressure, kJ/kg·K
$c_{p,f}$	specific heat of primary/process air at constant pressure, kJ/kg·K
$c_{p,m}$	specific heat of moist air at constant pressure, kJ/kg·K
$c_{p,v}$	specific heat of water vapour at constant pressure, kJ/kg·K
$c_{p,w}$	specific heat of water film at constant pressure, kJ/kg·K
$C_{cp,con}$	capital cost of the conventional mechanical compression system, €
$C_{cp,dew}$	capital cost of the dew point system, €
$C_{m,con}$	maintenance cost of the conventional mechanical compression system, euro
$C_{m,dew}$	maintenance cost of the dew point system, €
$C_{net,bill,sav}$	net bill saving during the life cycle time, €
$C_{opt,con}$	operating cost of the dew point system, €
$C_{opt,dew}$	operating cost of the conventional mechanical compression system, €
d	cross sectional diameter of extension duct, m
D_H	hydraulic diameter of channel, m
DB	dry-bulb
DEC	direct evaporative cooler
DP	dew-point
ECER	evaporative cooler efficiency ratio
EER	energy efficiency ratio, Btu/Wh
Em_{co2}	annual carbon emission reduction relative to 100 m^2 of building area using a 8 kW rating dew point unit, ton
En_a	annual electricity power saving relative to 100 m^2 of building area using a 8 kW rating dew point unit, kWh
$f_{c,c}$	carbon conversion factor relative to grid electricity power, 0.544 kg CO^2 emission per kWh power

F	cross sectional area of ducts, m^2
F_i	small equal area divided from cross section of ducts, m^2
g	gravitational acceleration, m/s^2
h	heat transfer coefficient, $W/m^2 \cdot K$
h_m	mass transfer coefficient, m/s
$h_{p,f}$	heat transfer coefficient between intake air and channel walls, $W/m^2 \cdot K$
h_w	heat transfer coefficient between water film and channel walls, $W/m^2 \cdot K$
$h_{w,f}$	heat transfer coefficient between working air and water film, $W/m^2 \cdot K$
$i_{db,r}$	specific enthalpy of air in room temperature, kJ/kg
$i_{db,1}$	specific enthalpy of intake air at dry bulb temperature, kJ/kg
$i_{db,2}$	specific enthalpy of supply air, kJ/kg
$i_{db,3}$	specific enthalpy of exhaust air at dry bulb temperature, kJ/kg
$i_{dp,1}$	specific enthalpy of intake air at dew point temperature, kJ/kg
i_0	latent heat of water at reference temperature, i.e. 0^oC, kJ/kg
i_v	specific enthalpy of water vapour at water film temperature, kJ/kg
$i_{w,f}$	specific enthalpy of working air, kJ/kg
IEC	Indirect evaporative cooler
$K_{p,f}$	overall heat transfer coefficient between water film and intake air, $W/m^2 \cdot K$
l	characteristic length, m
l_d	length of dry channel, m
l_w	length of wet channel, m
l_0	thermal inlet undeveloped region of channel, m
l_1	hydrodynamic entrance distance, m
Le	Lewis number
$m_{p,f}$	mass flow rate of primary/process air, kg/s
m_w	mass flow rate of water film, kg/s
$m_{w,f}$	mass flow rate of working air, kg/s
n	numbers of heat exchanger plates
n_p	numbers of measurement points

Nu	Nusselt number
Δp	total pressure drop, Pa
Δp_{fr}	frictional pressure drop, Pa
Δp_l	local pressure drop, Pa
$\Delta P_{p,f}$	pressure drop of product airflow, Pa
$\Delta P_{w,f}$	pressure drop of working airflow, Pa
P	wetted perimeter of the cross-section, m
$\mathrm{PP_{dew}}$	payback period of dew point system relative to conventional system, year
Pr	Prandtl number
$Q_{\mathrm{cooling,IA}}$	sensible cooling of intake air, W
$Q_{\mathrm{cooling,r}}$	cooling capacity of evaporative cooler, W
Q_e	effective cooling output, W
Q_l	latent heat
Q_o	outdoor fresh air cooling output, W
Q_s	sensible heat
Q_{total}	total cooling capacity of system including sensible and latent cooling, W;
Q_w	heat transfer rate of water film, W
Re	Reynolds number
RH_1	relative humidity of intake air, %
RH_2	relative humidity of outlet air, %
RH_3	relative humidity of exhaust air, %
$t_{db,r}$	reference dry-bulb temperature of room, i.e. 26.7^{o}C
$t_{db,1}$	inlet air dry-bulb temperature, ^{o}C
$t_{db,2}$	outlet air dry-bulb temperature, ^{o}C
$t_{dp.1}$	inlet air dew-point temperature, ^{o}C
t_i	measured temperature in each smaller area, ^{o}C
t_{in}	indoor design temperature, ^{o}C
$t_{p,f}$	dry-bulb temperature of primary/process air, ^{o}C

t_w	temperature of water film, ^oC
$t_{w,1}$	inlet temperature of feed water, ^oC
$t_{w,2}$	outlet temperature of feed water, ^oC
$t_{wb,1}$	inlet air wet-bulb temperature, ^oC
$t_{w,f}$	dry-bulb temperature of working air, ^oC
$t'_{w,f,1}$	inlet dry-bulb temperature of working air, ^oC
$t''_{w,f,1}$	inlet wet-bulb temperature of working air, ^oC
$\bar{t}_f$	air average temperature of cross section, ^oC
T	temperature, ^oC
temp.	temperature, ^oC
u_f	average air velocity, m/s
u_i	measured velocity in each smaller area, m/s
$\bar{u}_f$	mean air velocity across the measured cross section of ducts, m/s
u_2	measured supply air velocity, m/s
u_3	exhaust air velocity, m/s
V_{daily}	daily water consumption for the standard office building, litre
V_f	air volume flow rate through duct, m^3/s
$V_{p,f}$	volume flow rate of product air, m^3/s
V_w	water evaporation rate, litre/h
$V_{w,f}$	volume flow rate of working air, m^3/s
V_2	airflow rate of supply air, m^3/h
V_3	secondary air/working air flow rate, m^3/h
$w_{w,f}$	moisture content of working air, kg/kg (dry air)
w_1	inlet moisture content of primary/intake air, kg/kg (dry air)
w_2	inlet moisture content of secondary air, kg/kg (dry air)
w_3	outlet moisture content of secondary air, kg/kg (dry air)
W_{p}	theoretical power consumption of product air fan, W
W_{pump}	power consumption of water pump, W
W_{w}	theoretical power consumption of working air fan, W
WB	wet-bulb

Greek symbols

$\varepsilon_{\mathrm{DEC}}$	wet-bulb effectiveness of direct evaporative cooler
$\varepsilon_{\mathrm{IEC}}$	wet-bulb effectiveness of indirect evaporative cooler
ε_{wb}	wet-bulb effectiveness
ε_{dp}	dew-point effectiveness
ρ_f	density of air, kg/m^3;
ρ_w	water film density, kg/m^3
$\rho_{w,f}$	secondary air/ working air density, kg/m^3
$\rho_{w,s}$	density of saturated air at the water temperature, kg/m^3
σ	surface wettability factor
ν_f	kinematic viscosity of air, m^2/s
ν_w	kinematic viscosity of water film, m^2/s
λ	thermal conductivity of the fluid, W/m·K
λ_{fr}	frictional pressure drop factor
λ_w	thermal conductivity of water film, W/m·K
λ_{wall}	thermal conductivity of channel walls, W/m·K
μ_f	dynamic viscosity of air at the mean temperature of working air, N·s/m^2
μ_w	dynamic viscosity of air at the temperature of channel wall, N·s/m^2
δ_w	thickness of water film, m
δ_{wall}	thickness of channel walls, m
Γ	spraying density of feed water over wet plates, kg/m·s
ζ	local /minor pressure drop coefficient

List of Figures

List of Tables

Chapter1.
Introduction

1.1 Background

The rapid growth of world energy consumption has raised serious concerns over the depletion of energy resources and the associated environmental impact of global climate change. The increasing world energy consumption is caused by the facts such as continuous growth of world population, economic growth in emerging regions (Pérez-Lombard 2008), the development of communication networks and the promotion of life style of developed nations. Over the last two decades, the world primary energy consumption (fossil fuels) has increased by 49% and carbon dioxide emissions by 43% (Petroleum 2009). Despite the latest energy review shows that the world energy consumption was decreased by 1.1% in 2009 due to the unpredicted global economic recession, energy consumption still continues to increase rapidly in several developing countries, specifically in some regions of Asia with rapid economic growth.

For the reasons of rapid growth in population, improvement of building services and the increasing time spent in buildings, the proportion of energy consumption in buildings for developed countries (over 20–40% of total energy consumption), such as EU and USA, has exceeded the proportion distributed in industry and transports sectors. In 2004, energy consumption of buildings in EU countries accounted for 37% of total energy use, higher than those for industry (28%) and transport (32%). In the UK, the proportion of energy consumption in building was 39%, which is slightly higher than the European figure (Pérez-Lombard et al. 2008).

In developed countries, the energy consumption in heating ventilation and air-conditioning (HVAC) systems has accounted for 50% of the energy consumption in buildings and 20% of total energy consumption. In some developing countries, such as China, due to the facts of poor insulation, inefficient HVAC systems and inefficient transformation of energy to heat, the energy consumption of HVAC accounted for 50-70% of energy consumption in buildings (Jiang 2008).

In the HVAC systems, air conditioning proportion has grown rapidly due to global warming, improved insulation of buildings, and increased indoor facilities. The CMM market monitoring data shows that the air-conditioning market share increased by 34.1% per annum, retail sales increased by 29.2% (Xia 2010).

To meet the need of increasing air conditioning appliances without the use of conventional air conditioning that consumes substantial amount of electricity energy, it is necessary to develop sustainable cooling systems that are CFC-free and driven by a natural energy source, e.g., vaporisation of water.

Evaporative cooling systems utilize the latent heat of water evaporation, i.e. a kind of natural energy existed in the atmosphere, to perform air conditioning for buildings. These systems consume 20% of electrical energy by vapour-compression air conditioning, equivalent to reducing nearly 44% carbon dioxide emissions produced by vapour-compression air conditioning. Therefore, they are little dependency of fossil fuel energy and environment friendly.

Given the global significance of cooling building space and the recognised energy saving benefits of evaporative cooling over more conventional methods, understanding the energy saving of different design features of such a system is necessary to help understand its importance in achieving regional emissions reduction and energy savings goals.

However, despite that evaporative cooling has shown great potentials of energy saving and carbon emissions reduction, this type of system still has some technical barriers in existence that have impeded its wide applications. These barriers are addressed as follows:

The currently available evaporative cooling systems include both direct and indirect types. Direct evaporative cooling systems can lower the temperature of air by using the latent heat of water evaporation. As a result, warm dry air is changed into cool moist air, but the energy in the air remains the same. Since such a system adds moisture to the air supplied to rooms, it is only suitable for use in dry and hot climates, or rooms needing both cooling and humidification (ASHRAE 1996). Indirect evaporative cooling systems are able to lower the air temperature and avoid adding moisture to the air. This feature makes these systems more attractive than direct

systems. Thermodynamically, an indirect evaporative air cooler passes supply (product) air over the dry side of a heat/mass exchanging sheet, and cooling (working) air over its opposite wet side. The wet side absorbs heat from the dry side by evaporating water and therefore cooling the dry side, while the latent heat of vaporizing water is given to the wet side air. Under the ideal operating condition, the product air temperature on the dry side of the sheet will reach the wet-bulb temperature of the incoming working air, and the temperature of the working air on the wet side of the sheet will increase from its incoming dry-bulb temperature to the incoming product air dry-bulb temperature and be saturated. However, practical systems are far from this ideal. It has been suggested that only 50 to 60% of wet-bulb effectiveness can be achieved for a typical indirect evaporative cooling system (ASHRAE 1996). This means that the outlet product (supply) air would be at a temperature level between the wet-bulb temperature of the inlet working air and the dry-bulb temperature of the inlet product air, which is usually too high to cool the served room space.

If the structure of the heat and mass exchanger in an indirect evaporative cooling system is modified, a new thermal process called dew point cooling can be produced (Maisotsenko et al. 2004). This exchanger could cool product air to a temperature below the wet-bulb, and toward the dew-point of the incoming working air. Fig. 1-1 shows the principle and psychrometric representation of an ideal exchanger configuration for dew point cooling in which the working and product air have the same inlet condition (Idalex Technologies 2003). In this example, the incoming working air with state 1 flow over the dry side of a sheet, which is soaked with water on its other side and perforated along the flow path. When the working air moves along the dry side (working air dry channel), it is cooled and partially diverted to the wet side through the holes, resulting in a change of state from 1 to 3', in which 3' is a variable depending on the position of the holes. At the end of the dry working air channel, only a very small percentage of air remains and this is cooled to the lowest level (close to the dew-point of the incoming working air) and is also diverted to the wet side. The air in the wet side (working air wet channel) has a lowered temperature, and so is able to absorb heat from its two adjacent sides, i.e., the dry working air side and the dry product air side. This results in changes of state from 3', 3'' to 3 due to vaporization of the water from the wet side of the sheet into the air, and transportation of sensible heat from the adjacent air streams. In addition to the heat and mass transfer, the working air flows over the wet side of the sheet in a reverse direction, and is

finally discharged to the atmosphere. In the meantime, the product air flows over the other adjacent dry side (product air dry channel) and is cooled from state 1 to 2.

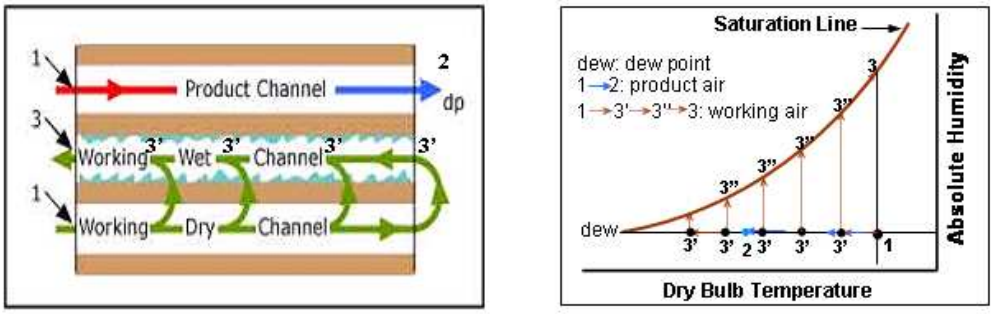

Fig. 1-1 Principle of the dew point evaporative cooling

For simplicity of manufacture, actual heat and mass exchangers for dew point cooling differ slightly from the ideal design, and one of these is shown schematically in Fig. 1-2 (ISAW 2005; Coolerado 2006). In this structure, part of the surface on the dry side is designed to allow for the passage of working air and the remainder is for the flow of product air. Both product and working air are guided to flow over the dry side along channels that are arranged in parallel. There are numerous holes distributed regularly on the working air channels and each of these allows a certain percentage of air to pass through and enter the wet side of the sheet. The air is gradually delivered to the wet side as it flows along the dry side, and this produces a uniform airflow distribution over the wet surface. This arrangement allows the working air to be pre-cooled before entering the wet side of the sheet, by losing heat to the opposite. The pre-cooled air entering the wet side flows over the wet surface along channels arranged at right angles to the dry side channels, absorbing heat from the dry-side working air and product air. As a result, the product air is cooled before being delivered to spaces where cooling is required, and the working air is humidified and heated, and discharged to the atmosphere. This type of exchanger consists of several rectangular sheets of a cellulose-blended fibre designed to wick fluids evenly. The sheets are stacked together, separated by channel guides located on one side of the sheet. One side of each sheet is also coated with polyethylene to avoid penetration of water. The guides are fabricated from ethyl vinyl acetate (EVA), and run along the length of one sheet, and the width of the next sheet to form a cross flow within the exchanger. Testing has indicated that the exchanger could obtain a wet-bulb effectiveness of 110% to 122%, and a dew-point effectiveness of 55% to 85% (ISAW 2005; Coolerado 2006).

This type of exchanger structure improves the performance of many types (Idalex Technologies 2003; ISAW 2005; Coolerado 2006) of indirect evaporative cooling systems, and thus, enables the systems used for cooling of buildings, due to lowered supply (product) air temperature. However, work done on this type of exchanger is very beginning. Currently, there is only one exchanger configuration available on market, as shown above. Although this configuration creates a uniform air flow distribution over the wet surface, it also lowers the cooling effectiveness owing to the large quantity of air flowing along the shortcuts through the holes. This obviously results in incomplete cooling of the working air, and so less effective cooling of the product air. In addition, a cross-flow arrangement between the working and product air is not the best flow pattern in terms of heat exchange. A counter flow arrangement would be preferable as it can create a higher temperature difference (logarithmic average) between the two adjacent airstreams. Moreover, no work was done on numerical analyses of fluid flow and heat/mass transfer within this or similar types of exchanger, and material selection, structure design and geometrical optimization of the exchangers were not being carried out yet.

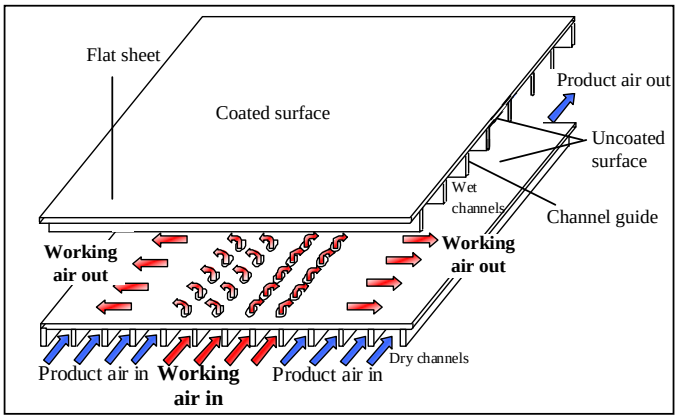

Fig. 1-2 Structure and operating principle of a heat and mass exchanger for dew point cooling

1.2 Descriptions of the research

1.2.1 Research concept

A polygonal-sheets-stacked structure will be proposed to replace the existing rectangular exchanger design. The polygonal sheets could be stacked together using guides of the same material, as shown in Fig. 1-3, and one side of each sheet is coated with a water-proof material to avoid water penetration. The intake air would be

brought into the dry channels from the lower part of the left-hand side of the stack. Operation would be as follows: The air flows through the channels and is divided into two parts at the other end of the channels: One part of the air stream keeps moving at the same direction and is finally delivered to the space where cooling is required, and the other part of the air stream is diverted into the adjacent wet channels where the surfaces are wetted by water. The wet channels allow heat to be absorbed through the channel walls by vaporising the water on the surfaces. The air in the wet channels flows in a reverse direction and is finally discharged to atmosphere from the bottom part of the right side of the stack. In this design, the dry channels contain both product and working air, and the wet channels take only working air, a division of the intake air. The remaining intake air flows out as product air (conditioned air to be supplied to space), which has been cooled towards the dew-point temperature of entering air because of the total heat transfer (i.e. sensible and latent heat) with the working air in the adjacent wet channels. Latent heat and sensible heat has been exchanged through vaporising the water of wet surface into working air and absorbing the heat through channel walls from dry channel to wet channel. The working air in the wet channels will be humidified and heat eventually.

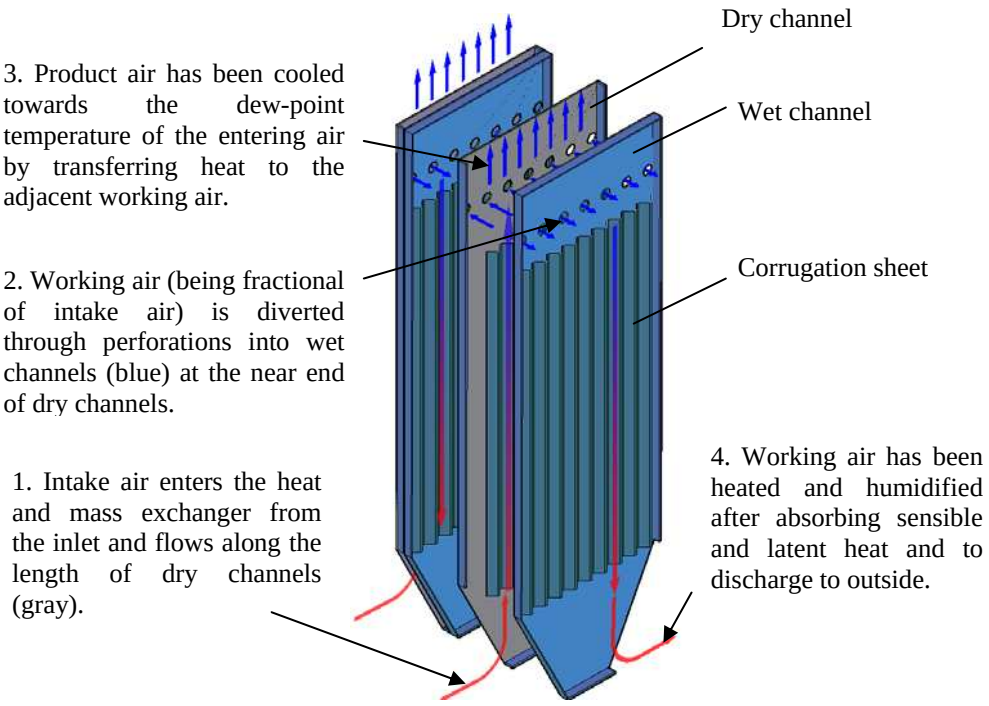

Fig. 1-3 **Working principle of counter-flow heat and mass exchanger**

The air treatment process occurring in the heat and mass exchanger (see Fig.1-4 (a)), can be indicated on the psychrometric chart, as shown in Fig. 1-4 (b). The airstream in dry channel experiences constant moisture cooling process (From state 1 to 2) and is cooled towards dew-point temperature of intake air (T_{dp}) due to the enhanced heat and mass transfer between the product and working air. The maximum heat exchanging is caused because the inlet temperature of working air (fraction of intake air) has been fully pre-cooled towards dew-point of intake air. In the wet channel, meanwhile, because of the water evaporation, the working air would experience a constant enthalpy cooling process to become saturated (From state 2 to 3'). Continuously, saturated working air exchanges heat with the air in dry channel sensibly and latently until being discharged (From state 3' to 3). In fact, the latent and sensible heat transfer has been occurred simultaneously. The real heat and mass transfer process of working air going through could not be indicated by an individual process on the psychrometric chart (such as constant enthalpy process), but, it is also very helpful for understanding and calculation by separating the simultaneous occurring latent and sensible heat transfer into individual process as used in the typical two-stage indirect/direct evaporative cooling system.

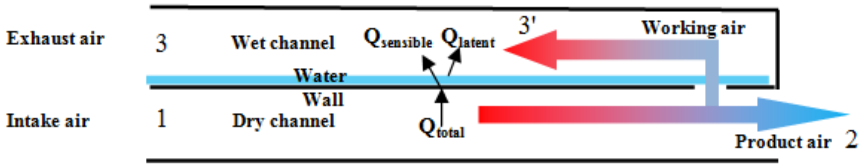

(a) Air flows in the counter-flow heat/mass exchanger

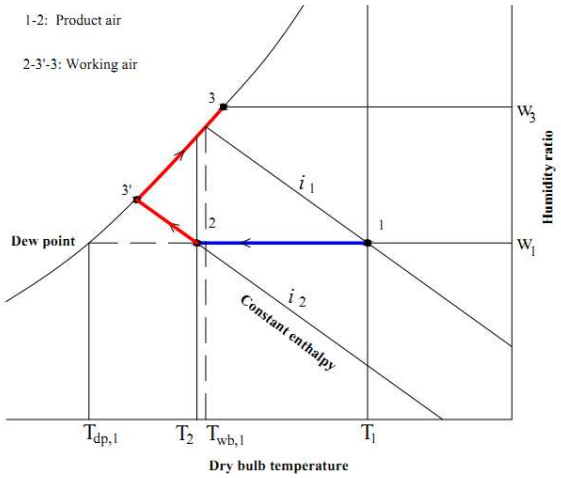

(b) The air treatment process showing on the psychrometric chart

Fig. 1-4 (a) Schematic of air flows in the counter-flow heat/mass exchanger and (b) the air treatment process showing on the psychrometric chart

1.2.2 Research Objectives

The proposed research aims to optimise the design of the exchanger in terms of its material, structure and geometrical sizes, and as a result of the research, to develop a new type of exchanger configuration. The new exchanger will lead to a 15 to 35% improvement in both wet-bulb and dew-point effectiveness. In most areas of the EU, the dew-points of outdoor air in summer are usually below 15-19^{o}C (CIBSE 2001). Use of the new exchanger would be able to produce a cold supply air stream that is below 16 to 20^{o}C and is suitable for cooling the building. This innovation will eliminate the need of fossil fuel based electricity for cooling, and will have obvious benefits in terms of reduced fossil fuel consumption and CO_2 emission to the environment. The specific objectives of the research include:

1. Optimisation of the exchanger design, in terms of material, structure/geometric sizes and initial cost issues.
2. Construction and laboratory testing of prototype exchangers, and finalisation of the exchanger design and computerised optimisation tool.
3. Economic, environmental and regional acceptance analyses.

1.2.3 Research methodology

Approaches for objective 1: Conceptual design of the proposed heat/mass exchanger module and module-based air cooler

The approaches enabling this objective is (1) undertaking the conceptual design of the heat/mass exchanger module and the module-based air conditioning system; (2) providing the list of components involved in the system.

Developing a computer model to optimise the heat/mass exchanger configuration and predict its operating performance: The approach enabling this objective is to develop a computer model and use the model to analyse the performance of the exchanger, e.g. cooling effectiveness, supply air temperature, energy efficiency ratio. The results from the simulation are further analysed to (1) determing the optimal geometrical sizes of the exchanger, through side by side comparison between different sets of results; (2) selecting the appropriate materials for constructing the heat/mass exchanger by comparing thermal and physical properties of the proposed materials and initial costs;

(3) recommending the adequate system operating conditions including temperature, humidity, intake flow rate and working into intake ratio of the heat exchanger, by comparing the results obtained from various operating conditions.

Approaches for objective 2: Constructing and testing a prototype dew point indirect evaporative air cooler in laboratory

The approaches enabling this objective are to construct and test an experimental prototype under the laboratory condition. The test results will be used to 1) determine the cooling effectiveness of the system under various operating conditions; 2) estimate the energy efficiency of the system by taking into account the fans and pump power consumed in the system operation. Further, the system performance will be verified based on the comparison between the computer prediction and experiment, thus giving the actual figures of the system cooling effectiveness and energy efficiency. As a result, a design/optimisation model for the dew point heat/mass exchanger and an experimental unit will be generated. These will be used to examine whether or not the expected increased cooling efficiency can be achieved, and what is the system's real operational energy efficiency.

Approaches for objective 3: Economic, environmental and regional acceptance analyses

The approaches enabling this objective is to develop a dedicated calculation approach and use this approach to evaluate the economic and environmental impact of the technology to the Europe and China and analyse its regional acceptance level within the European and China region.

The four approaches are joined together to enable the overall objective of the research to be achieved, i.e., developing a novel dew point indirect evaporative cooler with enhanced cooling effectiveness and energy efficicency. This technology is expected to achieve wide range of application in Europe and China building sector and so, will contribute to Europe's and China's governmental target on reducing energy consumption in buildings and cutting CO_2 emission to the environment.

1.2.4 Novelty and timeliness

This research has developed a novel dew point evaporative heat and mass exchanger that could achieve enhanced cooling effectiveness and thus aid to wide deployment of this low energy cooling systems. To summarise, the proposed system has the following innovative features:

- A unique counter current heat and mass exchanger module allows the product air to be cooled towards the dew point tempearature of entering air. This enables more areas of exchanger to engage in transferring the heat and mass and results in an enhanced cooling effectiveness compared with cross-flow heat and mass exchanger.
- A unique aluminium film coated cellulose fibre medium is employed in constructing the heat/mass exchanger. This composite material is composed of water-proof aluminium film and hydrophilic cellulous fibre evaporative media. This enables higher thermal conductivity, water absorption/ retaining and tensile strength to be achieved than the single evaporative medium. This new type of material helps increase the performance of the system.
- A new structure of water distribution of the heat exchanger enables the feed water to distribute over the evaporative medium uniformly. This enlarges the wetting area of evaporative media and allows the performance of the system to be increased.

The proposed research aims to develop a polygonal-sheets-stacked heat/mass exchanger that allows dew point cooling widely used for air conditioning of buildings in Europe, China, even worldwide regions. It contributes to the target of EPBD (European Directive on Energy Performance of Buildings) and UK's Part L building regulations in terms of improving performance of buildings, and eventually the Europe's target of 60% of CO_2 emission reduction by 2050, relative to 1990 level.

The proposed dew point cooling system consumes very little energy for the system operation (fans and pump only). The energy efficiency of the system will therefore be extremely high and its development would allow consumption of fossil fuels in cooling buildings to be reduced substantially or avoided. This would lead to a reduction of greenhouse gases and pollutant emissions, an increase in the use of natural energy and security of energy supplies, and improvement in energy efficiency. In addition, it will enhance the competitiveness of European sustainable development

industry and improve the quality of life both within the Europe, China and global region.

1.2.5 Thesis structure

Chapter 1 briefly introduced the background, significance, objectives, research concept of the proposed polygonal perforation heat and mass exchanger for evaporative cooling, methodology and novelty of the PhD research.

Chapter 2 presented an extensive literature review towards the evaporative cooling technologies, which concerns with the working principle, materials, structure, performance, disadvantages and advantages of various evaporative systems. The technical features and problems relevant to the evaporative cooling systems were identified. The innovative features of this research relevant to the previous studies were also identified as the result of comparison between the past works and proposed research. Further, the fundamental terms such as terminology, definitions and concepts relevant to the evaporative cooling were presented.

Chapter 3 involved development of a dedicated numerical computer model and use of the model to simulate the performance of the proposed counter-flow heat and mass exchanger. Differential equations of the model were established based on assumptions and approximations. A simplified model was developed to analyses the effects of various parameters on the performance of the heat exchanger and further to optimise the design.

In the Chapter 4, a prototype of dew point cooling system was designed, constructed and tested in laboratory to validate the simulation. The details of material selection and prototype set-up were described in this chapter.

The results of experiments and the effects of various parameters on the performance of prototype were investigated in the Chapter 5. The studied parameters include intake air dry-bulb and wet-bulb temperature, intake air channel velocity, working-to-intake air ratio, feed water temperature. Further, the discrepancy between experiment and simulation results was examined and the reasons causing the discrepancy were analysed.

Chapter 6 involved study of economic and environmental impacts and regional acceptance level of the dew point cooling system.

Economic and environmental analyses will be carried out against the new dew point cooling system. The polygonal stack is expected to provide higher effectiveness than the rectangular stack structure, but its advantage is likely to be offset by the higher construction costs. Estimates will be made of the construction cost, the total cost annual running cost for typical European and China regions and comparisons will be made. The simple payback period for the polygonal stack structures will be calculated taking into account investment cost and energy prices likely to be encountered in the near and medium future. The environmental benefit of the structure will also be assessed in terms of reduced carbon dioxide emission.

The dew-point of several typical European regions in summer season will be investigated, and the temperatures of the supply air under these climate conditions will be estimated, in response to the novel dew point cooling application. The potential of the dew point cooling system used for air conditioning of the buildings will be evaluated and its relevant parameters, including air flow rate, working-to-intake-air ratio and water temperature, will be determined. Regional acceptance of the system, as the alternative of the existing air conditioning systems, will be estimated based on the above analyses. This will provide an indication where the system is most applicable and where it is less. For humid climate where the dew-point of the air is high, the approach of air pre-treatment will be suggested that can still bring the dew point cooling into use.

Chapter 7 presents the conclusive remarks derived from the research in terms of cooling effectiveness, velocity, inlet conditions, geometrical sizes and materials et al.

The further work in the Chapter 8 was suggested to develop a commercially viable product which has already started up; and the preliminary design of the unit has been presented for the interest of readers.

All chapters are joined together to enable the overall objective of the project, i.e. to optimise the design of the exchanger in terms of its material, structure and geometrical sizes, and to develop a new type of exchanger configuration. The new exchanger will lead to a 15 to 35% improvement in both wet-bulb and dew-point effectiveness, which

allows the dew point cooling become a widely applicable system for building air conditioning in most regions of Europe and even global. This innovation will eliminate the need of fossil fuel for cooling, and will have obvious benefits in terms of reduced fossil fuel consumption and CO_2 emission to the environment.

Chapter2.
Literature Review

2.1 Background

Compared with the popular conventional vapour-compression and absorption refrigeration, the evaporative cooling has a few significant advantages cover: 1) large capacity of energy saving and carbon dioxide emission reduction because no energy-intensive compressors exist in evaporative cooling systems; 2) more environmental friendly cooling technology because only water participate in the cooling process rather than pollutant refrigerants; 3) more simple in terms of structure, construction, and control strategies.

Most of conventional air conditioning systems are based on vapour-compression and absorption refrigeration cycles, which are mature technology and have been widely applied in residential and commercial buildings. The performances of vapour-compression and absorption refrigeration systems are stable and sufficient to provide cooling for buildings. However, they are energy intensive refrigeration technologies owing to using the energy-consuming compressors, fans and pumps. The typical values of Energy Efficiency Ratio (EER) for some typical refrigeration cycles are summarised in Table 2-1 (Afonso 2006). Due to no compressors involved, the EER values of evaporative cooling systems are much higher than those of conventional refrigeration cycles. The energy consumption of evaporative cooling systems is usually 30-50% that of compression air conditioning system with the same capacity. Thus, the EER value of an evaporative cooling system is 2-3 time that of a typical vapour-compression system (Maisotsenko and Reyzin 2005).

Table2-1 The typical values of Energy Efficiency Ratio for some typical refrigeration cycles

Refrigeration cycle	Vapour-compression	Absorption	Adsorption	Desiccants	Ejector	Thermoelectric
EER(Btu/Wh)	7-17	2-3.4	0.7-2.7	1.7-5.1	0.9-2.7	1.7-3.4

The current mainstream refrigerants employed in vapour-compression air conditioning systems are HCFCs (such as R-22) and HFCs (such as R-134a, R-410A). HCFCs and HFCs have large global warming potential (GWP) and they can trap heat more

effectively than carbon dioxide (Wuebbles 1994). Evaporative cooling, however, utilises the latent heat of water evaporation to provide cooling instead of using harmful refrigerants and thereby has a great potential of slowing down global warming.

As two major types of evaporative cooling, direct evaporative cooling (DEC) adds moisture to room air, which causes discomfort and health problems. Indirect evaporative cooling (IEC) lowers air temperature and avoids adding moisture to the air, but it limits the temperature of supply air to some degrees (2 to 5^{o}C) above the wet bulb of the outdoor air (usually 40-60% wet-bulb effectiveness), which is too high to perform air conditioning of buildings. Especially for the regions with humid climates, the IEC systems usually have poor performances. To solve this, a pre-dehumidifier, direct expansion (DX) compressor or chilled water coil can be combined together with the IEC modules to form a hybrid system, which can provide a low supply air at a lower cost than conventional air conditioning system and can be applied in various climate conditions. The potential market of the IEC systems can be very large as long as the existing technical difficulties/barriers can be solved, i.e., relatively low effectiveness, high initial costs and large size occupations, etc.

By studying the relevant literatures, some basic knowledge, e.g. evaporative medium, apparatus types, work principles, performance and characteristics of various evaporative cooling systems, have been identified. Then performance evaluation standards of IEC systems have been indicated, which will be used in comparing the performances of different types of evaporative systems. The previous research works conducted on the IEC-related systems are too scattered and ambiguous to identify the focuses of research and technical problems surrounding the IEC technology. Therefore, it is very necessary to sort out the current developing status of the evaporative cooling technology, remaining difficulties or problems and technical barriers of practical applications by analysing the related R&D and application projects of IEC systems.

2.2 Work Principles of Evaporative Cooling Systems

2.2.1 Direct evaporative cooling systems (DEC)

Direct evaporative cooling adds moisture to the process air. The working diagram of direct evaporative cooling and the working process representing on the psychrometric chart are shown in Fig. 2-1.

(a) Working diagram of direct evaporative cooling

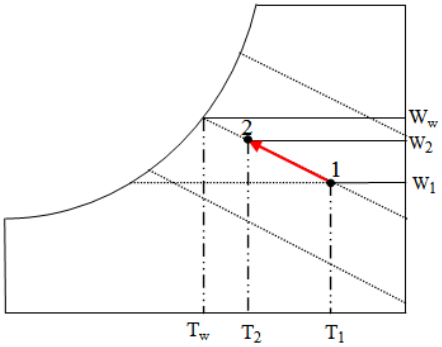

(b) The thermal process showing on the psychometric chart

Fig. 2-1 Working diagram (a) and thermal process showing on the psychometric chart (b) of direct evaporative cooling

Inlet air (state 1) enters into the wet channel and exchanges the heat and moisture with water. As water is continuously evaporated into the airstream along the wet channel, consequently, the dry bulb temperature of entering air has been reduced with rising moisture content (state 2). In the process, the sensible heat of air decreased with latent heat increases due to the evaporation of water. As shown on the psychometric chart of Fig. 2-1 (b), the entering air experiences an approximate isenthalpic process from state 1 to state 2 regardless of the enthalpy of water being evaporated. Fig. 2-2 illustrates temperature variation process occurring between the process air and direct contact water (ASHRAE 1996). Theoretically, the thermodynamic process of direct evaporative cooling is limited by the wet- bulb temperature of entering air. The

continuously cycled water will reach an equilibrium temperature equal to the wet-bulb temperature of the entering air. The dry-bulb temperature of air decreased because of the heat and mass transfer between air and water. Meanwhile, the humidity of air increased at a constant wet bulb temperature.

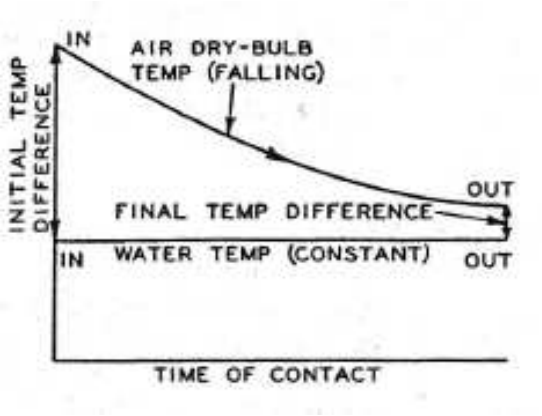

Fig. 2-2 Thermal process showing on the temperature decreasing process of air in contact with water in direct evaporative cooling system

An important technical term for evaluating effectiveness of evaporative cooling systems is the degree of outlet air approaching to wet-bulb temperature of inlet air, i.e., wet-bulb effectiveness, which is defined as follow:

$$\varepsilon_{\mathrm{DEC}} = \frac{t_{db,1} - t_{db,2}}{t_{db,1} - t_{wb,1}} \qquad (2\text{-}1)$$

The wet-bulb effectiveness of current direct evaporative cooling systems is ranged from 70% to 95% depending on the configurations and the air velocity of passing the evaporative medium. This type of systems has been widely used for the reasons of simple structure, cheap initial and operating costs.

2.2.2 Indirect evaporative cooling systems (IEC)

Indirect evaporative cooling systems can lower the air temperature without adding moisture to the air. The improvements in comfort feeling make these systems more attractive than direct systems. In an indirect evaporative air cooling system, primary (product) air passes over the dry side of a plate, and secondary (working) air passes over the opposite wet side. The wet side absorbs heat from the dry side by evaporating

water and therefore cooling the dry side, while the latent heat of vaporizing water is transferred to the working air in wet side.

Ideally, if the product air of IEC system travels in a counter flow manner to the working air, and the two airstreams have a good balance of flow-rates with an infinite surface area, the product air temperature on the dry side of the plate will reach the wet-bulb temperature of the incoming working air. The temperature of the working air on the wet side of plate will be decreased from its incoming dry-bulb temperature to the incoming wet-bulb temperature. However, It is shown that only 54% of the incoming air wet-bulb temperature can be achieved for a typical indirect evaporative cooler, and this poor performance is due mainly to the following reasons: 1) an infinite exchanging-surface area is unachievable; 2) a pure counter flow is difficult and expensive to achieve in mechanical design; 3) the uniform and even water distribution over the wet sides is hard to obtain.

Fig. 2-3 illustrates the working diagram and thermal process of indirect evaporative cooling system representing on a psychrometric chart. The intake air (state 1) enters into the dry channel while the working air (state 1) normally from the same source with intake air enters into the adjacent wet channel. The intake air (primary air) has been cooled by latent heat transfer of water evaporation and sensible heat transfer of convection heat transfer with the working air (secondary air) in the adjacent wet channel. As shown on the psychrometric chart, the intake air (state 1) is cooled at the constant humid ratio toward the wet-bulb temperature of working air. Meanwhile, the temperature of working air is increased from state 1 to 3 along the isenthalpic line, as the thermal process of direct evaporative cooling.

The efficiency of indirect evaporative cooling, i.e. wet-bulb effectiveness, is limited by the wet-bulb temperature of secondary air, which can be defined as the following formula, i.e. the ratio of the temperature decrease of primary air dry-bulb to the temperature distance of the primary air dry-bulb to the secondary air wet bulb.

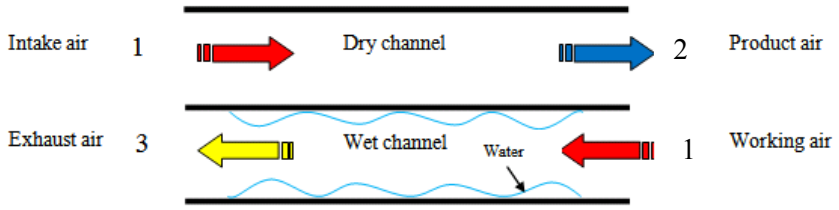

(a) Working diagram of indirect evaporative cooling

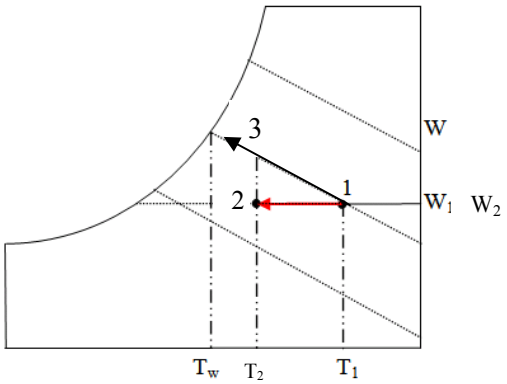

(b) The thermal process showing on the psychometric chart

Fig. 2-3 Working diagram (a) and thermal process representing on the psychrometric chart (b) of indirect evaporative cooling

$$\varepsilon_{\mathrm{IEC}} = \frac{t_{db,1} - t_{db,2}}{t_{db,1} - t_{wb,1}} \qquad (2\text{-}2)$$

The wet-bulb effectiveness of current typical indirect evaporative cooling systems may range between 55% and 75% or higher, which is lower than that of direct evaporative cooling (ASHRAE 1996). However, due to no moisture addition to the supply air, the IEC system doesn't have to supply the same cooling with the DEC system to provide the same comfort feeling.

2.2.3 Combination systems

Indirect cooling is often coupled with a second direct evaporative cooling stage, to increase the effectiveness of the overall system. The first stage indirect cooling lowers both the dry-bulb and wet-bulb temperature of the incoming air. Then the leaving air from the first stage enters to the direct evaporative cooler where the air is cooled in further but with moisture addition. The secondary air of indirect cooling may be the exhaust air from the conditioned space or outdoor air. Fig. 2-4 indicates the thermal

process of process air on a psychometric chart (ASHRAE 1996). The first-stage indirect cooling follows a line of constant humidity ratio because no moisture is added to the air. The second stage direct cooling follows the wet-bulb temperature line after the primary air leaving the first stage.

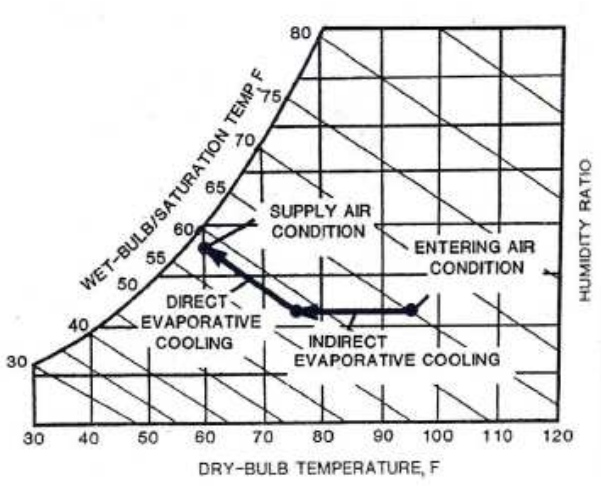

Fig. 2-4 Thermal process showing on the thermal process of indirect and direct combination cooling showing on psychometric chart

In dry or mild climate conditions, the two-stage IEC/DEC systems can be designed to supply the entire cooling to the conditioned space of buildings. The most typical two-stage IEC/DEC systems include the first stage indirect cooler with the heat exchanger in the configuration of plates, rotary wheel or heat pipe and the second stage direct evaporative cooler and second direct cooler stage. The overall wet-bulb effectiveness of two stage IEC/DEC systems ranges from 70-110% depending on different systems (Heidarinejad et al. 2009; Kulkarni and Rajput 2011). In humid climate conditions, a third cooling stage may be needed to supply sufficient cooling for the conditioned spaces. A chilled water coil or direct-expansion refrigeration unit may be added downstream from the indirect cooler and either upstream or downstream from the direct cooler. The third stage unit is activated only the upstream evaporative coolers cannot attain the required supply air temperature. The typical three-stage hybrid systems can provide supply air temperature slightly below the wet-bulb temperature of outdoor air with the overall wet bulb effectiveness ranges from 100% to 115% (ASHRAE 1996).

2.2.4 Dew point evaporative cooling based on Maisotsenko-cycle (M-cycle)

Maisotenko invented a novel thermodynamic cycle, i.e. Maisotenko-cycle (Idalex Technologies 2003). The M-cycle is designed to capture extra amount of energy from atmosphere using the latent heat of evaporation through a multi-perforated cross-flow plate heat exchanger. The exchanger is able to cool air (or liquid) to a temperature below the wet bulb and above the dew point of the cooling air, with no moisture added to the supply medium. That is why it is called dew point evaporative cooling.

Fig. 2-5 shows the principle and psychrometric representation of an ideal M-cycle, in which the working and product air have the same inlet condition. The intake and working air at state 1 flows over the dry side of a plate which is perforated along the flow path. When the air moves along the dry side (working air in dry channel), it is cooled and partially diverted to the wet side through the perforations, resulting in a change of state from 1 to 3'. State 3' is a variable point depending upon the position of the perforations. At the far end of the dry working air channel, only a very small percentage of air remains, which is cooled to the lowest level (close to the dew point of the entering working air) and is also diverted to the wet side. The air in the wet side (working air of wet channel) has a lowered temperature, and therefore, is able to absorb heat from its two adjacent sides, i.e., the dry working airflow side and the dry product airflow side. This results in a change of state from 3' to 3'' due to the water evaporation from the wet side of the plate to the working air. In which, the working air undergoes an isothermal humidification process from state 3' to 3''(state 3'' corresponds to the saturation point of state 3') and another change from 3'' to 3 due to transfer of sensible heat from the adjacent air streams, and is finally discharged to the atmosphere. In the meantime, the product air (or fluid) flows over the other adjacent dry side (product air of dry channel) and is cooled from state 1 to 2.

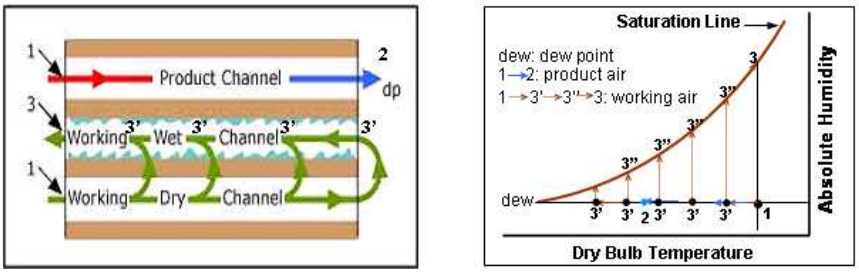

Fig. 2-5 Principle of the heat and mass exchanger based on M-cycle and its representation on psychrometric chart

For the simplicity of manufacture, actual heat and mass exchangers based on the M-cycle differ slightly from the ideal counter-flow design. Fig. 2-6 shows the structure of the actual exchangers based on the M-cycle (Elberling 2006). Part of the surface on the dry side is designed to allow for working air to pass through and the rest for the product air. Both product and working air are guided to flow over the dry side along the channels that are arranged in parallel. There are numerous perforations distributed regularly on the area covered by the working air and each of these allows a certain percentage of air to enter crossly the wet side of the sheet. The air is gradually delivered to the wet side as it flows along the dry side, and this produces well-distributed airflow over the wet surface. This arrangement allows the working air to be pre-cooled before entering the wet side of the sheet, by losing heat to the adjacent wet surface. The pre-cooled air delivered to the wet side flows over the wet surface along channels arranged at right angles to the dry side channels, absorbing heat from the working and product air. As a result, the product air is cooled before being delivered to spaces where cooling is required, and the working air is humidified and heated, and then discharged to the atmosphere. A testing report indicated that a module of this type of exchanger could obtain a wet bulb effectiveness of 81% to 91% with an average of 86% (Elberling 2006).

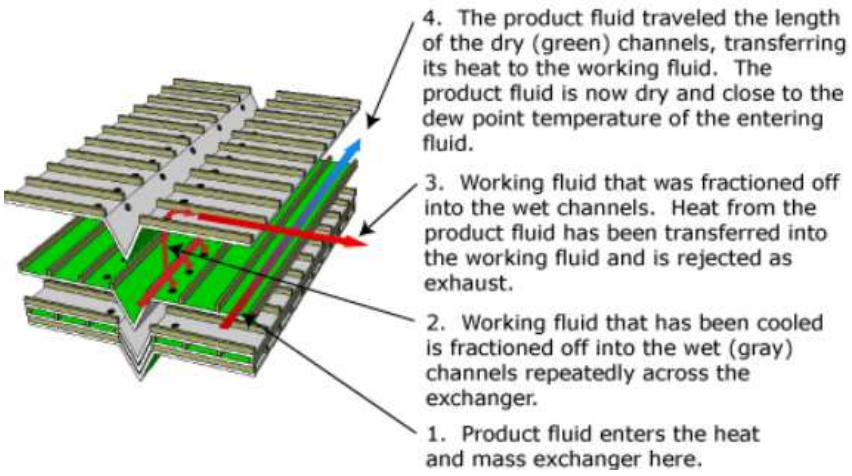

Fig. 2-6 Schematic of a heat and mass exchange module based on M-cycle

2.3 Performance Evaluation Standards of IEC

IEC system are usually evaluated by the following parameters, i.e. supply air temperature and flow rate, secondary to primary air ratio, wet-bulb effectiveness, cooling capacity, power consumption, energy efficiency and water consumption. The definitions of the essential parameters are specified below.

2.3.1 Wet-bulb/dew-point effectiveness

The cooling effectiveness of the indirect evaporative cooling system can be used to rate the IEC. Wet-bulb effectiveness is the temperature difference of intake and supply air divided by the temperature difference between the dry bulb and wet-bulb of intake air, which is expressed in the following equation:

$$\varepsilon_{wb} = \frac{t_{db,1} - t_{db,2}}{t_{db,1} - t_{wb,1}} \quad (2\text{-}3)$$

where,

ε_{wb}- Wet-bulb effectiveness；

$t_{db,1}$- Intake primary air dry bulb temperature, ^{o}C ;

$t_{wb,1}$- Intake secondary air wet bulb temperature. The temperature of intake secondary air of system is usually the same as that of intake primary air, ^{o}C ;

$t_{db,2}$- Leaving dry bulb temperature of primary air, ^{o}C ;

Dew point evaporative cooling systems can provide a supply air lower than the wet-bulb temperature of intake primary air toward its dew point temperature. In this situation, dew point effectiveness defined as the following formula can be used to rate the coolers.

$$\varepsilon_{dp} = \frac{t_{db,1} - t_{db,2}}{t_{db,1} - t_{dp.1}} \quad (2\text{-}4)$$

where,

ε_{dp}- Dew point effectiveness；

$t_{dp,1}$- Intake primary air dew point temperature, ^{o}C ;

2.3.2 Secondary to primary air ratio

For indirect evaporative coolers, primary air (product air) is the airflow in the indirect section whereas secondary air (working air) flows in the direct section. The ratio of secondary airflow rate to primary airflow rate has an effect on the performances of IEC systems. Assuming the total airflow rate is constant, the cooling effectiveness of an IEC system is enhanced when the secondary to primary ratio increases due to more secondary air working in the direct section to absorb sensible and latent heat from the primary air. However, the supply airflow rate of the IEC system is reduced.

For some IEC systems, the secondary air is the fraction of intake air entering into the indirect section. 'Secondary to primary air ratio' can be replaced by the similar parameter, i.e. 'working to intake air ratio', which is the ratio of working air (secondary air) flow rate to intake air flow rate.

2.3.3 Cooling capacity

There are two methods to define the cooling capacity of evaporative cooling systems depending on if the intake air of the system uses the return air from indoor or the outside air. When the return air of the room sent to the intake of system, the cooling capacity of cooler can be calculated by the following equation:

$$Q_{\text{cooling,r}} = \frac{c_{p,f}\rho_f V_2\left(t_{db,r} - t_{db,2}\right)}{3.6} \quad (2\text{-}5)$$

where,

$Q_{\text{cooling,r}}$- Cooling capacity of evaporative cooler, W;

$c_{p,f}$- Specific heat of air at constant pressure, kJ/(kg k);

ρ_f- Density of air, kg/m^3;

V_2- Airflow rate of supply air, m^3/h;

$t_{db,r}$- Reference dry-bulb temperature of room, i.e. 26.7^{o}C, which is selected because it is used in the ARI test standards for rating conventional air conditioning systems (ARI 2003);

$t_{db,2}$- Dry-bulb temperature of supply air, ^{o}C.

For the indirect evaporative cooling, however, the above equation only calculates the sensible cooling of the system. It can not reflect the thermal comfort improvement because of no moisture addition. The total cooling capacity of system including latent and sensible cooling can be evaluated using the following equation:

$$Q_{\text{total}} = \frac{\rho_f V_2 (i_{db,r} - i_{db,2})}{3.6} \quad (2\text{-}6)$$

where,

Q_{total}- Total cooling capacity of system, W;

$i_{db,r}$- Specific enthalpy of air in room temperature, kJ/kg;

$i_{db,2}$- Specific enthalpy of supply air, kJ/kg.

When the indirect evaporative systems use outside air as the intake air of systems, the cooling capacity of coolers can be evaluated using the sensible cooling of intake air. The calculation equation is given as below, which is developed by ASHRAE Standard 143 (ASHRAE 2000). This cooling capacity definition will be used in the following research.

$$Q_{\text{cooling,IA}} = \frac{c_{p,f} \rho_f V_2 (t_{db,1} - t_{db,2})}{3.6} \quad (2\text{-}7)$$

where,

$Q_{\text{cooling,IA}}$- Sensible cooling of intake air, W;

$c_{p,f}$- Specific heat of air at constant pressure, kJ/(kg k);

ρ_f- Density of air, kg/m^3;

V_2- Airflow rate of supply air, m^3/h;

$t_{db,1}$- Dry-bulb temperature of intake air, ^{o}C.

$t_{db,2}$- Dry-bulb temperature of supply air, ^{o}C.

2.3.4 Energy efficiency

The air conditioners usually use energy efficiency or coefficient of performance (COP), i.e. cooling capacity (W) divided by power consumption (W), to rate the system efficiency. Depending on the two different definitions of cooling capacity, there are two methods to calculate energy efficiency.

According to a test method developed by California Energy Commission (Commission 2008), the Evaporative Cooler Efficiency Ratio (ECER) can be calculated after substituting Eqs.(2-3) and (2-5) into the following equation:

$$\begin{aligned} \text{ECER} &= \frac{Q_{\text{cooling,r}}}{W} = \frac{c_{p,f}\rho_f V_2\left(t_{db,r} - t_{db,2}\right)}{3.6W} \\ &= \frac{c_{p,f}\rho_f V_2\left(t_{db,r} - \left(t_{db,1} - \varepsilon_{wb}(t_{db,1} - t_{wb,1})\right)\right)}{3.6W} \end{aligned} \quad (2\text{-}8)$$

where,

$t_{db,1}$- Outdoor dry-bulb temperature, 32.8 ^{o}C;

$t_{wb,1}$- Outdoor wet-bulb temperature, 20.6 ^{o}C;

$t_{db,r}$- Indoor dry-bulb temperature, 26.7^{o}C;

ε_{wb}- Measured wet bulb effectiveness;

V_2- Measured supply air flow rate, m^3/h;

W- Measured total power consumption, W;

where ε_{wb}, V_2 and W are measured with an external static pressure of 74.7 Pa. The energy efficiency of evaporative coolers can be calculated by substituting Equation (2-7) into the following formula which will be used to rate the energy efficiency of the dew point cooler in this research:

$$\text{Energy efficiency} = \frac{Q_{\text{cooling,IA}}}{W} = \frac{c_{p,f}\rho_f V_2\left(t_{db,1} - t_{db,2}\right)}{3.6W} \quad (2\text{-}9)$$

2.3.5 Water evaporation rate

The water consumption of IEC systems depends on the airflow, the contaminant load, the effectiveness of the evaporator medium, and the dry-bulb and wet-bulb difference of the intake air. Ideally, the water evaporation rate is determined by taking the moisture rise from inlet to outlet of secondary air and multiplying by the secondary air mass flow rate divided by the density of water film. It can be calculated by the following formula:

$$V_w = \frac{1000 V_3 \rho_{w,f}}{\rho_w} (w_3 - w_1) \quad (2\text{-}10)$$

where,

V_w- Water evaporation rate, litre/h;

V_3- Secondary air flow rate, m^3/h;

$\rho_{w,f}$- Secondary air density, kg/m^3;

ρ_w- Water film density, kg/m^3;

w_1- Inlet moisture content of secondary air, kg/kg (dry air);

w_3- Outlet moisture content of secondary air, kg/kg (dry air).

2.4 Evaporative Cooling System Types

The existing evaporative cooling systems can be classified into three main categories: direct evaporative cooling systems (DEC), indirect evaporative cooling systems (IEC) and indirect/direct evaporative combination systems. Table 2-2 shows the performance and characterise of various typical evaporative cooling system types including typical system configurations, evaporative media, face velocity, pressure drop, wet-bulb effectiveness, secondary to primary air ratio, advantages and disadvantages (ASHRAE 1996; Palmer et al. 2002).

DEC systems can be divided into three types according to evaporative media and system configurations, i.e., random media air coolers, rigid media air coolers, slinger packaged air coolers, packaged rotary air coolers and remote pad evaporative cooling system.

Random media air coolers usually have low effectiveness and short life time due to using the cheap and inefficient evaporative pads, which is usually made of aspen wood or plastic fibre or foam. The typical structure of this type of coolers for large airflow unit is shown in Fig. 2-7 (ASHRAE 1996). The cooler is mainly equipped with an evaporative pad, a centrifugal fan, water distribution system, a water pump and a reservoir. It operates in this way: The pump lifts water in the reservoir to the distribution system and the water flows down through the pads and then is collected in the reservoir. In the meantime, the centrifugal fan drives air through the evaporative pads and delivers it to the conditioned space.

(To be continued, please see the next page)

Table 2-2 Performance and characteristics of various typical evaporative cooling system types

Category	No.	System type	Configuration	Medium	Face* velocity (m/s)	Pressure drop (Pa)	Wet-bulb effectiveness	Secondary-to-primary air ratio†	Advantages	Disadvantages
DEC	1	Random media air coolers	Fig. 2-7	-Aspen; -Plastic fibre; -Foam	0.5-1.3	24.9	≈80% depending on the thickness of media and velocity of the air passes the media.	—	-Low initial cost -Simple controls -Simple construction	-Low system effectiveness -Short life time and not easy to clean
	2	Rigid media air coolers	Fig. 2-8	-Cellulose (Cardboard box/kraft paper); -Fibreglass	2.0-3.0		70-95% depending on the thickness of media and velocity of the air passes the media.	—	-Lower supply air temperature, airflow rate and energy use than random media air coolers; -Reduced pressure drop; -Cleaner air, longer service life and simple controls.	-Higher initial cost than aspen pad coolers
	3	Slinger packaged air coolers	Fig. 2-9	-Latex-coated fibre; -Fibreglass; -Coated nonferrous metal	1.5-3.0		< 80% depending on the thickness of media and velocity of the air passes the media.	—	-Well-distributed water film by water spray	-More energy consumption -Bacteria and fungi growth

Table 2-2 (Continued)

DEC	4	Packaged rotary air coolers	Fig. 2-10	-Latex-coated fibre; -Fibreglass; -Coated nonferrous metal	0.5-3.0	124		—	-No water spray or circulation system needed	-More energy consumption
	5	Remote pad evaporative cooling system	Fig. 2-11	-Standard random media -Rigid media	0.8, 1.3, 2.0		70-95% depending on the thickness of media and velocity of the air passes the media.	—	- Low cost cooling for the applications like greenhouses, animal shelters, automotive paint booths, etc.	- large space occupation - bacteria or fungi growth
IEC	6	Air to air heat exchanger	Plate and pleated media; Heat pipes; rotary heat wheel; Shell and tube (Fig. 2-12)	-Cellulous fibre -Porous ceramic -Cotton or other moisture-retaining cloths		50-500	40-80% depending on the primary and secondary airflow rate	0.3-1.0	-No moisture is added to the supply air results in improved comfort -Cleaner supply air than DEC. -Supply air has no contamination.	-More initial cost than DEC -More complicated structure than DEC

Table 2-2 (Continued)

IEC	7	Cooling tower and coil systems	—	- Film fill (allows water to spread into a thin film, usually PVC) -Splash fill (interrupts water flow)		—	55-75%	—	-Cooling tower can be located remote from the cooling coil;	-Large occupation space
Combination	8	Two-stage IEC/DEC or refrigerated (direct-expansion or chilled water coil) cooling system	Fig. 2-13 Fig. 2-14	—		—	70-110%	—	-Higher overall system effectiveness -Lower supply air dry bulb temperature.	-More complicated system construction - More space occupation -Higher initial cost
	9	Three-stage IEC/DEC/refrigerated (direct-expansion or chilled water coil) cooling system	Fig. 2-15	—		—	100-115%	—	-Higher overall system efficiency; -Lower cooling capacity compared with refrigeration system; -Reduction in size of the refrigeration cooling system;	-More complicated system construction - More space occupation -Higher initial cost -Pollutant refrigerant

* Face velocity - average velocity of air passes through the face of evaporative media
† Secondary to primary air ratio - the ratio of secondary airflow rate to primary airflow rate.

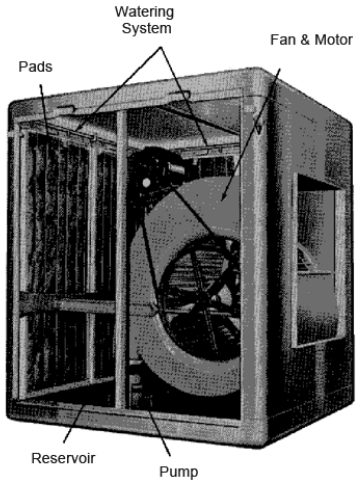

Fig. 2-7 Typical random media evaporative cooler

A rigid media air cooler, however, has a higher effectiveness and reduced pressure drop due to using a type of cross-corrugated "rigid media", which is usually made of cellulose, cardboard box/kraft paper, or fibreglass that have been treated chemically with antiriot and rigidifying resins. The advantages of rigid media are described in Section 2.5. The typical configuration of this cooler is shown in Fig. 2-8 (Munters, 2011; ASHRAE 1996). The cooler usually operates in this way: The airflow passes through the rigid media while the circulating water, lifted by a pump from a bottom reservoir, flows over the media surfaces from a top flooding header and water distribution chamber.

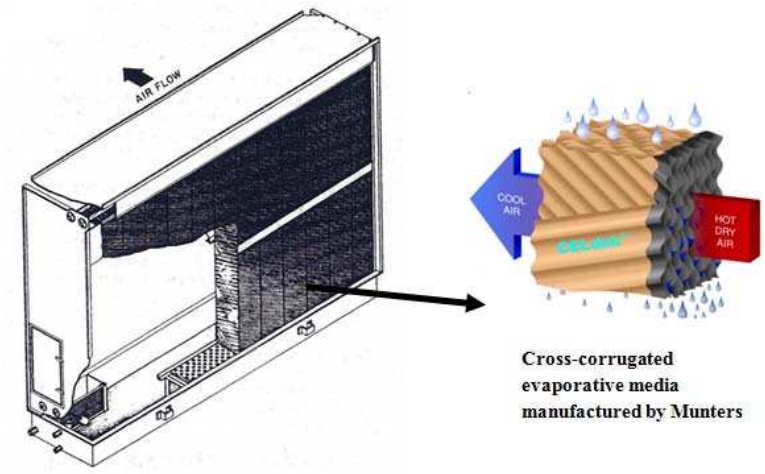

Fig. 2-8 Typical rigid media air cooler

A slinger packaged air cooler usually consists of a spray section and a blower section as shown in Fig. 2-9 (ASHRAE 1996). Airflow flows through a water spray created by

a motor-driven, vertical, clog-proof disk (the slinger) and then passes through an evaporative pad and an eliminator pad using to collect the moisture of air. This type of cooler usually consumes much more energy than random media air coolers in the same condition because of the centrifugal fan and water slinger. However, the water spray created by the slinger can provide well-distributed water film which significantly improves the efficiency of evaporative cooling.

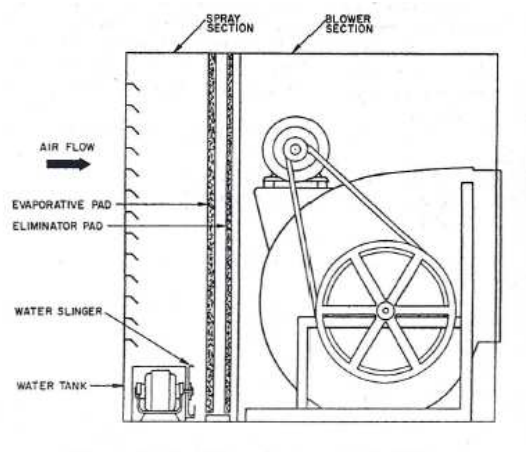

Fig. 2-9 Typical slinger packaged air cooler

A packaged rotary air cooler also consists of a cooling section and a fan section, as shown in Fig. 2-10 (ASHRAE 1996). However, the cooler wets and washes the evaporative pad by rotating it through a water tank. An automatic flush value may be equipped to drain off the water in the tank periodically thereby to reduce the minerals and solids in the water. The most obvious advantage of this cooler is that the water spray or circulation system is no needed in the cooler. However, additional energy consumption may be needed to drive the rotary pad.

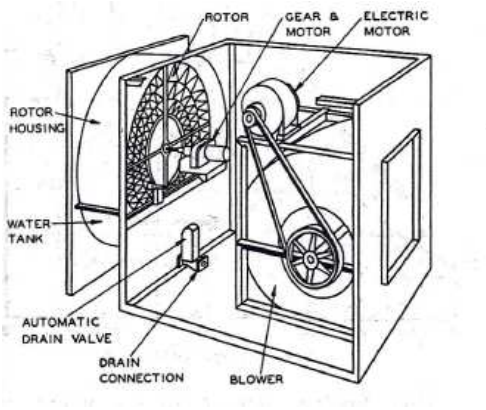

Fig. 2-10 Typical packaged rotary evaporative cooler

a remote pad evaporative cooling system usually consists of evaporative pads, water distribution and collecting system and has been widely applied in greenhouses (see Fig. 2-11) (Beijing Fenglong Agriculture Technology Co. 2006), animal shelters, automotive paint booths, etc. The evaporative pads are often mounted in the wall or roof of a building to compact space occupation. The system works in this way: Drawn by fans, the outdoor air flows through the wet pads flooded from the top perforated pipe. The extra water is either wasted to outside or collected from a bottom reservoir for recirculation.

Fig. 2-11 Remote pad evaporative cooling system applied in greenhouse

Compared with DEC systems, indirect evaporative cooling (IEC) systems usually have lower effectiveness and higher initial cost. However, The IEC systems can provide cool supply air without moisture addition which improves the thermal comfort of conditioned spaces.

The IEC systems have two typical types, i.e. air-to-air heat exchanger and cooling tower/coil system. In terms of the IEC systems with air-to-air heat exchanger, a shown in Fig. 2-12 (E-Source 2009), the operation is in this way: Drawn by a supply fan, the outdoor air flows through the dry sides of heat exchanger. Meanwhile, another airflow (secondary air), possibly from outdoor air, drawn by a secondary fan, flows through the wet sides of exchanger. The outdoor air in dry sides is cooled sensibly and latently by the secondary air in the adjacent wet sides of exchanger and thereby is delivered to the conditioned space. Water pump is often used to lift the extra water in the bottom reservoir to the top distribution system for recirculation. Regarding to the configurations of air-to-air heat exchanger, four types can be found in the most cases: 1) plate and pleated media; 2) heat pipes; 3) rotary heat wheel; 4) shell and tube. The wet-bulb effectiveness of the IEC systems with air-to-air heat exchanger ranges from

40 to 80% depending on the configuration and primary/secondary air passing through the exchanger.

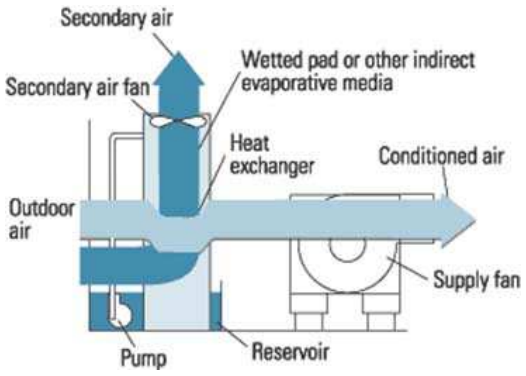

Fig. 2-12 Diagram of typical IEC with air-to-air heat exchanger

The cooling tower and coil system usually consist of a cooling tower, water-to-air heat exchanger coil and a water circulation pump. It works in this way: Chilled water is pump from the tank of cooling tower to the heat exchanger coil and returns to the top distribution system of tower for recirculation. In the cooling tower, the water is cooled toward the wet-bulb temperature of ambient after circulating for enough time and it flows through the coil to exchange the heat with the process air. The heat of process air is removed when it passes through the chilled water coil. As a result, the temperature of water increases and the process air is cooled without moisture addition. The water then returns to cooling tower where it is cooled again.

Also the IEC, DEC and refrigerated cooling system (direct expansion or chilled water coil) can be combined together to be used in applications where require lower supply air or in the regions with higher wet-bulb design temperatures. A diagram of two-stage IEC/DEC combination system with rotary wheel or heat pipe heat exchanger is shown in Fig. 2-13 (ASHRAE 1996). In which, the IEC system is located upstream of DEC system. As high as 110% wet-bulb effectiveness can be achieved for the typical combination systems, however, more initial cost, space occupation and system complexity may impede the wide applications. A diagram of two-stage combination system with a second stage of chilled water coil is shown in Fig. 2-14. In which, the outdoor air is pre-cooled by an IEC section and mixes with the return air before passing through a cooling coil. Also, the return air can be mixed together with the outdoor air before pre-cooling. Compared with the conventional refrigeration systems, the combination systems need less cooling capacity to provide the same thermal comfort feeling. With an indirect evaporative cooling section, the combination system

needs less initial cost than a refrigerated system with the same capacity. Fig. 2-15 shows a diagram of three-stage IEC/DEC/cooling coil combination system. The cooling coil section is activated when the wet-bulb of outdoor air is high or when the dehumidification is necessary.

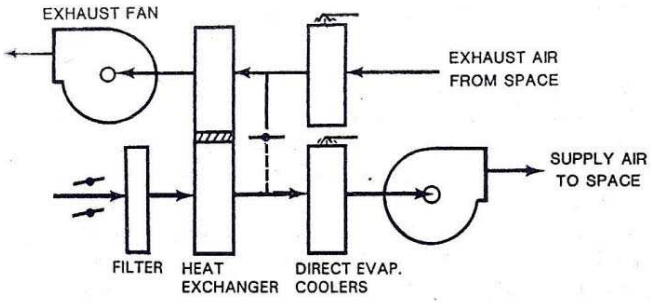

Fig. 2-13 Diagram of two-stage IEC/DEC combination system with heat exchanger (rotary wheel or heat pipe)

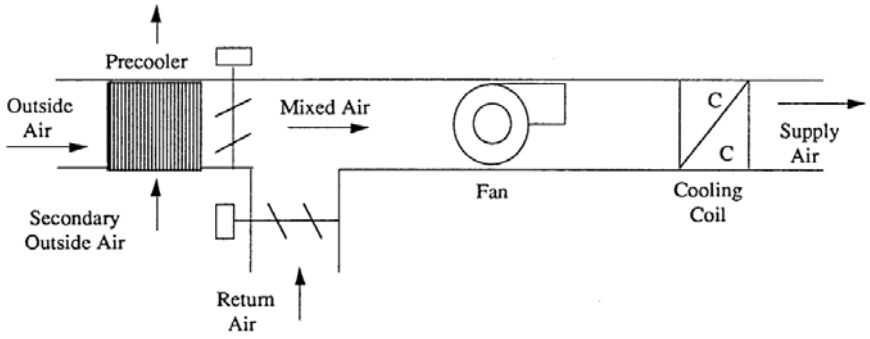

Fig. 2-14 Diagram of two-stage IEC/cooling coil combination system (IEC as pre-cooler)

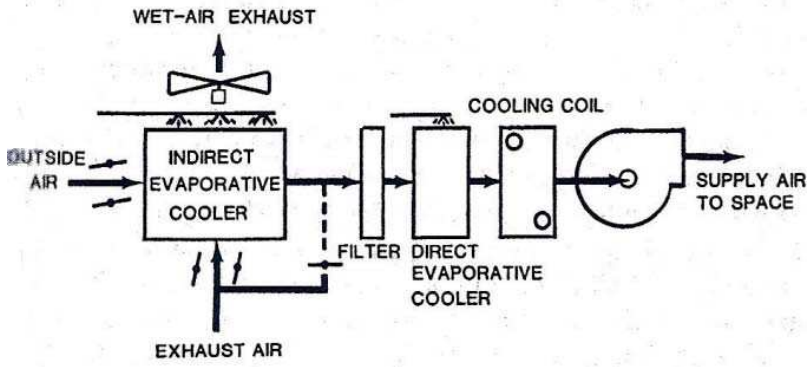

Fig. 2-15 Diagram of three-stage IEC/DEC/cooling coil combination system (IEC as pre-cooler)

2.5 Evaporative Medium Types

A wide range of material types can be used as a medium to evaporate water, i.e. metal, fibre, ceramics, zeolite and carbon. The properties of several selected evaporative medium types commonly used in evaporative cooling are summarised in Table 2-3 (Zhao et al. 2008).

The wet sides of heat and mass exchanger are usually formed by the wicking materials to enable water evaporation. The following properties of the wicking material (evaporative medium), such as wicking ability (capillary forces), thermal conductivity, hygroscopic and tensile strength should be considered in selecting the preferable wicking materials for the heat and mass exchanger: 1) A wicking material with high wicking ability enable a fast, thin and uniform wetting on the wet surface of the plate(Higgins and Reichmuth 2007); 2) A wicking material with high thermal conductivity allows a large amount of heat to be conducted from the dry side of the plate to the wet side; 3) The tensile strength of the wicking material should be well enough to process or shape into various geometries; 4) The coating compatibility of a wicking material with a hydrophobic material should be good enough to reduce the thermal contact resistance between them; 5) The wicking material should be inexpensive and be ease of cleaning and replacement.

Table 2-3 The properties of selected evaporative medium types

Material type	Index					
	Thermal conductivity (W/m K)	Porosity (%)	Hardness (shaping ability)	Compatibility with coating	Contamination risk	Cost (£) per sheet [36] 100 mm × 100 mm × 0.5 mm
Metal	High	20–90	High	Compatible with the solid metal	Low (sintered metal)	30–100
Fibre	Low	1–60	Low	Compatible to polyethylene	High	< 5
Ceramic	Variable	1–80	High	Compatible with the solid metal	High	150–250
Zeolite	Low	40–80	Medium	Compatible to polyethylene or wax	High	150–250
Carbon	Variable	Variable	Medium	Compatible to polyethylene or wax	High	30–80

The dry sides of heat/mass exchanger are usually formed by hydrophobic materials which prevent water penetrating from wet sides. Actually, the wicking and evaporation capacities of the materials will be improved after the hydrophobic material coated on the evaporative medium surface.

Several works related to the evaporative medium in use have been reviewed. A patent reports that the wicking materials, such as cellulous fibre or kraft paper, is often coated with hydrophobic synthetic resin, plastic or wax to form the heat exchanger plate (Gillan et al. 2010). For the case of Coolerado Cooler module based on the M-cycle, cellulose-blended fibre and polyethylene were used as the wicking and the hydrophobic coating materials as shown in Fig. 2-16. It is shown that this special cellulous material enables uniform and thin wetting on the wet side of heat exchanger without extra water and therefore focusing on the cooling of the process air. Because the wicking of cellulose material disrupts the surface tension of water and thereby causing a higher heat and mass transfer rate (Higgins and Reichmuth 2007). For the case of an indirect evaporative chiller, PVC padding and aluminium foil padding were used as the evaporative media in the direct evaporative cooler, as shown in Fig. 2-17. The research studied the mass transfer coefficient, pressure drop and costs of the two materials. It is found that the mass transfer coefficient of aluminium foil padding is two times greater than that of PVC padding and thereby has an obvious higher heat and mass transfer rate. However, aluminium foil padding has a shorter life time considering its relatively high cost, which impedes its wide applications (Jiang and Xie 2010).

As another typical evaporative media, the properties of porous ceramic (see Fig. 2-18) were investigated (Zhao et al. 2008). Porous ceramic tubes or pipes are the most favourite configurations for this type of material, which has several advantages, such as good construction facility, accessibility, and filtering property, i.e., water evaporates in the pores without carrying of water droplets, which acts as a filter to avoid the propagation of bacteria (Velasco Gómez et al. 2005).

A type of rigid evaporative media (See Fig. 2-19), originally manufactured by Munters Corp., have been widely used in direct evaporative coolers. The rigid media have many advantages over other materials, such as, high wet-bulb effectiveness, low pressure drop resulting in low operating costs, high wetting properties, low scaling, self-cleaning, long life time, etc. (Munters 2010; ASHRAE 1996). In the process of fabrication, the corrugated cellulose media, treated chemically with antiriot and rigidifying resins, have been stacked together in different flute angles (one sheet is 60 degree and the other is 30 degree), which are designed to maximise the mixture of air and water.

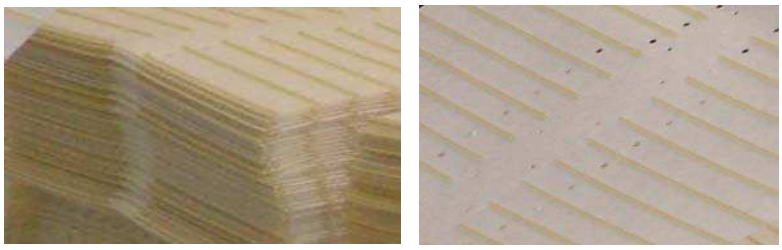

(a) Cellulous-blended fibre (b) The wicking surface of the fibre

Fig. 2-16 Cellulose-blended fibre wicking material used in the Coolerado Cooler heat and mass exchanger

(a) PVC padding (b) Aluminium foil padding

Fig. 2-17 The evaporative media used in an indirect evaporative chiller (a) PVC padding (b) aluminium foil padding

Fig. 2-18 Porous ceramic materials

(a) Corrugated cellulose paper sheets (b) Rigid evaporative media pad

Fig. 2-19 The rigid evaporative media used in DEC (a) corrugated cellulose paper sheets stacked together (b) rigid evaporative media pad

2.6 R&D Progress and Practical Application of the IEC Systems

2.6.1 Overview of the related R&D works

A great many research works have been carried out to study the heat and mass transfer process and performance of various types of flow patterns, optimise the geometries, suggest the preferable operating conditions and evaluate the cooling capacity, energy efficiency, energy saving and emissions reduction related to the IEC systems with plate heat exchanger. The important technical parameters, results and conclusions of the studied research works have been summarised as follows.

Maclaine-cross and Banks (1981) analysed the performance of a wet surface heat exchanger by establishing a one-dimensional mathematical model. The calculations for the model based on several assumptions, such as an average temperature and humidity ratio at the inlet and outlet of the heat exchanger and a complete surface wetting, etc. The results predicted by the model were 20 percent higher than the experimental data.

Stoitchkov and Dimitrov (1998) improved the wet surface cross-flow heat exchanger model originally developed by Maclaine-cross and Banks. the effectiveness predicted by their improved model had a better approximation by introducing with flowing water film, determination of mean water surface temperature and derivation of an equation for calculating the ratio of total to sensible heat taking into account the barometric pressure. The corrected model was validated with some published data. The errors between the results of test and model were found satisfactory.

Based on an earlier heat exchanger model (Pescod 1979), Alonso et al. (1998) developed a simplified heat and mass transfer model for calculating the primary air outlet temperature of a cross-flow indirect evaporative cooler. Alonso's model can be applied to simulate the primary air outlet temperature of the cross-flow indirect evaporative coolers with different geometries and operating conditions. In their study, an equivalent water temperature was introduced to include the energy transfer between primary and secondary air, which assumed the global process to an adiabatic saturation process. The model was verified and validated with other experimental data and Pescod and Erens 's models (Pescod 1979; Erens and Dreyer 1993). It is found that a good agreement was obtained between the experimental data and the model.

Compared with the Pescod's model, the results of Alonso's model were much closer to that of Erens's model.

Navon and Arkin (1994) conducted a feasibility study to evaluate the economic value and thermal comfort level of a wet coil DEC/IEC combined system compared with a conventional air conditioner (AC). A life cycle cost calculation method was exploited to compare the annual equivalent cost (AE) of a wet coil type DEC/IEC to that of an AC in two cities of Israel with extreme summer conditions. The maximum initial cost of the DEC/IEC system was estimated. The results show that the economic potential of the DEC/IEC is very promising considering the significant electricity cost cut compared to AC, although the rise in water consumption cost may undermine this advantage.

Lilly and Misemer (1996) et al. assessed the California market potential of using indirect/direct evaporative cooling and estimated the impacts of key deployment barriers. The assessment covers a wide range of evaluation factors including market potential, market barriers, technology potential and costs, energy savings potential for residential and commercial buildings and applicability factors, i.e., climate, humidity requirements, initial cost, etc.

Tulsidasani et al. (1997, Part 1) analysed and optimised the pressure drop, power consumption and COP of a tube type IEC in terms of the velocities of primary and secondary airs. The performance of the tube type IEC was studied theoretically and experimentally. It is found that the test results have a satisfactory agreement with the theoretical predictions. The reported maximum COP of the unit was 22 at the primary air velocity of 3.5 m/s and secondary air velocity of 3 m/s with the temperature drop of 10.4^{o}C. The study also suggests that the COP of the IEC increases with decreasing secondary air velocity without significantly affecting the cooling capacity of primary air.

Tulsidasani et al. (1997, Part 2) also studied the thermal performance of a non-conditioned building equipped with an IEC system. For the three different climatic conditions of India, i.e. hot, dry, warm, humid and combination, the research investigated the effects of various design parameters of the IEC on the discomfort standards. The analysis shows that the IEC system is effective in providing thermal comfort to buildings in dry, hot and combined climates.

Guo and Zhao (1998) investigated the thermal performance of a cross-flow heat exchanger by analysing the effects of various parameters, i.e. primary and secondary air velocities, channel width, inlet relative humidity and wettability of plate. A numerical method was used to solve differential equations. However, the accuracy of the numerical model was not validated with the experimental data or other models. Therefore, the model has no universality and only can be used as an approximate guidance for the direction of system or product design. Their study suggests that a smaller channel width, a lower inlet relative humidity of the secondary air, a higher wettability of plate, and a higher ratio of secondary to primary air can result in a higher effectiveness.

Brooks and Field (2003) invented a type of cross-flow indirect evaporative cooler. The cooler is made from extruded, twin-walled, corrugated, fluted plastic sheeting. The corrugated sheets were stacked vertically together to form the primary and secondary channels of the heat exchanger. The reasons for causing the poor cooling effectiveness were analysed which include the poor water distribution, poor air distribution across the inlet and the insufficient heat transfer surface area. To solve the poor water distribution problem, an evaporative mesh extending through and below the heat exchanger was suggested to use. It allows the water falls directly to the bottom area of the heat exchanges passages. The mesh also can be used as the pre-cooling of the secondary air to increase cooling effectiveness of the system. The study also suggests that heat transfer and surface area can be increased by roughening the surface of sheets.

Wang et al. (2005) studied the water absorbing fibre materials wrapped on an indirect evaporative cooler in the ellipse tube configuration theoretically and experimentally. It is found that only using one type of fibre material cannot achieve the desirable evaporative cooling. multi-function can be achieved by taking advantage of compound fibres. On one hand, the abnormity terylene fibre acts as the hygroscopic material with fast wetting and dry ability to enhance water evaporation. On the other hand, the Lanseal fibre can tighten the external tube surface with the hygroscopic material to reduce the thermal contact resistance between them. The above two types of fibres can be blended into a rhombic structure to enhance the evaporative cooling. An experiment was conducted to compare within cotton, polyurethane and compound blended fibres in terms of heat transfer efficiency. It is found that the compound blended fibres material had the highest heat transfer efficiency over the others.

Ren and Yang (2006) developed an analytical model of the heat and mass transfer processes in parallel/counter-current indirect evaporative cooling under real operating conditions. In their study, an analytical approach was developed by combining the simplicity of solution and the accuracy of detailed models. Many parameters originally assumed constant in other models were considered to be various in their study, i.e. Lewis factor, surface wetting condition, effects of spray water evaporation, spray water flow rate, spray water temperature and spray water enthalpy. The results of analytical solutions were compared with those of numerical results and a good agreement was found as a result. The performances of the four types of flow configurations in plate heat exchanger were also analysed. It is found that the counter current configuration, i.e., the primary air flows counter current both to the secondary air and water film, had the best performance of all. The configuration of primary air flowing counter current to the secondary air but parallel to the water film had the better performance than the configuration of the primary air flowing parallel to the secondary air. It also suggests that decreasing spray water mass flow rate improves the performance of indirect evaporative cooler.

The performance of a cross-flow dew point indirect evaporative cooling unit based on the M-cycle was tested in laboratory (Elberling 2006). The effects of inlet air dry/wet bulb temperatures, outlet backpressure, fan speed, airflow rate on the performance of cooling unit including effectiveness, cooling capacity, power consumption, cooling capacity, energy efficiency and water evaporate rate were investigated experimentally. However, no information can be found addressing to the materials and geometries of heat exchanger in the study. The test results show that the wet-bulb effectiveness of the unit varied from 81% to 91% over all test conditions, which is nearly 20-30% higher than that of the typical IEC systems. For all test conditions, the unit can provide a supply air at 18.9-25.6^{o}C bulb-dry temperature with 30-80% relative humidity. The cooling capacity of the unit was from 9-12 kW. The average energy efficiency (or COP) of the unit was over 8.8. At the cost of increasing effectiveness, the power consumption of the unit was 40-80% greater than that of other evaluated evaporative coolers. However, the initial cost of the unit was $2900 approximately, which is much expensive than the typical IEC systems.

Qiu (2007) studied the practical performances of an IEC module product. The study indicates that real performance of a IEC module is much lower than that of the values given by the product specifications. The study found that the reason for the poor

performance of the cooler lied in the poor water distribution. It is noticed that only 1/2-2/3 of surfaces were wet when the module operated. To solve the problem, Qiu added a top water spraying device and integrated a solar-powered PV panel to supply the energy for fans and water pump in the module. It is shown that the cooling capacity and COP of the retrofitted IEC module were 3 times larger than that of the original module (the cooling capacity was 453 W and the COP was 12.2 at a primary air flow rate of 270 m^3/h and intake air condition of 35.6^oC and 38.7% RH). The primary air temperature drop from the inlet to outlet was in the range of 3-8^oC for all test conditions.

Hettiarachchi et al. (2007) investigated the effect of longitudinal heat conduction on the thermal performance of cross-flow compact plate evaporative coolers. Heat and mass transfer characteristics of the module were analysed by a NTU method. The numerical methods were used to solve equations and the results of numerical modelling were validated with other published data. The research found that the thermal performance deterioration of evaporative coolers due to the longitudinal heat conduction could be as high as 10% at some operating conditions. This effect could become significant at some design and operating conditions such as large NTU, conduction factor values (the effect of the two-dimensional longitudinal heat conduction on the deterioration of heat exchanger performance), low wet-bulb temperatures and certain primary to secondary air ratio. For the typical range of operating parameters, such as NTU < 6 and 1 < primary to secondary air ratio <3, the deterioration of performance was lower than 5%.

Zhao et al. (2008) investigated several types of evaporative media potentially used in forming the heat/mass exchanger of IEC systems, i.e. metals, fibres, ceramics, zeolite and carbon, in terms of their physical and thermal properties. The most appropriate materials and structures were identified by comparison. By analysing the heat and mass transfer principle of IEC, the study indicates that the thermal conductivity and water-retaining capacity (porosity) of materials play less important parts in selecting materials. In contrast, the shape formation/holding ability, durability, compatibility with water-proof coating, contamination risk as well as cost of materials play more important parts. The study analysed each material type in terms of the above criteria. For each type, the preferable structures were indicated as well. By comparison, it is found that the wick (sintered, meshes, groves and whiskers) attained metals (cooper or aluminium) are the most suitable material of forming the heat exchanger. Wick

attained aluminium sheet is more suitable for the applications of air conditioning than the wick attained cooper sheet for the reason of cheaper cost.

Zhao et al. (2008) also studied a new counter-flow indirect evaporative heat exchanger numerically. A simulation was conducted in terms of the geometries and operating conditions to enhance the performance of the exchanger. The simulation predicted that the wet-bulb effectiveness of the new exchanger could be as high as 130% under the UK's summer outdoor air design condition of 28^{o}C dry-bulb temperature and 20^{o}C wet-bulb temperature. The results of simulation indicated that the channel size, air velocity and working to intake air ratio have more important effects on the cooling effectiveness and energy efficiency of the heat exchanger than the feed water temperature. Several parameters were suggested to direct the optimal design of the heat exchanger: 1) the channel spacing should be less than 6 mm; 2) the length of the channel should be longer than 1m or 200 time of the channel spacing; 3) the working to intake air ratio should be set to 0.4; 4) the intake air velocity should be set to 0.3-0.5 m/s.

A two-stage IEC/DEC system was investigated experimentally in various climatic conditions of Iran (Heidarinejad et al. 2009). The effects of various outdoor climatic conditions on the cooling efficiency of the system were investigated. The IEC/DEC system composes of a plastic wet surface heat exchanger and a 15 cm thick cellulose pad. The size of the IEC system is 500×500×400 mm and the channel spacing of heat exchanger is 7 mm. The primary and secondary air flow rate of the system was adjusted to 1700 and 850 m^3/h respectively to conduct testing. The results show that under various climatic conditions (inlet dry/wet-bulb temperature: 27-49^{o}C/15-33^{o}C), the wet-bulb effectiveness of the system was in a range of 108–111% higher than the single IEC system (55 and 61%). The average water consumption of the system was 55% more than the single direct evaporative cooling system. It is found that the energy efficiency (or COP) of the system was in a range of 8–9. Compared with typical mechanical vapour compression cooling systems (COP≈3), more than 60% of energy savings can be achieved by this combined system.

Jiang and Xie (2010) developed a novel indirect evaporative chiller which can provide the HVAC systems used in buildings with the chilled water at the temperature below wet-bulb temperature and closing to the dew point of the outdoor air. The indirect evaporative chiller composes of two major components, i.e. the air-to-water counter-

current heat exchanger and the air-to-water counter-current padding tower, which were designed by approximate calculations. Simulations were carried out to analyse the performance of the chiller, which include output water temperature, cooling efficiency, and Coefficient of Performance (COP). The first prototype of the chiller was built to supply cooling for a building in the west part of China for 5 years. The long-term test results show that the output water temperature provided by the prototype chiller was around 14–20^{o}C, which was below the wet-bulb temperature and above the dew point of outdoor air. The COP of the prototype chiller was about 9. More than 40% of energy can be saved if replacing conventional air conditioning systems (COP≈2-3) with this type of chiller.

2.6.2 Practical Applications

Coolerado Cooler™, manufactured by Idalex, is based on the M-cycle indirect evaporative heat and mass exchanger (HMX). A series of Coolerado Cooler products including pre-cooling, stand-alone and hybrid applications have been developed by the company. A laboratory test was conduct on a stand-alone early-2005 model Coolerado cooler (see Fig. 2-20) to investigate the real performance of the cooler (Elberling 2006). The test results show that the unit can provide 9-12 kW cooling capacity at the wet-bulb effectiveness ranged from 81% to 91% (averaging 86%) with average energy efficiency (COP) over 8.8 for all the test conditions.

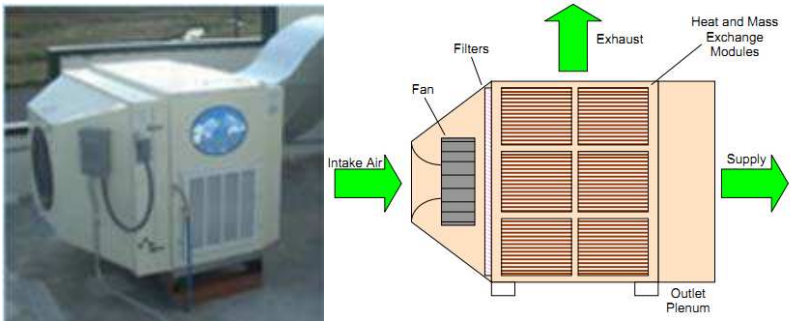

(a) Stand-alone Coolerado Cooler (b) Working diagram of the cooler

Fig. 2-20 The stand-alone Coolerado Cooler system (a)photograph of the system; (b) diagram of the system

A Coolerado hybrid system combines an indirect evaporative cooler with a refrigeration direct expansion (DX) system, as shown in Fig. 2-21, The performance of the hybrid system were investigated experimentally in a laboratory (Kozuba and Slayzak 2009). The system operates in this way: The outdoor air mixes with the return air of the system before entering into the indirect evaporative section. a 54-57% of the

entering mix air is cooled by the evaporative section and then passes through an evaporator coil to be delivered by a fan. Other part of the entering air, as the secondary air, was cooled and humidified in the indirect evaporative module and then passes through the condenser coil of DX system. The secondary air gains some heat from the fluid in condenser and exhausts to outside. The results of test show that the total cooling capacity of the unit was 16.8 kW (sensible cooling 13.4 kW) with a total COP of 15.2 (sensible COP 12.1) at the outdoor air condition of 32.2^{o}C dry-bulb and 17.7^{o}C wet-bulb temperature. The water consumption of the hybrid unit was 9.27 litre/ton h (sensible) with a water evaporation of 7.42 litre/ton·h (sensible).

Desert Aire Corporation designed and manufactured a type of Desert CoolAire ^{TM} hybrid air conditioning package unit (see Fig. 2-22) which combines the Coolerado M-cycle indirect evaporative heat exchanger module with vapour compression cooling and gas heating to produce a 17.6 kW cooling capacity. The unit has the capacity of 50% energy savings during the summer peak (Higgins and Reichmuth 2007). The laboratory and field research testing were carried out to investigate the performance of both indirect evaporative module and the overall package unit. The laboratory testing shows that the evaporative module can produce a supply air at dry bulb temperature of 18.3-22.2^{o}C. The wet-bulb effectiveness of the evaporative module was in the range of 78-98% with an average of 82% for all test conditions. Under the extreme outside air condition (38.3^{o}C dry-bulb and 32% relative humidity), the cooling capacity of the evaporative module was 19 kW with a COP of 9.7 while the total cooling capacity of the package unit was 27 kW with a COP at 3.8. The field research shows that the prototype unit (average COP =3.6) can achieve 23% of energy savings compared to a conventional direct expansion (DX) compressor system with a daily average COP of 2.8. It is also found that the cooling load of conditioned-space can be satisfied without the assistance of compression section during moderate cooling seasons. During the hot seasons, 20% of cooling capacity can be increased with the assistance of compression cooling.

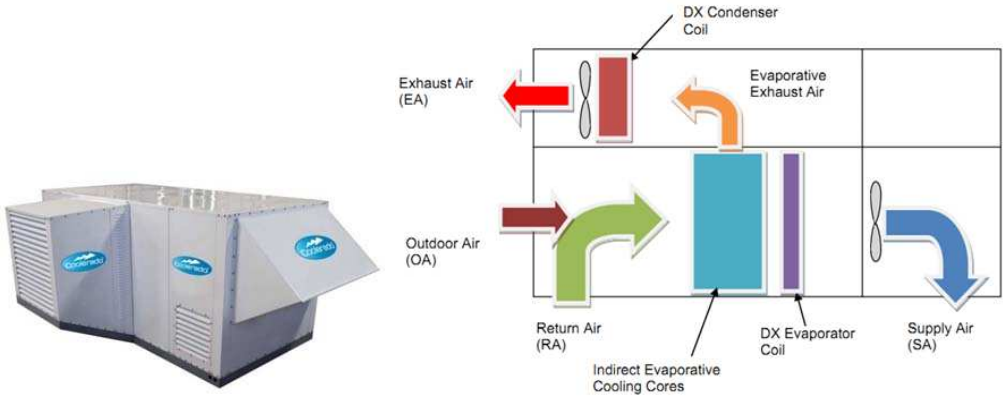

(a) Hybrid Coolerado Cooler (b) Working diagram of the system

Fig. 2-21 The hybrid Coolerado Cooler system (a)photography of the system; (b) diagram of the system

AMAX Indirect/Direct Evaporative Cooler (see Fig. 2-23), manufactured by AMAX company, mainly consists of an indirect cooling coil, a direct evaporative cooling media, a drop stop media, a primary fan and a secondary fan. As shown in Figure 2-23 (b) and (c), the cooler operates in this way: Chilled water was treated by an integrated 'cooling tower' toward to the wet-bulb temperature of ambient air. The water is pumped through the indirect coil to pre-cool fresh outdoor air. The pre-cooled air then passes through direct evaporative media and is delivered to the conditioned space at a temperature below the ambient wet-bulb. Through evaporative cooling, the heat of outdoor air can be transferred to exhaust air by a constant water circulation.

(a) Desert Cool Aire indirect evaporative hybrid package unit

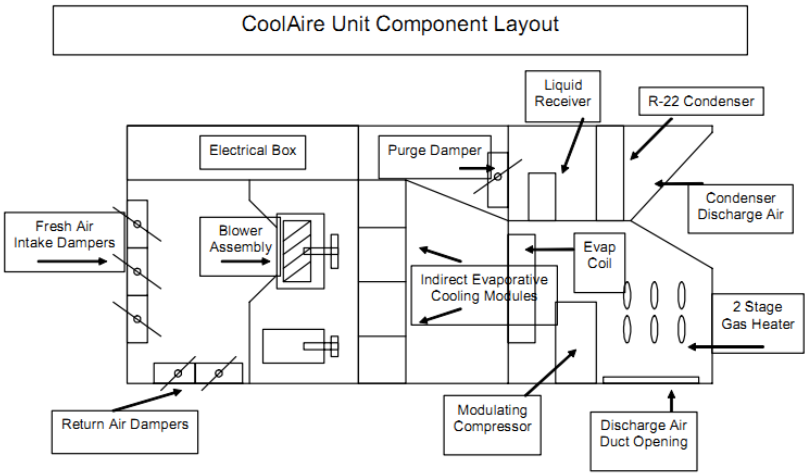

(b) Working diagram of the unit

Fig. 2-22 Desert Cool Aire indirect evaporative hybrid package unit (a) Photograph of unit; (b) Diagram of the unit

(a) AMAX Indirect/Direct Evaporative Cooler

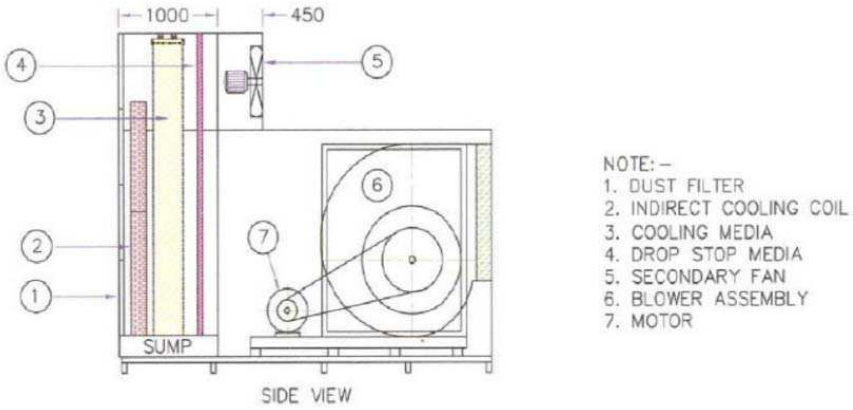

(b) Components of the cooler

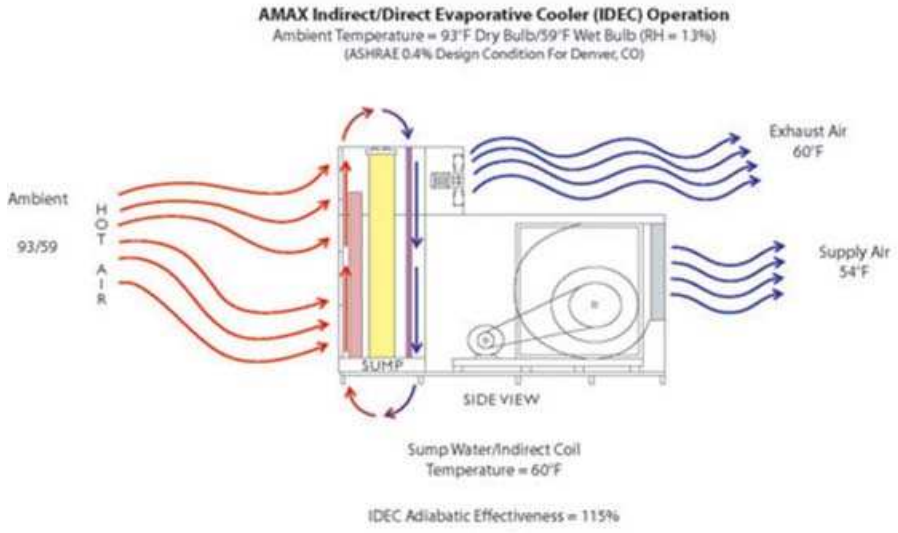

(c) Working diagram of the cooler operation

Fig. 2-23 AMAX indirect/direct evaporative cooler (a) Photography of the cooler; (b) Components of the cooler; (c) diagram of the cooler operation

Also, this cooler can be combined with integrated chilled water coils or a compressor circuit to achieve additional cooling. According to the specifications produced by the AMAX company, their cooling modules can be sized to provide supply air from 8500 to 85000 m^3/h flow rate with as high as 115% of effectiveness and 11.7 of COP.

2.6.3 Analyses of the review works

The type of IEC systems with plate heat exchanger has been developed for many years and has been used in the residential and commercial applications in many places across the world, especially where the climate is dry and hot. This type of systems usually comprises of 1) air-to-air plate heat and mass exchanger; 2) water sprayer; 3) circulation pump with associated controllers; 4) reservoir for collecting unevaporated water; 5) fans with associated controllers; 6) air filters, louvers and enclosure.

To attain a clear understanding of the technical progressing routes, problems/barriers and main concerns of the research works in this subject, the above review works are further analysed from two angles: 1) research focuses; 2) research methodology.

Analysis of the review works in terms of research focuses

So far, the research works related to the IEC systems with plate heat exchanger have been focus on: i) studying the heat and mass transfer process of different flow patterns of heat exchanger by theoretical analysis and simulation, i.e., cross-flow, parallel-flow and counter-flow patterns (Maclainecross and Banks 1981; Erens and Dreyer 1993; Alonso et al. 1998; Stoitchkov and Dimitrov 1998; Ren and Yang 2006); ii) optimising the performance of the system in terms of selecting the appropriate evaporative material, designing the geometric size and operating conditions of the exchanger by theoretical analysis and simulation (Tulsidasani et al. 1997; Guo and Zhao 1998); iv) evaluating the performance of the IEC related systems and the feasibility of providing cooling for buildings in various climate conditions by stimulating/testing the supply air dry and wet-bulb temperature, effectiveness, energy efficiency, energy and water consumptions of the system at various operating parameters, i.e., inlet air dry and wet-bulb temperature, primary/secondary airflow rate and water temperature (Elberling 2006; Higgins and Reichmuth 2007; Heidarinejad et al. 2009; Kulkarni and Rajput 2011).

In overall, the typical IEC systems can achieve a wet-bulb effectiveness of 40-80% depending on the configurations and the air speed passing the heat exchanger. An IEC performance chart showing the relationship of wet-bulb effectiveness and pressure drop with face velocity and secondary to primary air ratio (V/P = Vaporizer air per primary air, or secondary to primary air ratio) is shown in Fig. 2-24 (Palmer et al. 2002). It is found that the effectiveness of IEC decreases with increasing face velocity and reducing secondary to primary air ratio whereas the pressure drop increases with increasing face velocity.

The theoretical wet-bulb effectiveness of IEC systems is largely dependent on the following design parameters of the heat exchanger: 1) the geometric size; 2) the operating conditions, i.e., the inlet air dry/wet-bulb temperature, primary air velocity, secondary air velocity, secondary to primary air ratio (Guo and Zhao 1998). However, the practical performance of IEC systems is largely determined by the following factors, which are difficult to achieve in real applications: 1) the uniformity of water film distribution over wet surfaces of heat exchanger; 2) the uniformity of air distribution at the inlet of heat exchanger (Brooks and Field 2003).

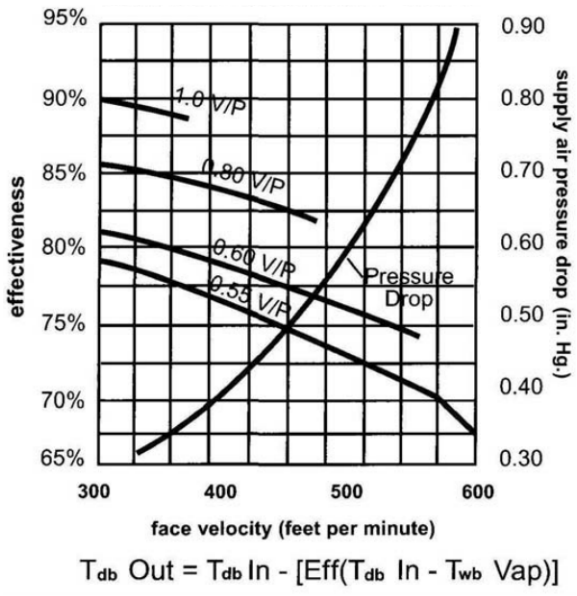

Fig. 2-24 Performance chart of IEC

The major problems surrounding the IEC systems with plate heat exchanger configurations lie in the relatively low performance and high initial and operating costs compared to DEC systems. The low performance is caused by the following reasons: i) the structures of the existing exchangers are not the most favourite as the temperature of secondary air of the exchanger is not low enough to remove more heat from the primary air; ii) the evaporative materials of forming the heat exchanger have poor wicking ability which results in an uneven water film distribution over the wet surfaces; iii) the water distribution sprayers or structures of the exchanger are too inefficient to distribute the water uniformly and entirely over the wet surface; iv) most of the installed air fans cannot supply an uniform inlet air distribution. It makes the exchanger operate in a low efficiency as some channels are under-loaded and some are over-loaded.

So far, the most preferable configuration for the air-to-air heat exchanger module has been the cross-flow flute heat exchanger stacked together with rectangular sheets, as shown in Fig. 2-6. This type of structure improves the performance of many types of IEC systems, and thus, enables the systems to use for cooling of buildings, due to the lowered supply (product) air temperature. However, work done on this type of exchanger is very beginning. Currently, there is only one exchanger configuration available on market. This configuration can only achieve a dew point effectiveness of 55% to 85%, which is still too low to produce cooled supply air for building air conditioning.

Analysis of the review works in terms of research methodology

The research methodology of the review works can be divided into: 1) theoretical analyses and computer simulation; 2) experimental and testing study; 3) combined simulation and experimental study; 4) economic, environmental analyses and feasibility study.

Theoretical analyses and computer simulation

Many theoretical works have been undertaken to investigate the heat and mass transfer process and mechanism of IEC heat exchanger model. These works were dedicated to 1) analyse and establish the theoretical heat and mass transfer model for the exchanger; 2) optimise the structural/geometrical parameters of the heat exchanger model including channel spacing and length; 3) suggest the favourite operational conditions, e.g. airflow rates, secondary to primary air ratio, inlet air temperature and humidity.

Those theoretical works cover 1) an one-dimensional simple mathematical model to predict the performance of a cross-flow plate heat exchanger by assuming the stationary water film and constant water temperature (Maclainecross and Banks 1981; Erens and Dreyer 1993; Zhan et al. 2011); 2) an one-dimensional mathematical model to predict the performance of cross-flow plate exchanger by taking into account the effects of flowing water film, water temperature variation and wettability (Erens and Dreyer 1993; Halasz 1998; Stoitchkov and Dimitrov 1998); 3) an analytical model addressing the heat and mass transfer processes of IEC in cross/parallel/counter flow patterns assuming a varied Lewis factor, water temperature and surface wettability (Ren and Yang 2006); 4) an one-dimensional differential model to study the effects of a wide variety of parameters such as primary and secondary air velocities, channel width, inlet relative humidity, and surface wettability on the thermal performance of exchanger (Guo and Zhao 1998).

In summary, so far the theoretical and simulation works conducted on the cross-flow exchangers have been sufficient and mature enough. However, few theoretical work has been conducted on the numerical and parametric analyses of fluid flow and heat/mass transfer within the counter-flow exchangers. The structure design and geometrical optimization of the counter-flow exchangers also have not carried out yet.

Experimental and combined simulation/experimental study

Experimental study including laboratory tests and field long-term tests have been undertaken to measure various operational parameters, e.g. inlet/outlet air temperature, humidity, air velocity, pressure drop, power/water consumption, which aims to 1) reveal the real performance of the IEC systems under the specified operating conditions; 2) validate the reliability and accuracy of the developed theoretical model and thereby provide test data for further correction to the model; 3) create the relationship between theoretical analysis and practical applications and find out the hidden factors that could affect the accuracy of numerical results.

The previous experimental and combined simulation/experimental studies cover 1) the effects of operating parameters, such as air velocity, secondary to primary air ratio, inlet air dry/wet-bulb temperature, on the effectiveness and energy efficiency of the IEC or combined system (Elberling 2006; Heidarinejad et al. 2009; Delfani et al. 2010; Riangvilaikul and Kumar 2010; Kulkarni and Rajput 2011); 2) the energy saving potential of IEC or combined system under the specified climate conditions by analysing the laboratory test results or long-term field test results (Maheshwari et al. 2001; Delfani et al. 2010; Jaber 2011); 3) the comparisons between the numerical and experimental results of the IEC cross-flow plate exchanger and the related uncertainty and disagreement analyses (Alonso et al. 1998; Stoitchkov and Dimitrov 1998).

To sum up, some experimental and combined simulation/experimental studies have been done but no work has been conducted to achieve all above aims. The further work may lie in the measurements of the effects of various operating parameters on static and dynamic performance of an IEC system under various climate conditions and thereby compare and validate the results of computer simulation with experiment data.

Economic/environmental analyses and feasibility study

Several research works have been done on economic, environmental analyses and feasibility study of the IEC/combined systems by comparing their performance against conventional vapour compression systems. Electric energy and water consumptions are the main concerns of economic issue. Economic comparison, such as payback period and life cycle cost, were used to study the energy saving, operating cost saving

and capital cost increase of the IEC systems. In terms of environmental issue, no works have been found addressing to evaluate the capacity of carbon emission cut of the IEC systems. In terms of feasibility study, works were done addressing to access the capability of the IEC systems to replace the conventional refrigeration systems by studying the performance of the IEC systems under various climate conditions, the capability of providing the level of thermal comfort, the accessibility of water source and the economic cost of the systems.

Works related to economic, environmental analyses and feasibility study cover: 1) the energy saving potential and economic comparison by calculating payback period and life cycle cost of the IEC systems (Anderson 1986; Watt 1988; Navon and Arkin 1993; Maheshwari et al. 2001); 2) an annual equivalent cost (AE) approach were used to take into account the annual capital costs for acquisition and installation, operating costs, and the maintenance costs of a IEC system (Ruegg and Marshall 1990); 3) the feasibility studies of examining thermal performance, thermal comfort level and economic features (as above mentioned) of the IEC/combined systems in residential buildings with arid climates using the static or dynamic calculations methods (Navon and Arkin 1994 ; Steeman et al. 2009); 4) a market potential and barriers evaluation addressing the economic and non-economic factors including technology potential and costs, energy savings potential and climate conditions, i.e., climate, humidity requirements (Lilly and Misemer 1996).

In summary, the previous studies indicate the economic superiority of the IEC or combined systems applied in dry climate conditions. The further work may lie in evaluating the energy saving potential, payback period and life cycle cost by studying dynamic performance of the IEC related systems over a long term of running under various climate conditions taking into account the various parameters, e.g. supply air temperature, humidity and flow rate, water and energy consumptions.

2.6.4 Conclusive remarks of the review works

To summarise, the previous research works in the IEC technology focus on: 1) revealing the nature of heat and mass transfer process and mechanism occurring in the heat exchanger modules of IEC and the module-based systems; 2) establishing simple or complicated theoretical and computer model of the heat exchanger modules with different flow patterns by dealing with the approximations/assumptions differently; 3)

optimising the structural/geometrical parameters of the IEC systems and suggesting the appropriate operational conditions; 4) evaluating the performance of IEC related systems under various climate conditions; 5) creating the correlations between the theoretical analyses and practical applications; 6) assessing the economic, environmental benefits and feasibility of the IEC related systems as compared to prevailing air conditioning systems. All these efforts intended to create an energy and cost-efficient IEC system with simple structure.

2.7 Opportunities for the PhD works

2.7.1 Optimising materials/structure/geometries of new dew point heat exchanger

The existing dew point heat exchanger structure improves the performance of many types of IEC systems, and thus, enables the systems to be used for the cooling of buildings, due to the lower supply (product) air temperature (Idalex Technologies 2003). However, work done on this type of exchanger is very beginning. Currently, there is only one exchanger configuration available on market, as shown in Fig. 2-6. This configuration can only achieve a wet-bulb effectiveness of 81% to 91%, which is still too low to produce sufficiently cooled supply air for the conditioned spaces of buildings. No work was done on the numerical analyses of fluid flow and heat/mass transfer within this or similar types of exchanger. And the materials selection, structure design and geometrical optimization on the this type of exchangers were not being carried out yet. This opens up a way to optimise the performance of IEC heat exchanger by designing a new structure of counter-flow exchanger, selecting the appropriate materials of constructing the exchanger and designing the geometrical parameters using the numerical results.

2.7.2 Studying the real performance of new heat exchanger under various climates

Current research works on the parametric studies or real performance of the IEC related systems are very limited. To validate the accuracy of the numerical model established for the new exchanger as well as to create the correlation of theoretical analyses and practical application, an experimental prototype of the new IEC system will be constructed in laboratory based on the optimising structural/geometrical

parameters of the new heat exchanger. The real performance of the prototype under various climate conditions will be tested by stimulating various inlet air conditions. The real effects of operating parameters on the performance of new IEC system will be studied by comparing the experimental data with numerical results.

2.7.3 Economic and environmental and regional acceptance analyses

Previous works on economic and feasibility studies of IEC related systems are clear enough to provide a clue for evaluating the new IEC system. However, studies on the environmental benefits of IEC systems have not been found yet. For Europe and China where the IEC systems have a great potential to be used, the works on the economic and feasibility studies are very limited. For the new IEC system proposed in this PhD work, the overall economic, environmental analyses for the regions of Europe and China will be studied by taking into account the construction and operating costs, life-cycle costs, payback period, energy savings, carbon dioxide emission cut, etc. The regional acceptance/feasibility of the new IEC system to be used in the buildings of Europe and China will be evaluated based on the investigations of weather data, availability of water source and temperature, calculations of water consumption, cooling capacity and airflow rate over the summer cooling period.

2.8 Conclusions

This review studied the background, principle, fundamental knowledge, terminologies, system types, previous research and practical works of the evaporative cooling. By analysing the previous works, the opportunities for this PhD works have been sorted out. Firstly, the work principles of typical evaporative cooling system types, i.e., direct evaporative cooling (DEC), indirect evaporative cooling (IEC), combination and dew point evaporative cooling based on the M-cycle have been illustrated. Secondly, the parameters (including wet-bulb/dew-point effectiveness, secondary to primary air ratio, cooling capacity, energy efficiency and water evaporative rate) for evaluating the performance of indirect evaporative cooling systems have been indicated and the related calculation formulas have been presented. Thirdly, the performances and characteristics of various typical evaporative cooling system types and configurations have been studied. Fourthly, the review also discusses the properties of evaporative materials which are mostly concerned in selecting the preferable materials of forming the evaporative cooling heat/mass exchanger. Several cases of evaporative materials

used in practical applications have been studied. Finally, an analysis into the previous R&D works and practical applications of the IEC related systems has been carried out. The results of the review work contribute to understand the current status of the IEC technical development, to identify the remaining technical difficulties/barriers, and to propose the opportunities for further development in terms of materials, structures/configurations, design, performance and potential applicability of the IEC systems.

The previous research works in IEC technology focus on : 1) revealing the nature of heat and mass transfer process and mechanism occurring in the heat exchanger modules of IEC or modules-based systems; 2) establishing approximate/accurate theoretical and computer model of the heat exchanger modules with different flow patterns by dealing with the assumptions differently; 3) optimising the structural/geometrical parameters of the IEC systems and suggesting the appropriate operational conditions; 4) evaluating the performance of the IEC related systems under various climate conditions; 5) creating the correlation between the theoretical analyses and practical applications; 6) assessing the economic, environmental benefits and feasibility of the IEC related systems as compared to prevailing air conditioning systems. All these efforts were endeavoured to create an energy and cost-efficient IEC system with simple structure.

DEC systems add moisture to the air supplied to rooms. It is only suitable for use in dry and hot climate, or the rooms needing both cooling and humidification. The wet-bulb effectiveness of the current DEC systems ranges from 70% to 95% depending on the configurations and air velocity passing the medium. IEC systems, however, are able to lower the air temperature and avoid adding moisture to the air. This feature makes IEC systems more attractive than direct systems. The wet-bulb effectiveness of current typical IEC systems ranges between 55% and 75%.

The existing dew point heat exchanger based on the M-cycle improves the performance of many types of IEC systems, and thus, enables the systems to be used for the cooling of buildings due to a lower supply (product) air temperature. However, works done on this type of exchanger is very beginning. Currently, there is only one exchanger configuration available on market. This configuration can only achieve a wet-bulb effectiveness of 81% to 91%, which is still too low to produce adequate cool supply air for the conditioned spaces of buildings.

This opens up opportunities for this PhD work to develop a new counter-flow IEC heat/mass exchanger which can provide a lower supply air toward to the dew point of inlet air temperature. The opportunities cover i) designing and optimising a new structure/geometries of counter-flow IEC heat/mass exchanger by theoretical analysis and computer simulation; ii) selecting appropriate materials of constructing the heat exchanger; iii) constructing and testing the real performance of the new dew point cooler prototype under various operating conditions and further comparing the numerical results with experimental data; iv) conducting an economic, environmental and regional acceptance/feasibility analysis for the dew point cooler to be used in the buildings of Europe and China.

Chapter3.
Theoretical Analyses and Computer Simulation

3.1 Physical model of the heat/mass exchanger

The grids of counter-current heat and mass exchanger for simulation were designed to the corrugations with equilateral triangular flow channels, as shown in Fig. 3-1. The air velocity and temperature distribution over the cross section of flow channels were assumed uniform. Therefore, a two-dimensional physical model was formed for the counter-current heat and mass exchanger, as illustrated in Fig. 3-2. The model consists of a layer of dry and wet channel with channel walls in between. The primary air (the sum of product and working air) of dry channel is cooled through exchanging sensible and latent heat (Q_s and Q_l) with the working air in the adjacent wet channel.

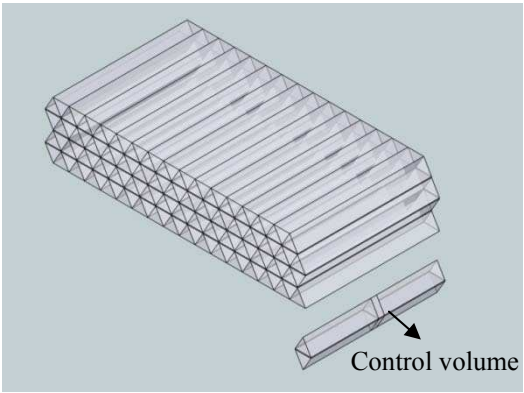

Fig. 3-1 Flow channels for simulation with equilateral triangle cross section

To simplify the modelling process and mathematical analysis, the following assumptions were made:

i. The heat and mass transfer process is considered as steady state. The exchanger enclosure is considered as the system boundary.
ii. The heat and mass transfer process is adiabatic. No heat transfer to the surroundings;
iii. Heat is transferred vertically through the channel walls. No heat and mass transfer in the airflow (x) direction. Within the air streams, the convective

heat transfer is considered the dominant mechanism for heat transfer. The channel walls are impervious to mass transfer;

iv. Water film on the wet surface is assumed static. The temperature of spraying water is constant. Water-to-air interface temperature is assumed identical with the water-in temperature;

v. The wet surface of the heat transfer sheet is completely saturated. The water film is distributed uniformly across the wet channel.

vi. Each control volume has a uniform wall surface temperature. An analysis (Zhao 2008) indicates that the thermal conductivity of the heat transfer sheet has a little effect on the magnitude of the heat and mass transfer rates owing to its tiny thickness (0.24 mm). The temperature difference between dry and wet sides of the wall can therefore be ignored.

vii. Air is treated as an incompressible gas. The velocity and properties of all air streams are considered to be uniform in a differential control volume.

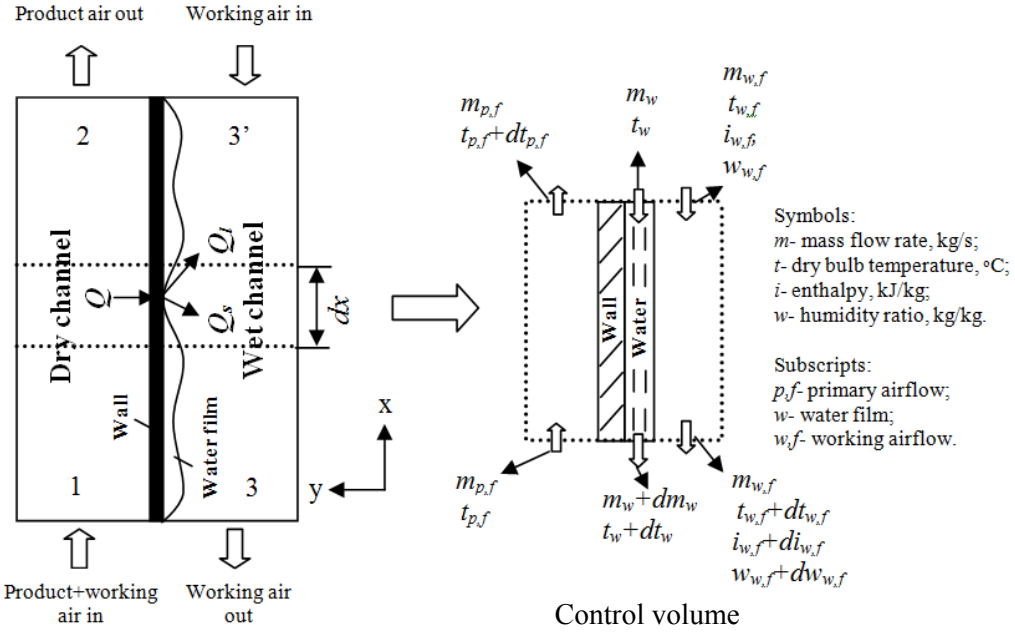

Fig. 3-2 Physical model of counter-current heat and mass exchanger

3.2 Mass and energy conservation

A set of differential equations were established for a control volume (see Fig. 3-2) using the energy and mass conservation laws:

The energy balance equation for the working air and water film of wet channel:

$$m_{w,f}di_{w,f} = \left[h_{w,f}\left(t_w - t_{w,f}\right) + i_v h_m\left(\rho_{w,s} - \rho_{w,f}\right)\sigma\right]\mathrm{A_w}\frac{dx}{\mathrm{l_w}} \quad (3\text{-}1)$$

where the specific enthalpy of water vapour at a water film temperature is

$$i_v = c_{p,v}t_w + i_0 \quad (3\text{-}2)$$

where i_0 represents the latent heat of water at the reference temperature, i.e., 0^oC.

The air in dry/wet channel can be treated as laminar flow (Re < 1930) due to the small size of channels and low air velocity. For the laminar flow forced convection condition at constant surface temperature in narrow channels, the following empirical correlation can be used to determine the thermal inlet undeveloped region (l_0) (P, Incropera et al. 2007):

$$\frac{l_0}{\mathrm{D_H}} = 0.05\mathrm{RePr} \quad (3\text{-}3)$$

where the Reynolds number is defined as:

$$\mathrm{Re} = \frac{u_f \mathrm{D_H}}{\nu_f} \quad (3\text{-}4)$$

where $\mathrm{D_H}$ is the hydraulic diameter of flow channel which is defined as:

$$\mathrm{D_H} = \frac{4\mathrm{A_{cross}}}{\mathrm{P}} \quad (3\text{-}5)$$

The Nusselt number of air can be classified into two regions, i.e., the entrance undeveloped region ($l \le l_0$) and the following fully developed region ($l_0 \le l \le l$).

For the entrance region ($l \le l_0$), the Nusselt number can be calculated using the following empirical correlation (P, Incropera et al. 2007):

$$\mathrm{Nu} = \frac{hl}{\lambda} = 1.86\left(\frac{\mathrm{RePr}}{l/\mathrm{D_H}}\right)^{1/3}\left(\frac{\mu_f}{\mu_w}\right)^{0.14} \quad (3\text{-}6)$$

For the fully developed region ($l_0 \le l \le l_1$), the Nusselt number is constant (P, Incropera et al. 2007):

$$\mathrm{Nu} = 2.47 \tag{3-7}$$

The convective heat transfer coefficient, defined as below, can be solved from the above equations:

$$h = \frac{\mathrm{Nu}\lambda_f}{l} \tag{3-8}$$

The mass balance equation for the working air and water film of wet channel is expressed as:

$$m_{w,f} dw_{w,f} = h_m(\rho_{w,s} - \rho_{w,f})\sigma \mathrm{A_w} \frac{dx}{\mathrm{l_w}} \tag{3-9}$$

$$dm_w = -m_{w,f} dw_{w,f} \tag{3-10}$$

In which, the mass transfer coefficient can be calculated using the analogy between heat transfer and mass transfer defined as:

$$\frac{h}{h_m} = \rho_f c_f \mathrm{Le}^{\frac{2}{3}} \tag{3-11}$$

The energy balance equation for the intake air (primary air) of dry channel is expressed as:

$$c_{p,f} m_{p,f} dt_{p,f} = K_{p,f}(t_w - t_{p,f})\mathrm{A_d} \frac{dx}{\mathrm{l_d}} \tag{3-12}$$

where the overall heat transfer coefficient between the water film and intake air is given by

$$K_{p,f} = \frac{1}{\frac{1}{h_{p,f}} + \frac{\delta_{wall}}{\lambda_{wall}} + \frac{1}{h_w}} \tag{3-13}$$

where $h_{p,f}$ represents the convective heat transfer coefficient between the intake air and channel walls. δ_{wall} and λ_{wall} represents the thickness and thermal conductivity of channel walls respectively. h_w is the heat transfer coefficient between the water film and channel walls. For the static water film condition, h_w can be negligible, i.e., $h_w = 0$. For the flowing water film condition, h_w is the function of water film mass flow rate, i.e., $h_w = f(m_w)$.

Eq. (3-6) can be used to determine the heat transfer coefficient between intake air and channel walls ($h_{p,f}$) and the coefficient between working air and water film ($h_{w,f}$).

Alternatively, the following empirical correlation developed by Stoitchkov can be used (P, Incropera et al. 2007):

$$h = 36.31(\rho_f v_f)^{0.68}\left(\frac{l}{\mathrm{D_H}}\right)^{-0.08} \quad (3\text{-}14)$$

The energy balance equation for the control volume is expressed as:

$$c_{p,w}m_w dt_w + c_{p,w}t_w dm_w + c_{p,f}m_{p,f}dt_{p,f} + m_{w,f}di_{w,f} = 0 \quad (3\text{-}15)$$

The specific enthalpy of moist air is defined as:

$$i_{w,f} = c_{p,m}t_{w,f} + w_{w,f}i_0 \quad (3\text{-}16)$$

where the specific heat of moist air is defined as:

$$c_{p,m} = c_{p,a} + w_{w,f}c_{p,v} \quad (3\text{-}17)$$

Since the computed heat/mass exchanger model is in counter-current configuration, thus both the length and the heat transfer area of dry and wet channel are identical, i.e., $\mathrm{l_w} = \mathrm{l_d} = \mathrm{l}$, $\mathrm{A_w} = \mathrm{A_d} = \mathrm{A}$.

Rearranging Eqs. (3-1), (3-2), (3-9) and (3-10), we have the following equations:

$$\frac{dt_{w,f}}{dx} = \left(\frac{h_{w,f}\mathrm{A}}{c_{p,m}m_{w,f}\mathrm{l}} + \frac{c_{p,v}}{c_{p,m}}\frac{dw_{w,f}}{dx}\right)(t_w - t_{w,f}) \quad (3\text{-}18)$$

$$\frac{dw_{w,f}}{dx} = \frac{h_m\mathrm{A}\sigma}{m_{w,f}\mathrm{l}}(w_{w,s} - w_{w,f}) \quad (3\text{-}19)$$

$$\frac{dt_{p,f}}{dx} = \frac{h_{p,f}\mathrm{A}}{c_{p,f}m_{p,f}\mathrm{l}}(t_w - t_{p,f}) \quad (3\text{-}20)$$

$$\frac{dt_w}{dx} = -\frac{\mathrm{A}}{m_w\mathrm{l}}\left[\frac{h_{p,f}}{c_{p,w}}\left(t_w - t_{i,f}\right) + \frac{h_{w,f}}{c_{p,w}}\left(t_w - t_{w,f}\right)\right. \quad (3\text{-}21)$$

$$\left. + h_m\sigma\left(\frac{c_{p,v}}{c_{p,w}} + \frac{i_0}{c_{p,w}} - t_w\right)(w_{w,s} - w_{w,f})\right]$$

If the heat exchanger geometries ($\mathrm{A}, \mathrm{l}, \mathrm{D_H}$), the mass flow rates of two streams ($m_{p,f}, m_{w,f}$), the physical properties ($(\rho v)_{p,f}$, $(\rho v)_{w,f}$), the mass flow rate of the water (m_w) and the initial temperature conditions ($t_{db,1}, t_{wb,1}, t_{db,2}, t_{wb,2}$) are given, Eqs. (3-18) and (3-21) can be solved. For the studied counter-current heat/mass exchanger

model, inlet temperature of working air is equal to outlet air temperature of product air, i.e., $t_{w,f,1} = t_{db,2},\ t'_{w,f,1} = t_{wb,2}$. The outlet parameters including $t_{db,2}, t_{db,3}, t_{wb,3}, t_{w,2}$ can be solved using finite difference method with iteration. If water is recirculated in the cooler, the inlet feed water temperature ($t_{w,1}$) of the heat exchanger is unknown. The iteration is used until the following equation is satisfied:

$$\int_0^{l_d}\int_0^{l_w} dQ_w = \int_0^{l_d}\int_0^{l_w} d(c_{p,w} m_w dt_w) = 0 \tag{3-22}$$

If water is distributed directly without recirculation, the inlet feed water temperature ($t_{w,1}$) will be considered as a known value for simulation. As a result, the wet-bulb/ dew-point effectiveness of counter-current heat exchanger ($\varepsilon_{wb}, \varepsilon_{dp}$) can be obtained using the results of outlet parameters.

3.2.1 Discussion with extreme water conditions

When the spray water flow rate over the wet surfaces of exchanger is too small to be negligible, the enthalpy variation of water film can be neglected. Thus, in Eq. (3-13), the heat transfer coefficient between water film and channel walls can be negligible, i.e. $1/h_w = 0$. As a result, the overall thermal resistance between water film and primary air only include the thermal resistance of channel walls ($\frac{\delta_{wall}}{\lambda_{wall}}$) and the thermal resistance of primary airflow ($\frac{1}{h_{p,f}}$). On the other hand, when the spray water flow rate is very high, the temperature increase of water film can be negligible, i.e. $dt_w = 0$.

For general conditions, however, the spray water flow rate should be considered as a finite value and its temperature variation cannot be neglected. Thus, the heat transfer coefficient between water film and walls should be considered as a function of water mass flow rate, i.e., $h_w = f(m_w)$, which can be obtained from the following equations (Stoitchkov and Dimitrov 1998):

$$\mathrm{Nu} = \frac{h_w \delta_w}{\lambda_w} = 1.88 \tag{3-23}$$

where,

$$\delta_w = \left(\frac{3\nu_w \Gamma}{\rho_w \mathrm{g}}\right)^{1/3} \tag{3-24}$$

where,

$$\Gamma = \frac{m_w}{(n+1)\mathrm{l}} \tag{3-25}$$

3.3 Pressure drop

The total pressure drop of heat/mass exchanger model, as expressed in Eq. (3-26), consists of friction and minor loss (or local loss). Fig.3-3 shows the diagram of airflow routes in the heat/mass exchanger model and the circuit diagram of the pressure drops of airflow routes. The individual pressure drop of airflow routes is estimated and shown in Table 3-1.

$$\Delta p = \Delta p_{fr} + \Delta p_l \tag{3-26}$$

where the friction loss can be calculated using the following equation (P, Incropera et al. 2007):

$$\Delta p_{fr} = \lambda_{fr} \frac{\mathrm{l}}{\mathrm{D_H}} \frac{\rho_f {u_f}^2}{2} \tag{3-27}$$

For fully developed laminar in channels of equilateral triangular cross section, the frictional factor is a constant which can be calculated using the following empirical correlations (Incropera et al. 2007):

$$\lambda_{fr} = \frac{53.3}{\mathrm{Re}} \tag{3-28}$$

where,

$$\mathrm{Re} = \frac{u_f \mathrm{D_H}}{\nu_f} \tag{3-29}$$

For the hydrodynamic entrance distance (l_1), however, the friction factor varies by the effect of viscous action. The friction factor in entrance region varies with the increase of boundary layer, which is relatively thicker than that in fully developed region. The hydrodynamic entrance distance (l_1) of laminar flow can be determined by the following formula:

$$\frac{l_1}{\mathrm{D_H}} = 0.05\mathrm{Re} \tag{3-30}$$

The entrance region (l_1=0.19 m) was relatively shorter than the entire length of channel (l = 1 m) wherein fully developed flow is present. Therefore, the frictional factor in Eq. (3-27) are computed on the assumption that the entire length of channel is

fully developed laminar flow, which results in a lower predicted pressure loss than the actual value.

The length of dry and wet channel is assumed equal, i.e., $l = l_d = l_w$.

Substituting Eqs. (3-28) - (3-30) into Eq. (3-27), the following correlation can be achieved:

$$\Delta p_{fr} = \frac{53.3l}{2D_H^2}\rho_f u_f v_f \quad (3\text{-}31)$$

This equation indicates that channel geometries have a more important effect on friction loss than air velocity owing to that the friction loss has a quadratic nonlinear relationship with the hydraulic diameter of channels (D_H) but a linear relationship with the air velocity (u_f).

The minor loss (or local loss) can be calculated using the following equation (White 1979):

$$\Delta p_l = \zeta \frac{\rho_f {u_f}^2}{2} \quad (3\text{-}32)$$

As shown in Fig. 3-3, the inlet sudden contraction loss (ζ_1), is produced by dragging intake air into the narrow dry channels of exchanger from wide open outside. The intake air flows along the narrow dry channels in which the fractional intake air (as the product air) is supplied to the air-conditioned space at the end of channel (the outlet sudden expansion loss, ζ_2, is caused), while the remaining intake air (as the working air) diverts from the dry channel into the adjacent wet channel through the perforations. When the air flows through the perforations, the line flow loss (ζ_{1-2}) and branch flow loss ($\zeta_{1-2'}$) are caused in the process of air distribution like "T-type three-way pipe". The angle of branch flow directed through the perforations (θ) ranges from 90 to 180 degree depending upon the branch flow rate, line flow rate, sizes of perforations and channels. After passing through the perforations, the branch flow takes a sharp turning and diverts to the adjacent wet channel. The sharp diversion loss (ζ_{div}) is caused in this process. The outlet sudden expansion loss (ζ_3) is produced when working air exhausts to outside at the end of wet channel.

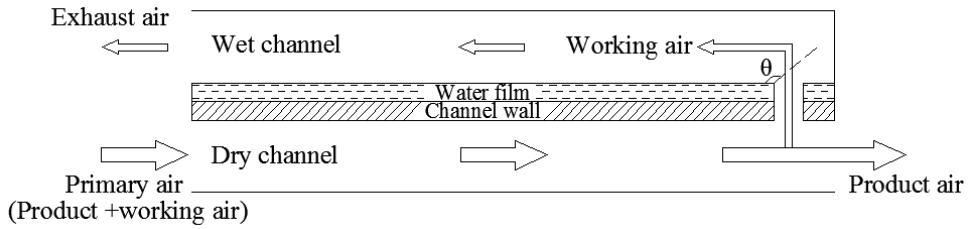

(a) Airflow routes of heat/mass exchanger

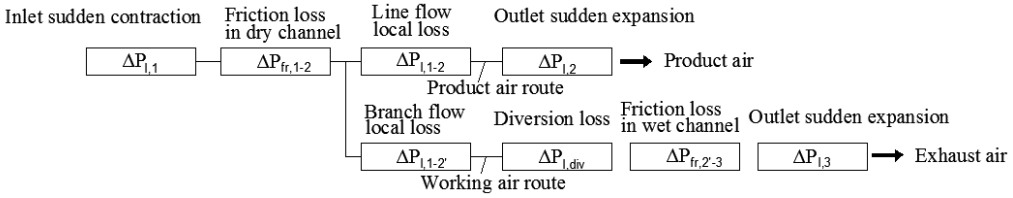

(b) Circuit diagram indicating pressure drop of airflow routes

Fig. 3-3 Diagram of pressure drop in heat/mass exchanger model: (a) airflow routes; (b) circuit diagram indicating pressure drop of airflow routes

(To be continued, please see the next page)

Table 3-1 Pressure drop of product and working air routes

No.	Item	Minor loss coefficient estimate (White 1979)	Frictional factor estimate	Basic equation
1	Inlet sudden contraction loss	ζ_1=0.5	—	$\Delta P_{\mathrm{l},1}=\zeta_1\frac{\rho_{i,f}{u_{i,f}}^2}{2}$
2	Frictional loss in dry channel	—	$f_{1-2}=\frac{53.3}{\mathrm{Re_f}}$	$\Delta P_{\mathrm{fr},1-2}=\frac{53.3l}{2\mathrm{D_H^2}}\rho_f u_f \nu_f$
3	Line flow loss coefficient	ζ_{1-2}=0.1	—	$\Delta P_{\mathrm{l},1-2}=\zeta_{1-2}\frac{\rho_f {u_f}^2}{2}$
4	Outlet sudden expansion local loss of dry channel	ζ_2=1.0	—	$\Delta P_{\mathrm{l},2}=\zeta_2\frac{\rho_f {u_f}^2}{2}$
5	Branch flow loss coefficient	$\zeta_{1-2'}$=0.9	—	$\Delta P_{\mathrm{l},1-2'}=\zeta_{1-2'}\frac{\rho_f {u_f}^2}{2}$
6	Diversion loss coefficient	ζ_{div}=1.5	—	$\Delta P_{\mathrm{l,div}}=\zeta_{\mathrm{div}}\frac{\rho_f {u_f}^2}{2}$
7	Frictional loss in wet channel	—	$f_{2'-3}=\frac{53.3}{\mathrm{Re_f}}$	$\Delta P_{\mathrm{fr},2'-3}=\frac{53.3l}{2\mathrm{D_H^2}}\rho_f u_f \nu_f$
8	Outlet sudden expansion local loss of wet channel	ζ_3=1.0	—	$\Delta P_{\mathrm{l},3}=\zeta_3\frac{\rho_f {u_f}^2}{2}$
9	Pressure drop of product air	—	—	$\Delta P_{\mathrm{primary}}=\Delta P_{l,1}+\Delta P_{fr,1-2}+\Delta P_{l,1-2}+\Delta P_{l,2}$
10	Pressure drop of working air	—	—	$\Delta P_{\mathrm{working}}=\Delta P_{\mathrm{l},1}+\Delta P_{\mathrm{fr},1-2}+\Delta P_{\mathrm{l},1-2'}+\Delta P_{\mathrm{l,div}}+\Delta P_{\mathrm{fr},2'-3}+\Delta P_{\mathrm{l},3}$

3.4 Key quantities of computer simulation

Numerical simulations were run to predict the performance of heat/mass exchanger model under various geometrical/operational parameters such as air velocity, channel sizes, ratio of working-to-intake air and feed water temperature. Several important technical criteria or quantities of evaluating the performance of heat/mass exchanger can be obtained as the results of simulations. Those key quantities include effectiveness (wet-bulb and dew-point effectiveness), power consumption, cooling capacity and

energy efficiency of exchanger. The wet-bulb and dew-point effectiveness can be calculated by the following formulas:

$$\varepsilon_{wb} = \frac{t_{db,1} - t_{db,2}}{t_{db,1} - t_{wb,1}} \quad (3\text{-}33)$$

$$\varepsilon_{dp} = \frac{t_{db,1} - t_{db,2}}{t_{db,1} - t_{dp.1}} \quad (3\text{-}34)$$

where,

ε_{wb}- Wet bulb effectiveness；

ε_{dp}- Dew point effectiveness；

$t_{db,1}$- Intake air dry bulb temperature, ^{o}C;

$t_{wb,1}$- Intake air wet bulb temperature, ^{o}C;

$t_{dp,1}$- Intake air dew point temperature, ^{o}C;

$t_{db,2}$- Product air dry bulb temperature, ^{o}C.

Because the air velocity of the heat/mass exchanger model is small, theoretical power consumptions of fans caused by blowing product and working air though dry and wet channels are low, which can be calculated using the following formulas respectively:

$$W_{\mathrm{p}} = \Delta P_{p,f}\, V_{p,f} \quad (3\text{-}35)$$

$$W_{\mathrm{w}} = \Delta P_{w,f}\, V_{w,f} \quad (3\text{-}36)$$

where,

W_{p}- Theoretical power consumption of product air fan, W;

W_{w}- Theoretical power consumption of working air fan, W;

$\Delta P_{p,f}$- Pressure drop of product airflow, Pa;

$\Delta P_{w,f}$- Pressure drop of working airflow, Pa;

$V_{p,f}$-Volume flow rate of product air, m^3/s;

$V_{w,f}$- Volume flow rate of working air, m^3/s.

The total cooling capacity of heat/mass exchanger, including sensible and latent cooling capacity, can be calculated by:

$$Q_{\text{total}} = m_{p,f}(i_1 - i_2) \quad (3\text{-}37)$$

where,

Q_{total}- Total cooling capacity of heat/mass exchanger, kW;

$m_{p,f}$- Mass flow rate of product air, kg/s

i_1- Specific enthalpy of intake air, kJ/kg;

i_2- Specific enthalpy of product air, kJ/kg.

The sensible cooling capacity supplied by the intake air of heat/mass exchanger can be calculated by:

$$Q_{\text{cooling,IA}} = \frac{c_{p,f}\rho_f V_2\left(t_{db,1} - t_{db,2}\right)}{3.6} \quad (3\text{-}38)$$

where,

$Q_{\text{cooling,IA}}$- Sensible cooling of intake air, W;

$c_{p,f}$- Specific heat of air at constant pressure, kJ/(kg k);

ρ_f- Density of air, kg/m^3;

V_2- Airflow rate of supply air, m^3/h;

$t_{db,1}$- Dry-bulb temperature of intake air, ^{o}C;

$t_{db,2}$- Dry-bulb temperature of supply air, ^{o}C.

The energy efficiency of heat/mass exchanger can be evaluated by energy efficiency, i.e. the ratio of sensible cooling capacity (W) to the sum of power consumptions by the product air fan (W_{p}) and working air fan (W_{w}), as expressed below:

$$\text{Energy efficiency} = \frac{Q_{\text{cooling,IA}}}{W_p + W_w} \quad (3\text{-}39)$$

3.5 Numerical method

The model of channels can be divided into numerous calculation cells along its flow direction, which is shown schematically in Fig. 3-4. The cell is a coupled triangular channel, which contains a triangular wet channel, a triangular dry channel and a heat transfer sheet in between.

The above established mass and energy balance equations were applied to each single cell, one after another, using the numerical iteration method, with the consideration of pre-set boundary conditions.

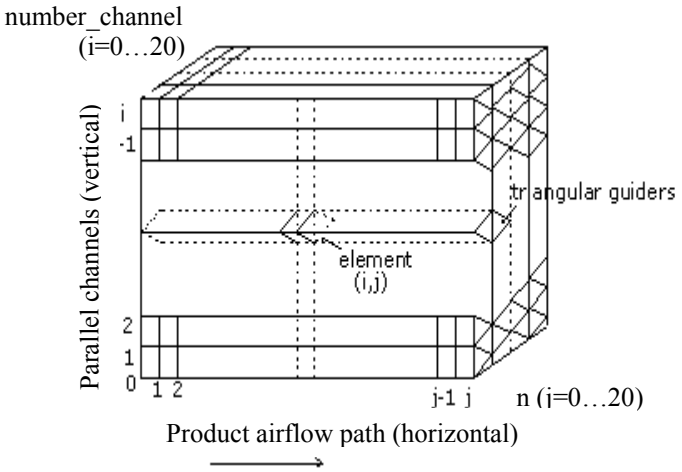

Fig. 3-4 The numbering of calculation cells

By solving the coupled differential equations stated above, the air temperature and moisture content of each cell were calculated to achieve the results of effectiveness and energy efficiency ratio. A computer model incorporating the above equations was developed in the EES (Engineering Equation Solver) environment (Klein 2010), by employing finite-element approach. The Newton iterative method was used to solve a set of equations in relation to the fluid flow and heat and mass transfer within the passages of the heat exchanger.

Simulations were run by varying a studies parameter while setting other parameters to the pre-set conditions as shown in Table 3-2.

The trial computational results show that under the specified conditions a change of 0.03 C (less than 0.2%) in the outlet air temperature resulted from increasing the

mesh grid from 20×20 to 40×40 (n×number_channel), as shown in Fig. 3-5. The significant increase in computing time for the 40×40 grid was not considered as a rational modelling burden for the relatively small temperature change. The mesh grid of 20×20 was considered to provide sufficient accuracy for engineering applications and was, therefore, adopted in the model set-up.

Table 3-2 Pre-set simulation conditions

intake DBT/WBT., °C	intake channel air velocity, m/s	Working-to- intake air ratio	feed water temp., °C	dry/wet channel length, m	dry/wet channel height (equilateral triangle), mm
35/24	0.5	0.5	22.5	1.0	6.0

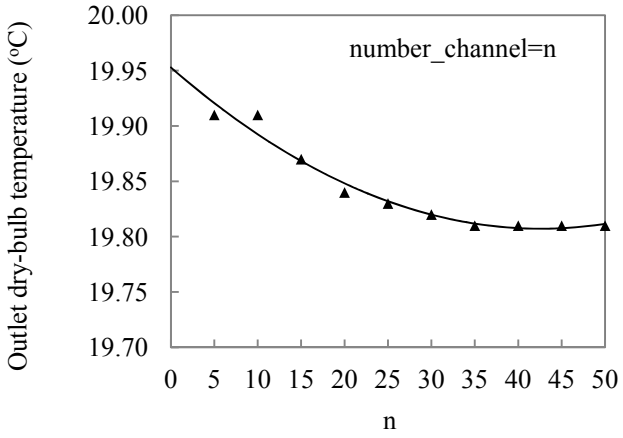

Fig. 3-5 Mesh sensitivity of the computer model

3.6 Simulation results and analyses

3.6.1 Effect of channel walls thermal conductivities

The channel wall of the counter current heat/mass exchanger is formed by a type of evaporative media and hydrophobic material. According to Eq. (3-13), the effect of thermal conductivities of channel walls on the magnitude of the heat and mass transfer rates can be negligible. A close analysis was given into the Eq. (3-13). If the thickness of channel wall is less than 0.5mm, the thermal conduction resistance could be lower than the convective heat transfer thermal resistance by three orders of magnitude, which

makes the thermal conduction resistance nearly negligible. The temperature difference between the dry and wet sides of wall can therefore be ignored.

3.6.2 Effect of feed water distribution flow rate

The feed water distribution flow rate (i.e., the falling water flow rate to the wet surface) has an effect on the pressure drop of working air and the heat and mass transfer process in the heat exchanger. For the ideal condition, the water film on wet surfaces totally evaporates to the working air and no extra water remains. To ensure the wet surfaces thoroughly wetted, however, abundant water beyond the evaporation value should always be feed in. The abundant water actually increases the water film thickness of the wet surfaces. The extra water film may result in the reducing of wet channel spacing and the increasing of water film thermal resistance. Often in the numerical simulation, the water film thickness is assumed very thin and can be negligible which results in a much higher predicted performance of the heat exchanger than the actual value.

3.6.3 Effect of channel geometries

A few simulations were carried out to investigate the effects of channel length and spacing on the wet-bulb/dew-point effectiveness of heat exchanger. The channel spacing was varied from 0.001 to 0.01 m while setting other parameters to the pre-set conditions as shown in Table 3-2. The result of simulation is shown in Fig. 3-6. The wet-bulb effectiveness decreased gradually from 1.4 to 1.1 with increasing the channel spacing from 1 to 10 mm, whereas the outlet air temperature of the heat exchanger increased gradually from 19.5 to 22.8^{o}C. Fig. 3-7 shows that the cooling capacity and energy efficiency reduce with increasing channel spacing. It is found that the unit cooling capacity (W/cell) and energy efficiency remained constant from 0.001 to 0.004 m and then rose gradually from 0.004 to 0.01 m. To compromise between effectiveness and energy efficiency, the most favorite channel spacing should be in the range of 5 to 6 mm.

Fig. 3-8 shows the predicted effectiveness and outlet air temperature as a function of channel length. The effectiveness of the heat exchanger increased steadily towards the peak when the channel length increased from 0.1 to 1 m. Then the effectiveness remained constant from 1 to 1.2 m. Meanwhile, the outlet air temperature of the heat exchanger reduced gradually from 28.5 to 19.8^{o}C and also remained unchanged from 1

to 1.2 m. Therefore, to obtain high effectiveness, the channel length of the heat exchanger should be set above1 m.

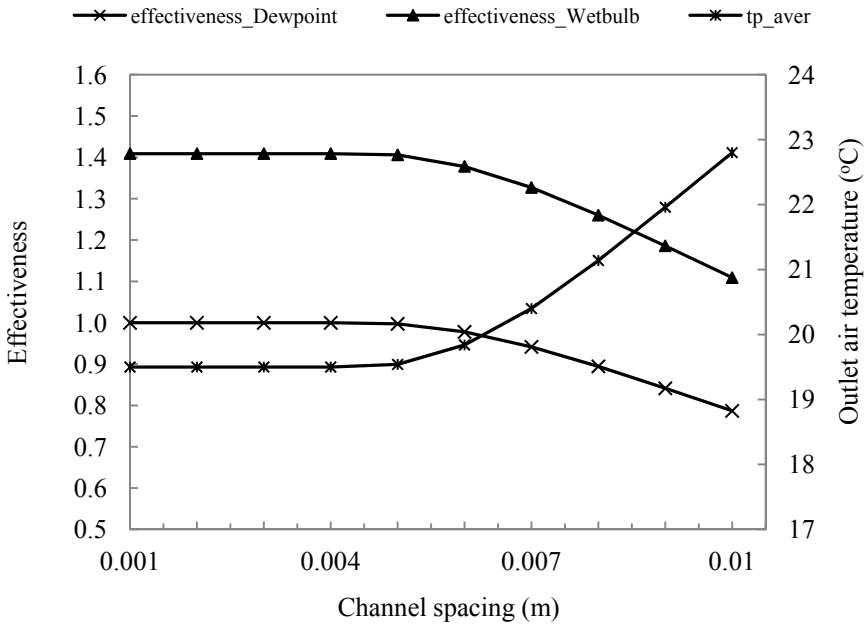

Fig. 3-6 Effectiveness and outlet air temperature with channel spacing

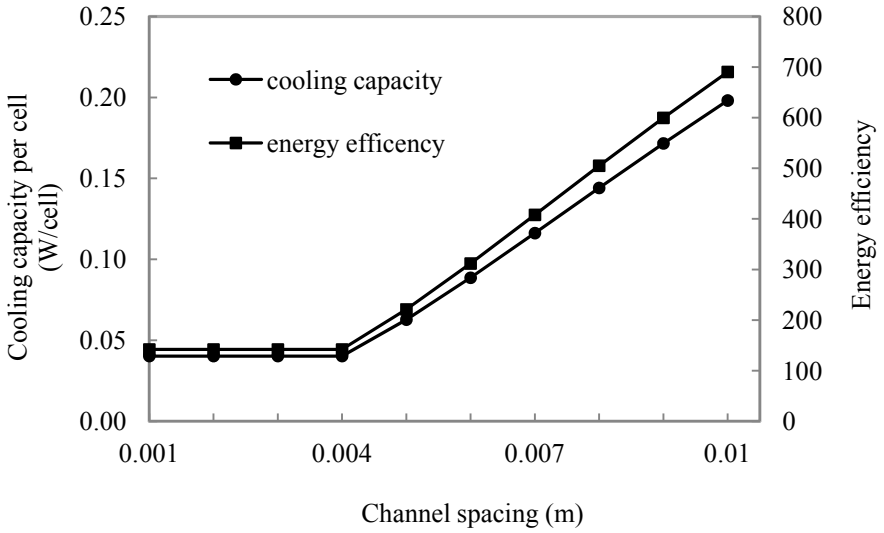

Fig. 3-7 Cooling capacity and energy efficiency per modelling cell with channel spacing

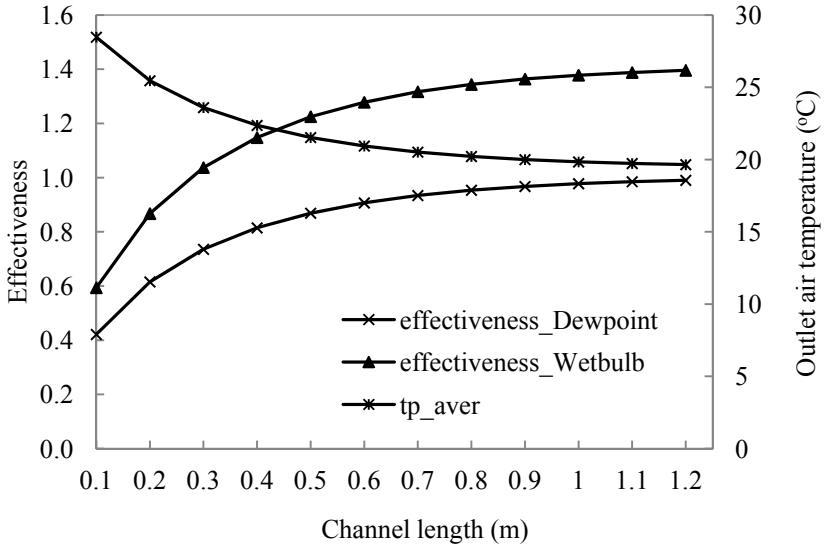

Fig. 3-8 Effectiveness and outlet air temperature varied with channel length

The variations of cooling capacity and energy efficiency with channel length are shown in Fig. 3-9. It is seen that the unit cooling capacity increased gradually when the channel length increased from 0.1 to 1 m and then remained nearly constant when the length increased from 1 to 1.2 m. Whereas, the energy efficiency decreased gradually from 0.1 to 1.2 m. To achieve the comprimise between effectiveness, cooling capacity and energy efficiency, the channel length should be set above 1 m.

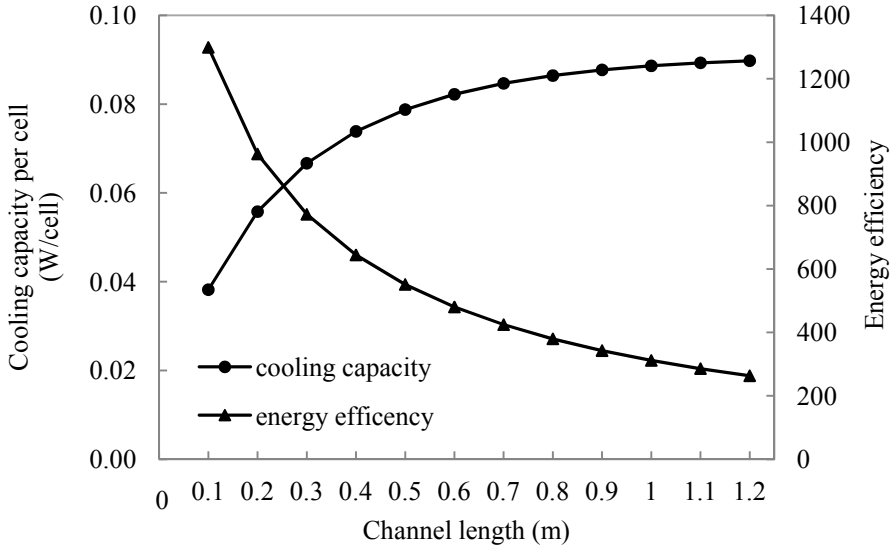

Fig. 3-9 Cooling capacity and energy efficiency per modelling cell with channel length

3.6.4 Effect of intake channel air velocity

The numeric results of effectiveness and outlet air temperature with intake channel air velocity are shown in Fig. 3-10. The effectiveness decreased slightly with the intake air velocity increasing from 0.2 to 0.5 m/s and then it decreased rapidly with increasing the velocity from 0.5 to 4 m/s. In the meanwhile, outlet air temperature of the heat exchanger increased a little with the velocity from 0.2 to 0.5 m/s and then continued rising from 0.5 to 4 m/s.

The effects of intake channel air velocity on the cooling capacity and energy efficiency of the model are shown in Fig. 3-11. The cooling capacity increases gradually with increasing intake channel air velocity. The energy efficiency dropped significantly with increasing the velocity from 0.2 to 1 m/s. Then it fell slightly with increasing the velocity from 1 to 4 m/s. The curve trend of energy efficiency with velocity can be explained from the relationship of pressure loss with velocity (pressure loss is proportional to the second-order of air velocity). As a result, it is suggested that the intake channel air velocity should be controlled between 0.2-0.5 m/s to achieve an enhanced effectiveness and energy efficiency. However, the cooling capacity of the exchanger reduces with decreasing the air velocity. Therefore, to compromise between the effectiveness and cooling capacity, the intake channel air velocity should be set between 0.5-1 m/s.

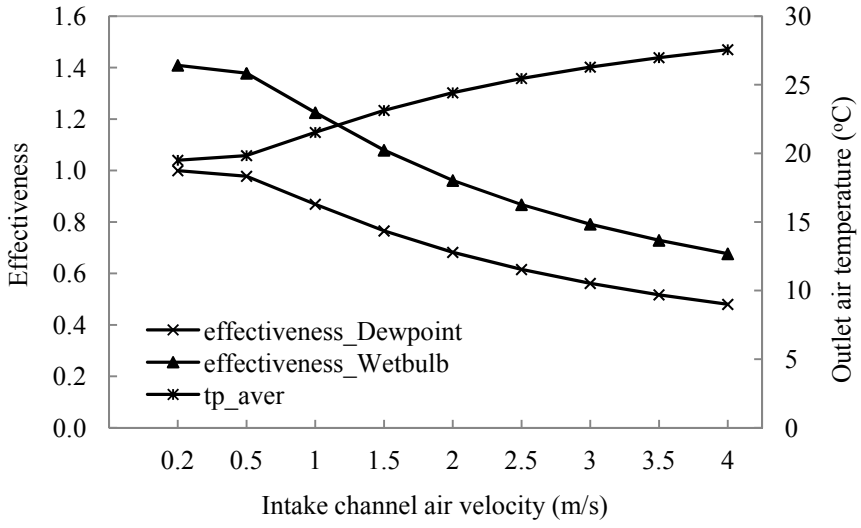

Fig. 3-10 Effectiveness and outlet air temperature with intake channel air velocity

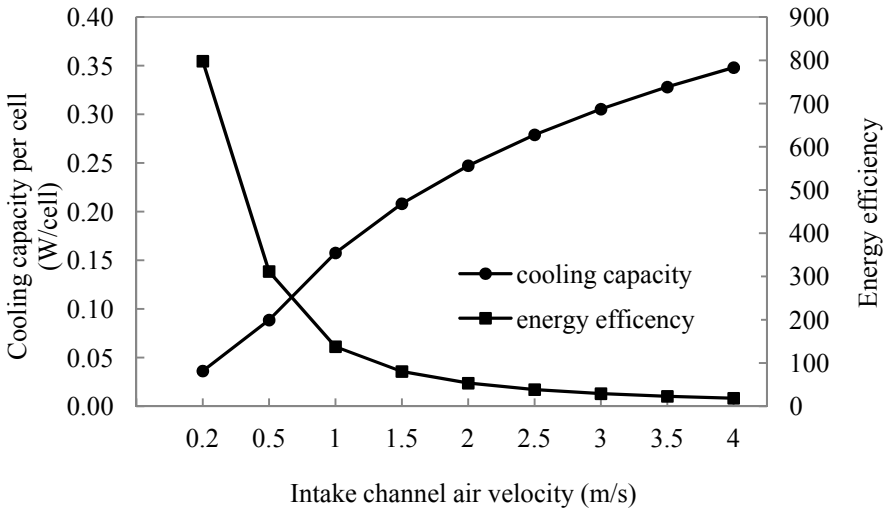

Fig. 3-11 Cooling capacity and energy efficiency per modelling cell with intake channel air velocity

3.6.5 Effect of working-to-intake air ratio

The working-to-intake air ratio represents the ratio of working air volume to total intake air volume. The predicted effectiveness and outlet air temperature with working-to-intake air ratio are shown in Fig. 3-12. It is shown that the wet-bulb effectiveness rose gradually from 1.05-1.4 when the working-to-intake air ratio increased from 0.2 to 0.6 and then it remained almost constant when the ratio varied from 0.6 to 0.9. The outlet air temperature gradually fell down from 23.5 to 19.7^{o}C when the working-to-intake air ratio increased from 0.2 to 0.6 and then it remained almost constant from 0.6 to 0.9. The effects of working-to-intake air ratio on the cooling capacity and energy efficiency of the model are shown in Fig. 3-13. It is found that either cooling capacity or energy efficiency decrease with increasing the working-to-intake air ratio. The cooling capacity per unit cell increased slightly when the working-to-intake air ratio increased from 0.2 to 0.3 and then it fell linearly from 0.3 to 0.9. The energy efficiency dropped slightly from 0.2 to 0.3 and then continued falling down from 0.3 to 0.9 in a linear trend. The above numerical simulations indicate that the working-to-intake air ratio should be set to 0.4-0.5 in order to achieve a high effectiveness, cooling capacity and energy efficiency.

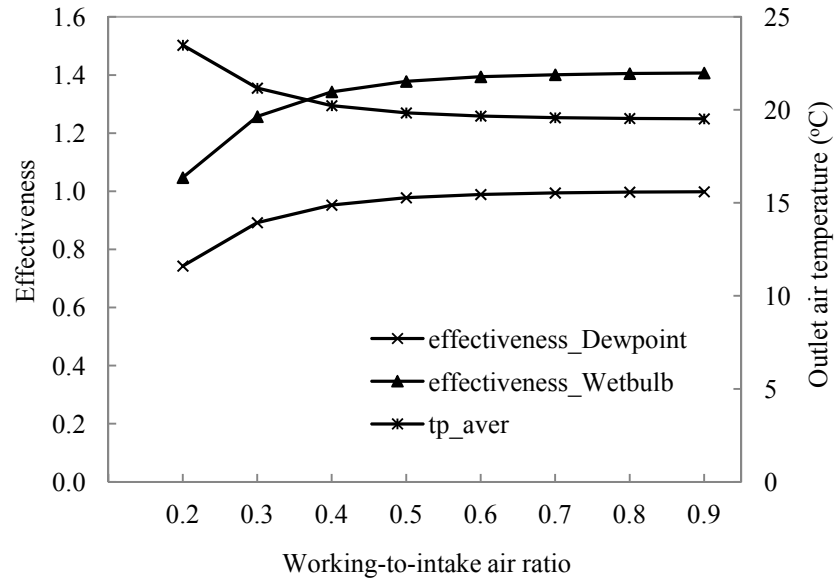

Fig. 3-12 Effectiveness and outlet air temperature with working-to-intake air ratio

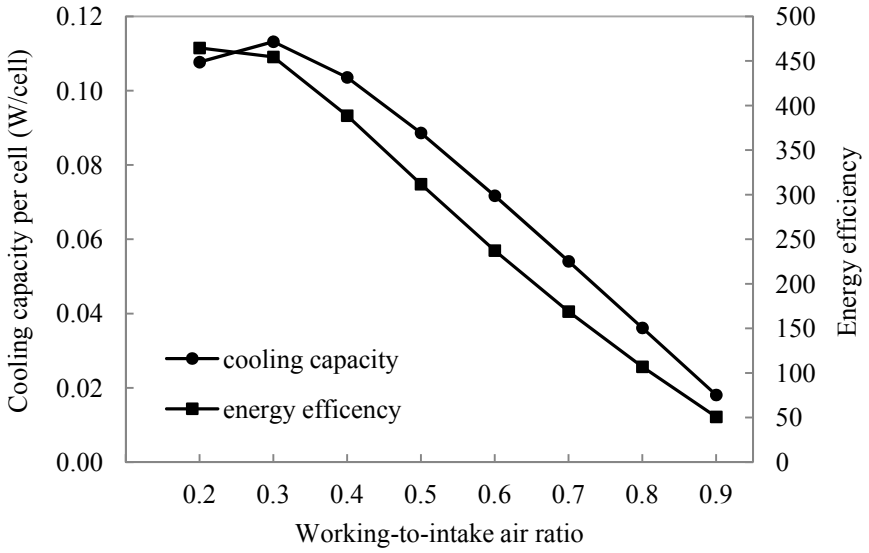

Fig. 3-13 Cooling capacity and energy efficiency per modelling cell with working-to-intake air ratio

3.6.6 Effect of feed water temperature

A simulation was conducted to investigate the effect of feed water temperature on the effectiveness of heat exchanger by varying the water temperature from 16 to 30°C while setting other parameters to the pre-set conditions Simulations were run by varying a

studies parameter while setting other parameters to the pre-set conditions as shown in Table 3-2.

The trial computational results show that under the specified conditions a change of 0.03 C (less than 0.2%) in the outlet air temperature resulted from increasing the mesh grid from 20×20 to 40×40 (n×number_channel), as shown in Fig. 3-5. The significant increase in computing time for the 40×40 grid was not considered as a rational modelling burden for the relatively small temperature change. The mesh grid of 20×20 was considered to provide sufficient accuracy for engineering applications and was, therefore, adopted in the model set-up.

The predicted effectiveness and outlet air temperature varied with feed water temperature are shown in Fig. 3-14. It is found that the feed water temperature has the negligible effects on the effectiveness and outlet air temperature. This is due to the fact that the cooling effect of heat exchanger is mainly achieved from water evaporation, i.e. latent cooling.

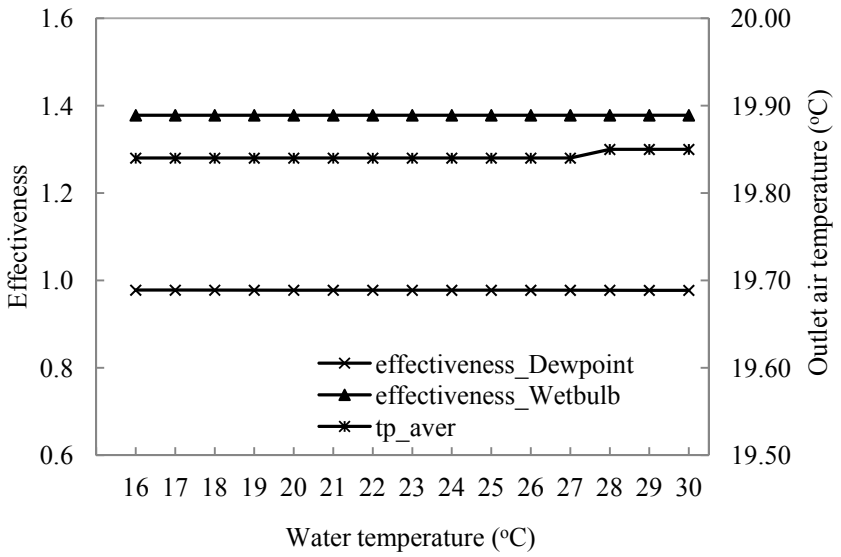

Fig. 3-14 Effectiveness and outlet air temperature with feed water temperature

3.6.7 Surface wetting factor

The surface wetting factor is the ratio of wetted surface area to the entire wall surface area of a heat exchanger plate. The undesirable surface wetting result in the decrease of actual heat/mass exchanging area (the reduced wet surface in the direction of channel length or width), which produce a reduced wet-bulb/dew-point effectiveness and

cooling capacity, as shown in Figs. 3-8 and 3-9. Due to this reason, an evaporative medium with great water absorbing and retaining abilities should be selected as the wet surface material of heat/mass exchanger.

3.7 Experimental validation of the model accuracy

Some previous published experiment data (Riangvilaikul and Kumar 2010) were chosen to validate the accuracy of established model. The model was set to run with the same operating conditions as the experiment (i.e. the same inlet air parameters and flow rates). The operational/geometrical conditions of the published experimental study are shown in Table 3-3. The counter-flow exchanger tested in the experimental study was stacked together with 4 dry and 5 wet channels (5 mm channel spacing) of rectangular cross section.

Table 3-3 The geometrical and operational parameters used in the published experiment (Riangvilaikul and Kumar 2010)

Wall material	Wall thickness	Channel length	Channel width	Channel spacing	Intake channel air velocity	Working air-to-intake air ratio
	mm	mm	mm	mm	m/s	kg/kg
Cotton sheet coated with polyurethane	0.5	1200	80	5	2.4	0.33

Fig. 3-15 shows the comparison between our numerical results and the data obtained from the experiment study (Riangvilaikul and Kumar 2010). The difference between experimental and numerical supply air temperature was 0.01-1.09°C for different moisture content of inlet air. The highest deviation of the numerical to experimental supply air temperature was 3.4%. When the moisture content was 6.9 g/kg dry air, it presented the biggest deviation between them.

(To be continued, please see the next page)

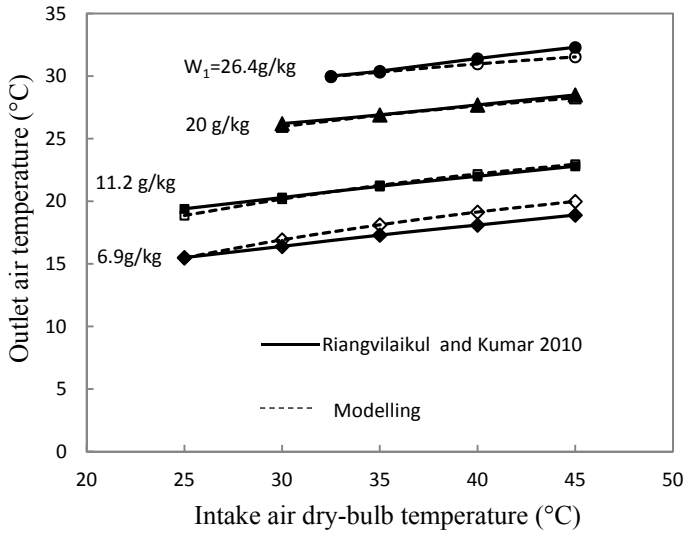

Fig. 3-15 Experimental validation-outlet air temperature versus intake air temperature

Chapter4.
Construction and Experiment of the Dew Point Air Cooler Prototype

4.1 Structural design

A stand-alone dew point air cooler prototype was designed based on the results of simulations. The diagram of the prototype is shown in Fig. 4-1. The prototype mainly consists of a dew point heat and mass exchanger, supply air tangential fan, exhaust air axial fan, water distributor, water collector, float switch and water pump. The air cooler operates in the following way: Intake air is dragged into the dry channels of heat exchanger. At the end of dry channels, fraction of intake air, as the working air, is directed into the adjacent wet channels through the perforations at the end of heat exchanger sheets. In the wet channels, the working air absorbs sensible and latent heat from the intake air of the dry channels and is finally discharged to outside by an axial fan. As a result of heat exchange sensibly and latently, the product air of dry channels is cooled and supplied to the air-conditioned space by using a tangential fan. The technical details of the system components are stated in the following sections.

Dew point heat and mass exchanger

Dew point heat and mass exchanger consists of numerous dry and wet channels which are formed by a type of evaporative and water-proof materials. The dry channels of exchanger are formed by a type of water-proof material which prevents water penetrating from wet channels. The wet channels of exchanger are formed by a type of evaporative material with high capillary forces and water absorption capacity which enable water retain on its surface uniformly. The retaining water on the media is then evaporated to the working air of wet channels. The dry/wet channels are normally supported with rectangular bars or corrugated sheets which can be used as air guiders of channels.

Supply air tangential fan

Characterised by compactness, quiet operation, and capability of providing high pressure coefficient, a tangential fan is mounted at the supply outlet of the system to provide supply airflow. The tangential fan can provide a wide range of airflow which is applicable to designed airflows of the heat exchanger.

Exhaust axial air fan

Characterised by small pressure drop and large airflow volume, an axial fan is equipped at the exhaust outlet of the system to blow exhaust air to outside.

Water distributor

The water distributor of dew point cooling unit consists of a top water tank and numerous small distributing tubes connecting between the water tank and wet channels of heat exchanger. The water tank, made of acrylic plastic material, stores feed water of cooling unit. The feed water flows through the distributing tubes from the tank to the wet channels of heat exchanger. By an unique water distribution structure in the wet channels, uniform water film is created on the surfaces of evaporative media. Of the feed water, only a small amount is evaporated to the working air of exchanger. The remaining water is dripped into the bottom water collector for recirculation.

Water collector

A water collector is equipped to collect the remaining water drained from the heat exchanger. The remaining water is lifted to the upper water tank by a water pump indulged in the water collector. The water collector is also fitted with drainage and overflow pipes.

Water pump

A small submersible water pump is merged in the water collector. It runs periodically in response to a float switch device which is mounted at a certain level of the water collector. The pump begins to lift water when the water level of the collector reaches to the activated level of the float switch.

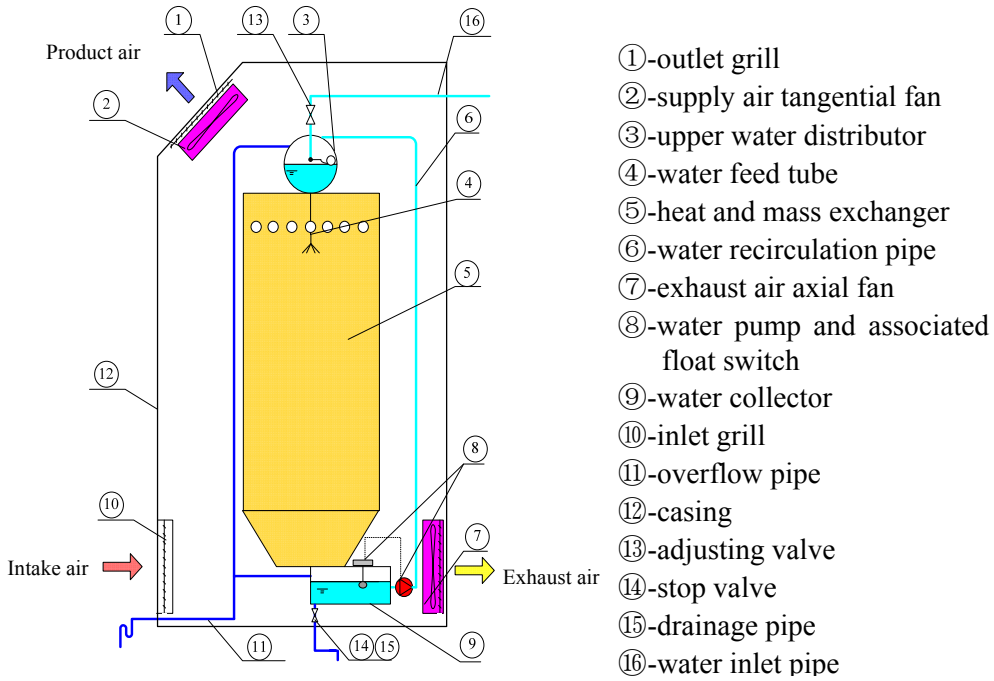

Fig. 4-1 Diagram of the stand-alone dew point cooler

Casing

The aluminium casing of dew point cooling unit is insulated with thick insulation materials to reduce the heat exchange with ambient conditions. For this purpose, the external surfaces of heat and mass exchanger are glued with thick insulations.

Electrical components

The electrical components of dew point cooling unit are comprised of two fans, a water pump and an associated float switch. The technical parameters of the components are presented in Table 4-1.

4.2 Material selection

The air-to-air heat and mass exchanger of dew point cooler consists of heat and mass transfer sheets and air guiders. The heat and mass transfer sheet is formed by coating a waterproof material on an evaporative material. The waterproof surface of exchanger enables product air pass through without moisture gains. However, the hydrophilic evaporative surface enables working air get saturated when passing through. For the air guider material, plastic corrugated sheets or rectangular bars/walls are widely used. Compared with the air guiders, the thermal and physical properties of evaporative

material play more significant roles on the heat and mass transfer of the exchanger. Therefore the following sections will place an emphasis on the study of evaporative materials.

Table 4-1 Technical parameters of the electric components in prototype

Items	Model	voltage	Air flow rate	Max Pressure/ head	Power input	Speed
		V	m^3/h	Pa	W	r/min
Tangential fan	ebmpapst-QLN65/30 30-3045L	230	410	62	72	1225
Axial fan	ebmpapst-Series 6078ES	230	420	150	26	2800
Submersible circulation pump	ebmpapst-P30-4330	230AC	0.75	N/A	48	N/A
Float switch	Cynergy3 RSF34W10 0RF	240Va.c./240 Vd.c. (Max)	–	–	100W (Max)	–

Heat and mass transfer sheets

According to the analysis of materials in Chapter 2, the thermal and physical properties of materials forming a heat/mass exchanger should meet the following requirements to maximise heat/mass transfer: 1) From the respect of heat transfer, thermal conductivity and thickness of materials have direct effects on the resistance of thermal conduction; 2) From the respect of mass transfer, wetting surfaces of materials should have good capacities of water absorption and retaining; 3) From the respect of construction, strength of materials should be strong enough to form the construction of heat exchanger.

Firstly, a test was conduct to measure the thickness of the selective materials by using a thickness gauge (measurement range: 0-5 mm, accuracy: 0.01 mm). The result of measurements is shown in Appendix A. It is found that all of the thickness values were below 0.5 mm. In cases where the wall thickness of heat/mass exchanger is below 0.5mm or even smaller, the heat conduction resistance can be negligible without regarding the thermal conductivity of materials (Zhao et al. 2008).

Secondly, to maximise mass transfer of heat exchanger, the evaporative surfaces of heat exchanger should be covered with thin and uniform water films. In doing so, the hydrophilic porous evaporative material forming the exchanger should have acceptable water retaining ability. This ability relates to the following properties of hydrophilic materials, i.e., capillary force, porosity (the fraction of void space over the total volume) and specific surface area (the total surface area per unit of mass).

Thirdly, both strength of the evaporative material and its coating ability with selected waterproof materials should be taken into account. The strength of evaporative material should be capable of constructing heat exchanger with waterproof coating. Table 2-3 in Chapter 2 reviews the strength and coating capability for several types of materials, i.e., metal, fibre, ceramics, zeolite and carbon.

Fibre, as a type of evaporative material, is relatively cheaper, thinner and has a higher water absorption and retaining capacities compared with ceramic and carbon types (Zhao et al. 2008). But it has the lowest strength among other types. In fact, properties of strength and water absorbing capacity are considered more important in choosing the suitable fibre material forming exchanger. Some types of fibres cannot be employed despite with great water absorbing capacity, such as hand towel. It is easy to fragile after wetting. In general, an enhanced strength is derived from increasing the thickness of fibre. The thicker fibres also can absorb more water than the thinner ones. However, increasing thickness of fibre may increase the thermal conduction resistance between dry and wet air.

Therefore, a suitable fibre option is the compromise among strength, water absorption (capillary forces) and thermal resistance.

An experiment was conducted to compare the capillary forces/ water absorption capacity among some fibres with or without coating materials. The materials for testing are shown in Fig. 4-2.

(a) Rough surface of textile fibre

(b) Smooth surface of textile fibre

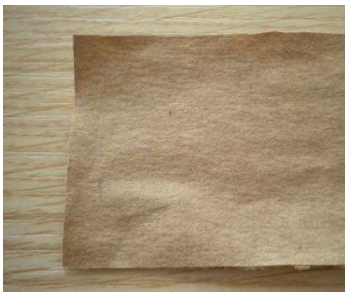

(c) Pure kraft paper

(d) Waxing kraft paper

(e) Aluminum-coating kraft paper (finish product)

(f) Non-woven fabric

(g) Aluminum film

Fig.4-2 The chosen materials for forming heat/mass exchanger

For the chosen materials, the heights of capillary rise were measured by a water absorbing detector (measurement range: 0-200 mm, accuracy: 1 mm), as shown in Fig. 4-3 (dyed water was employed to highlight the observations). The heights of capillary rise of different materials varied with time(within 2 hours) is shown in Fig. 4-4.

Of the three materials, i.e., pure textile fibre, pure kraft paper and waxing kraft paper, it is found that the pure textile fibre has the relatively higher water absorption capacity among others. And also it can be saturated in a very short time. It is noted that the pure textile fibre absorbed water very rapidly at the first 5 minutes. Actually, it already had absorbed over 90% of the total water absorption capacity within the first 5 minutes. The fast wetting ability of fibre is very desirable for evaporative cooling applications as it enables evaporative coolers to provide required cooling within a short time after they start up.

The pure kraft paper also has the relatively high water absorption capacity but it absorbs water in a gradual process. After absorbing for approximate 50 minutes, the height of capillary rise of pure kraft paper had reached to the same level with that of pure textile fibre.

Although strengths of fibres are poor, the other side of heat exchanger sheet, i.e., waterproof material, can strengthen the hardness of heat exchanger. Metal is the preferable type for the relatively high strength and thermal conductivity. Of the common metal types, aluminium foil can be served as the waterproof coating for its cheap initial cost, high thermal conductivity and good heat process capability.

In terms of coating methods between aluminium film and fibre sheet, both heating and gluing methods were used to test the water absorption capacities of materials after coating. Fig. 4-4 shows the heights of capillary rise of aluminium coating materials (by different coating methods) varied with time. It is found that the heating method is not as good as the gluing method. Coated by heat, the aluminium foil coating textile fibre (ATF1) has a worse water absorption capacity than the aluminium foil coating textile fibre (ATF2) which is coated by gluing. The water absorption capacity of fibre with coating is higher than that of pure fibre owing to the reason that coating increases the adhesion of fibre material to water.

Table 4-2 summarises the properties of chosen evaporative materials including thermal conductivity, thickness, water absorption capacity, weight of water absorption per area, strength, durability and cost. Aluminium coating textile fibre (ATF2) could be the best suitable composite material among the selected materials owing to the above mentioned superior properties, i.e., fast wetting, high water absorption capacity, low cost and small thermal contact resistance arising from the coating between aluminium and fibre.

(a) Water absorbing detector

(b) The observation after 1minute

(c) The observation after 1 hour

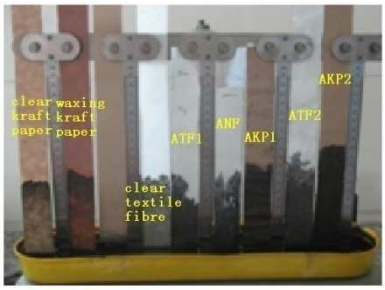

(d) The observation after2 hours

Fig. 4-3 Water absorbing experiment (a) water absorbing detector (b) observation after 1minute (c) observation after 1 hour (d) observation after2 hours

A test was further conducted on the selected materials with high water absorbing capacity to compare the weight of water absorbing per unit surface area. The chosen materials include pure textile fibre, pure Kraft paper, pure nonwoven fabric, waxing kraft paper, AKP2 and ATF2. The samples of those materials were simultaneously indulged in a sink to absorb water for a long period of time until they were saturated. The weights of samples before wetting and after wetting were measured by an electronic scale (measurement range: 0-120 g, accuracy: 0.01 g). The result of tests is shown in Fig. 4-6. It is found that the aluminium-coating textile fibre had the highest water absorbing capacity per unit surface area (≈261 g/m^2) among others. The pure textile fibre had the less value, i.e., about 210 g/m^2. The waxing kraft paper had the worst value, i.e., about 94 g/ m^2.

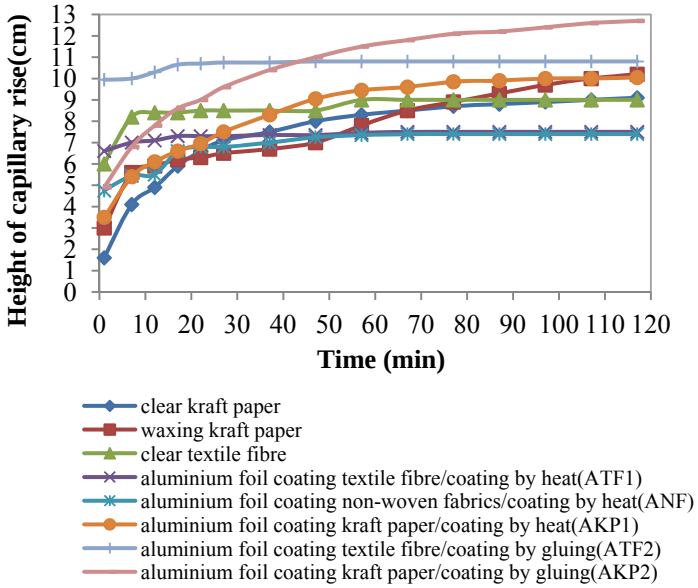

Fig. 4-4 Heights of capillary rise of the chosen materials versus time

Table 4-2 Properties of the chosen evaporative materials

Material	Thermal conducti -vity, W/m K	Thickne -ss, mm	Height of water absorpt -ion, mm	weight of water absorpt -ion per area, g/m^2	Strengt -h	Durabil -ity	Cost, £/m^2
pure textile fibre	0.026	0.259	9.0	210.44	Poor	Medium	<1.7
pure kraft paper,96g/m^2	0.049	0.180	9.1	121.21	Medium	Medium	<0.05
pure non-woven fabric	-	0.180	-	135.52	Poor	Medium	<0.5
aluminium foil	222	0.153	-	-	High	High	<0.14
aluminium coating textile fibre, coating by heat	-	0.370	7.5	-	High	High	<2.0
aluminium coating kraft paper, coating by heat	-	-	10.05	-	High	High	<0.2
waxing kraft paper	0.075	0.209	10.2	94.28	Medium	Medium	<0.1
aluminium coating non-woven fabric	-	0.280	7.4	-	High	High	<0.65
aluminium coating textile fibre, coating by glue	-	0.410	10.8	260.94	High	High	<2.0
aluminium coating kraft paper, by glue	-	0.470	12.7	-	High	High	<0.2
aluminium film coating kraft paper,130g/m^2,finished goods	0.077	0.200	curve	148.15	Medium	Medium	<0.2

(a) Electronic scale (b) The chosen materials (c) Water absorbing process

Fig. 4-5 The experiment on weight of water absorption of chosen materials (a) electronic scale (b) chosen materials (c) water absorbing process

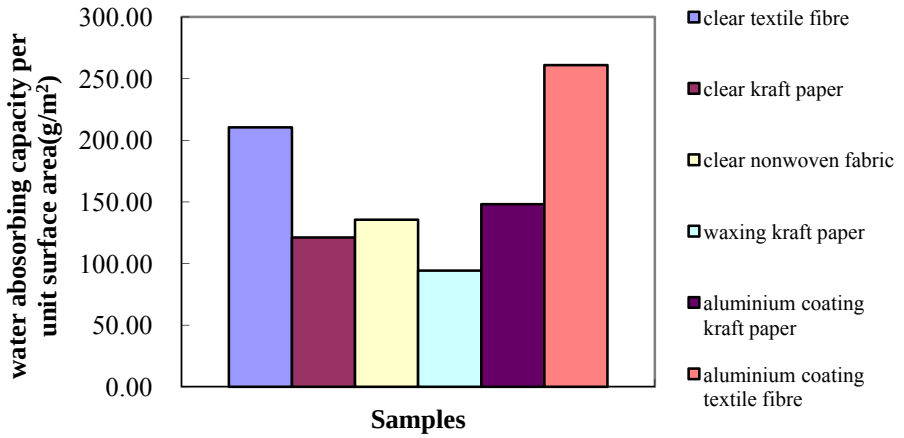

Fig. 4-6 Water absorbing capacities per unit surface area for the selected materials

From the results of above experiments, aluminium coating textile fibre (coating by gluing) would be the adequate material for forming the heat/mass exchanger of evaporative cooling. Instead of gluing, heating and pressing methods were used in coating between the aluminium foil and fibre sheet due to the limitation of fabrication in laboratory.

Supporting air guider

Regarding to the materials for supporting the channel walls of exchanger, plastic corrugated sheets were used for the characteristics of easy assembly and light weight, as shown in Fig. 4-7. The corrugated sheet, as the supporter of each channel, guides airflow to pass through the air channels of exchanger.

Fig. 4-7 The corrugated sheets for supporting channels of heat exchanger

4.3 Construction of the experiment prototype

The dew point cooling unit was constructed in laboratory. The procedures of construction is shown in Fig. 4-8. As the main part of the cooling unit, the heat and mass exchanger was formed by aluminium coating fibre sheets and plastic corrugated sheets: The aluminium foil (with perforations) and fibre sheet were stacked together using heating press method, as shown in Fig. 4-8 (a); Note that the smooth surface of fibres should be coated with aluminium foils because the coarse surface of fibre sheet is used to evaporate water. The plastic corrugated sheets were supported in both dry and wet channels to guide airflows, see Fig. 4-8 (b). The fibre and corrugated sheets were assembled into 5 groups (see Fig. 4-8 (c)), which were partitioned with several wooden plates to strengthen the structure of exchanger (see Fig. 4-8 (d)). The exchanger was then glued with thick insulation sheets to reduce its heat exchange with ambience (see Fig. 4-8 (e)).

All the components of cooling unit were installed to the right positions. The components include heat/mass exchanger, water tank and collector, outlet tangential fan, exhaust axial fan, filters, air speed controllers, water pump and float switch, as shown in Fig. 4-8 (f-j). The finished cooling unit prototype is shown in Fig. 4-8 (k-m).

(a) Aluminium coating fibre sheets

(b) Corrugated sheets

(c) Finished heat/mass exchanger sheets

(d) Assembly of heat/mass exchanger

(e) Insulation process

(f) Top water tank

(g) Finished heat/mass exchanger

(h) Fans and filter components of cooler

(i) Top view inside the cooler

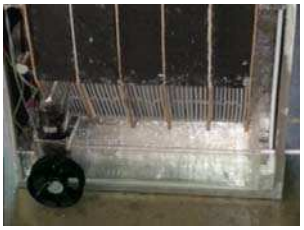

(j) Bottom view inside the cooler

(k) Back view of the cooler

(l) Internal view of the cooler

(m) Front view of the cooler

Fig. 4-8 The construction process of experiment prototype

4.4 Experiment set-up

Fig. 4-9 shows the schematic of dew point cooling experiment system and the locations of measuring instruments. The dew point cooler prototype was placed in a laboratory room in which air temperature and humidity remain constant. Intake air temperature and humidity of the prototype were controlled by a connected variable output resistance heater and a humidifier. To achieve a steady flow state before testing, extension ducts (each in 2 m length) was set to the intake, supply and exhaust vents of the system respectively. The intake, supply and exhaust air ducts of the test unit were separately connected to a sealed chamber where a variable speed fan was set to control the outlet static pressure and compensate for the additional resistance of ducts and measurement system. The photograph of the dew point cooling test system in laboratory is shown in Fig. 4-10.

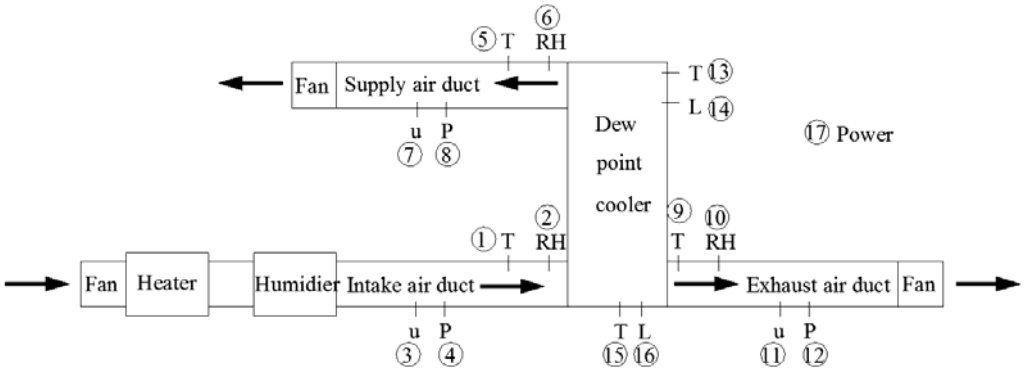

(The numbers for the locations of the instruments are described in Table 4-3)

Fig. 4-9 Test system and measurement locations

Fig. 4-10 The photograph of dew point cooler test system in laboratory

4.5 Measurements and instruments

The experiment set-up follows the ASHRAE indirect evaporator cooler test standard (ASHRAE 2000). All the details of measured parameters (as indicated in Fig. 4-9) and instruments are presented in Table 4-3, which include measurement range and accuracy. Fig.4-11 shows the photographs of the measurement instruments and types.

For the temperature measurement instrument of experiment, Type K thermocouples are accurate enough as the measurement range of dry-bulb temperatures in evaporative cooling is relatively small, i.e., 10-40^{o}C. For the humidity measurement instrument, a type of polymer thin film electronic humidity sensor with high accuracy (±1% RH after calibration) was used to measure the relative humidity of moist air. For measuring the static pressure of each air flow, four taps were fitted in the extension circular duct at a distance downstream equal to the four time the diameter of circular duct, and evenly distributed around the surface of the duct. The taps were connected together with a ring of tubing and tees, with an additional tee connecting to a micromanometer. The static pressure of each air flow was controlled by adjusting its associated fan speed.

All Type K thermocouples, PT100 resistances and humidity sensors were connected through a data logger device to a computer. All experiment data acquired by the data logger were transferred to the computer. The data logger was programmed and it instructed the connected instruments to read, report and save measured data on the display of computer at 5 seconds intervals. The operating parameters of the test system, such as intake air dry-bulb temperature, humidity and air velocities, were controlled by adjusting the inlet heater, humidifier and associated fan motor speed to desired conditions, which can be monitored on the display of computer.

The measurement methods for temperature, humidity and velocity/flow rate of air are described in the following sections.

Table 4-3 The measured parameters and the corresponding instruments

No.	Parameters	Instruments	Measurement range	Uncertainty
1	Intake air dry-bulb temperature	Type K thermocouples	-50 to +250°C	±1.5 K or ±0.4% of reading
2	Intake air relative humidity	Humidity sensor	0-100% RH	±1% RH
3	Intake air velocity	Hotwire anemometer	0-20 m/s	±0.03 m/s or 5% of reading
4	Intake static pressure	Micromanometer	0-1500 Pa	±0.01 mmH_2O
5	Supply air dry-bulb temperature	Type K thermocouples	-50 to +250°C	±1.5 K or ±0.4% of reading
6	Supply air relative humidity	Humidity sensor	0-100% RH	±1% RH
7	Supply air velocity	Hotwire anemometer	0-20 m/s	±0.03 m/s or 5% of reading
8	Supply static pressure	Micromanometer	0-1500 Pa	±0.01 mmH_2O
9	Exhaust air dry-bulb temperature	Type K thermocouples	-50 to +250°C	±1.5 K or ±0.4% of reading
10	Exhaust air relative humidity	Humidity sensor	0-100% RH	±1% RH
11	Exhaust air velocity	Hotwire anemometer	0-20 m/s	±0.03 m/s or 5% of reading
12	Exhaust static pressure	Micromanometer	0-1500 Pa	±0.01 mmH_2O
13	Feed water temperature	PT100 resistances temperature sensor	50 to +200°C	±1.0 K
14	Upper water level height *	Water level indicator	0-100 mm	±1.0 mm
15	Drain water temperature	PT100 resistances temperature sensor	50 to +200°C	±1.0 K
16	Lower water level height *	Water level indicator	0-100 mm	±1.0 mm
17	Total electric power consumption	Power meter	0-1000 W	±0.01 W

*Water consumptions of the dew point cooler are determined by measuring water level heights of the upper and lower water tanks.

(a) Type K thermocouples

(b) Humidity sensor (Vaisala HMP45A)

(c) Hotwire anemometer

(d) Micromanometer

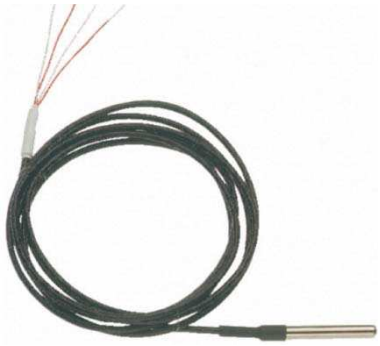

(e) PT100 resistances temperature sensor

(f) Power meter

Fig. 4-11 Photographs of the measurement instruments: (a) Type K thermocouples; (b) humidity sensor (Vaisala HMP45A); (c) hotwire anemometer (Type: Testo 425); (d) micromanometer; (e) PT100 resistances temperature sensor (Type: XQ-283-RS); (f) power meter

4.5.1 Air velocity and flow rate measurements methods

The airflow rate through ducts can be calculated by the following formula:

$$V_f = \mathrm{F}\bar{u}_f \tag{4-1}$$

where,

V_f-Air volume flow rate through ducts, m^3/s;

F-Cross sectional area of ducts, m^2;

$\bar{u}_f$-Mean air velocity across the measured cross section of ducts, m/s.

The airflow rate through ducts can be achieved by measuring mean air velocity and cross section area of ducts. For the accuracy of velocity measurements, the measured cross-section of duct should be set behind local resistance longer than 4 time diameter of circular duct and in front of local resistance longer than 1.5 time diameter of circular duct to achieve a steady and uniform flow. The measured cross section of duct is divided into a number of equal areas to determine mean air velocity. The velocities at the centre of each area were measured. The locations of these measurement points are indicated in Fig. 4-12 (Chen and Yue 1999). The mean air velocity of the circular duct is determined by taking arithmetic average of the measured velocities:

$$\bar{u}_f = \frac{\sum_{i=1}^{n} u_i}{\mathrm{n_p}} \tag{4-2}$$

where,

u_i- measured velocity in each smaller area, m/s;

$\mathrm{n_p}$-Numbers of measurement points.

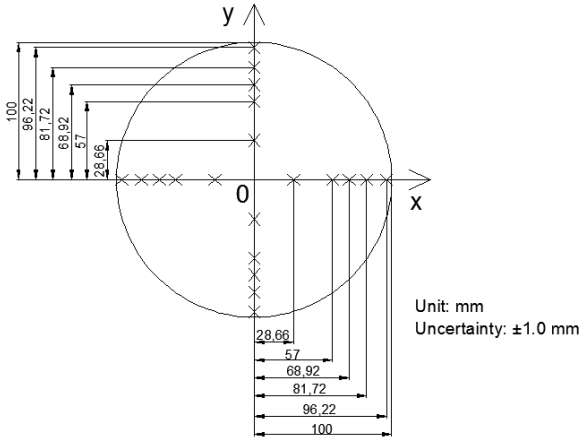

Fig. 4-12 Locations of measurement points on the cross section of circular duct (5 points in each radius)

4.5.2 Temperature measurements method

The average air temperature of a cross-section of circular duct is determined by the weighted mass flow average using the following equation (Incropera et al. 2007):

$$\bar{t}_f = \frac{\sum_{i=1}^{n} c_{p,f}\rho_f t_i u_i \mathrm{F}_i}{c_{p,f}\rho_f \bar{u}_f \mathrm{F}} \qquad (4\text{-}3)$$

where,

$\bar{t}_f$- Air average temperature of cross section, ^{o}C;

t_i- Measured temperature in each smaller area, ^{o}C;

F_i-Small equal area divided from the cross section of circular duct, m^2;

The temperature in each smaller area is measured at the same location as shown in Fig. 4-12. An average air temperatures of a duct can be solved after substituting the velocity and temperature measured in each smaller area into the above equation.

4.5.3 Humidity measurements method

As the variations of air relative humidity along the cross section of circular duct were very small (±2% RH difference), the relative humidity of air flows at the centre of cross section of ducts was considered as the average air relative humidity. The relative humidity was measured by a polymer thin film electronic humidity sensor which was fitted to the centre of the measured cross section. Based on the measured relative

humidity and dry-bulb temperature, the corresponding wet-bulb/dew-point temperatures of air were calculated by the programme of the data logger.

4.6 Testing conditions

Summer cooling design conditions (1% un-guaranteed frequency) for representative regions of Europe and China were studied based on ASHRAE standard for air conditionings (ASHRAE 1996), which are listed in Table 4-4.

Table 4-4 Cooling design temperatures for different regions in Europe/China

No.	Country	City	DBT (°C)	WBT (°C)
1	Denmark	Copenhagen	24	17.3
2	Czech Republic	Prague	27.7	18.6
3	Hungary	Budapest	30.6	19.7
4	Portugal	Lisbon	32.1	19.7
5	Israel	Ben-guion	33.1	22.4
7	Italy	Catania	34.1	21.6
8	Spain	Madrid	35.1	19.5
9	Turkey	Adana	35.1	23
10	Turkey	Izmir	35.5	20.4
11		London	27.4	18.7
12		Birmingham	25.7	17.5
13	UK	Bristol	26.3	18.2
14		Finningley	25.5	17.7
15		Manchester	25.2	17.3
16		Beijing	34.2	21.9
17		Jinan/Xi'an	34.8	22.9
18		Nanchang	35.7	26.8
19		Nanjing	34.6	27.1
20	China	Shanghai	34.4	27.4
21		Shijiazhuang	34.9	22.5
22		Wuhan	35.1	27.3
23		Zhangjiakou	31.9	18.4
24		Zhengzhou	34.7	23.6

4.7 Test procedure

The procedures of testing consist of preparation and test period.

Preparation

1) The data logger and computer were switched on, and all experimental instruments were inspected to ensure correct readings.

2) Before fans were turned on, the bottom tank of the system was filled with water by an external pump.

3) Room temperature and humidity were recorded.

4) The fans were started. All electronic instruments (heater, axial fans, triangle fan, and water pump) were checked to ensure well operating.

5) The inlet air temperature and humidity of the system were adjusted to expected inlet conditions by controlling the humidifier and heater connected to the inlet duct.

6) The static pressures of intake, supply and exhaust air ducts were controlled by adjusting the corresponding external fans speeds. The outlet airflow rate and exhaust airflow rate of system were regulated by the exhaust axial and outlet triangle fans.

7) Before testing, it allowed the cooling system to operate for 2 hours until the wet surfaces of heat exchanger were thoroughly wetted.

Test period

1) By monitoring the displays showing on the computer, once the desired inlet air conditions were achieved and stabled for at least 15 minutes, the data logger began to record the data read by the connected thermocouples and humidity sensors and meanwhile to send them back to the computer.

2) The readings displaying on the power meter were recorded during a stable test period.

3) At the beginning and then end of a steady-state operating period, the readings of upper and lower water level indicators were recorded.

4) The inlet air condition of system was then adjusted to the next setting.

4.8 Uncertainty analysis

Uncertainty analysis for the experimental results were conducted according to the following equations (Coleman and Steele 1989; Heidarinejad et al. 2009):

$$\Delta y = \left[\left(\frac{\partial f}{\partial x_1}\right)^2 (\Delta x_1)^2 + \left(\frac{\partial f}{\partial x_2}\right)^2 (\Delta x_2)^2 \cdots + \left(\frac{\partial f}{\partial x_n}\right)^2 (\Delta x_n)^2\right]^{1/2} \quad (4\text{-}4)$$

$$\frac{\Delta y}{y}=\left[\left(\frac{\partial f}{\partial x_1}\right)^2\left(\frac{\Delta x_1}{y}\right)^2+\left(\frac{\partial f}{\partial x_2}\right)^2\left(\frac{\Delta x_2}{y}\right)^2\cdots+\left(\frac{\partial f}{\partial x_n}\right)^2\left(\frac{\Delta x_n}{y}\right)^2\right]^{1/2} \quad (4\text{-}5)$$

where Δy and $\Delta y/y$ represent the absolute and relative uncertainty of dependent variables respectively; f is the function of several independent variables, i.e. $x_1,\cdots,x_n$; Δx represents the absolute uncertainty of the independent variables.

Based on the above equations, uncertainty analysis were carried out on the following concerned dependent variables, i.e., wet-bulb/dew-point effectiveness, sensible cooling capacity of intake air, energy efficiency, and water consumption rate.

Wet-bulb and dew-point effectiveness (ε_{wb} and ε_{dp}) are defined in Eqs.(4-6) and (4-7) respectively:

$$\varepsilon_{wb}=\frac{t_{db,1}-t_{db,2}}{t_{db,1}-t_{wb,1}} \quad (4\text{-}6)$$

$$\varepsilon_{dp}=\frac{t_{db,1}-t_{db,2}}{t_{db,1}-t_{dp.1}} \quad (4\text{-}7)$$

where intake air dry-bulb temperature ($t_{db,1}$) and outlet air dry-bulb temperature ($t_{db,2}$) are measured variables. The intake air wet-bulb and dew point temperatures ($t_{wb,1}$, $t_{dp.1}$) are calculated variables which are determined by the direct measured relative humidity (RH_1) and dry bulb temperature of intake air ($t_{db,1}$).

The sensible cooling capacity of intake air for the dew point cooler can be calculated by the following equation:

$$Q_{\text{cooling,IA}}=\frac{c_{p,f}\rho_f V_2\left(t_{db,1}-t_{db,2}\right)}{3.6} \quad (4\text{-}8)$$

where the supply air volume flow rate (V_2) is determined by the measured supply air velocity (u_2) and the associated diameter of cross-sectional area (d). The specific heat ($c_{p,f}$) and density of outlet air are dependent on the dry bulb temperature ($t_{db,2}$) and relative humidity of outlet air (RH_2).

The energy efficiency of the dew point cooler is defined as:

$$\text{Energy efficency}=\frac{Q_{\text{cooling,IA}}}{W_{\text{p}}+W_{\text{w}}+W_{\text{pump}}} \quad (4\text{-}9)$$

where the power consumptions of fans and pump are measured variables and the uncertainty of sensible cooling capacity is decided by Eq.(4-8).

The water consumption rate (or water evaporative rate) of the dew point cooler is determined by the following formula:

$$V_w = \frac{1000 V_3 \rho_{w,f}}{\rho_w} (w_3 - w_1) \quad (4\text{-}10)$$

where exhaust air volume flow rate (V_3) is dependent upon the measured exhaust air velocity (u_3) and the associated diameter of cross-sectional area (d); Exhaust air humidity ratio (w_3) is determined by the measured dry-bulb temperature ($t_{db,3}$) and relative humidity of exhaust air (RH_3); Intake air humidity ratio (w_1) is decided by the measured dry-bulb temperature ($t_{db,1}$) and relative humidity of intake air (RH_1).

Based on the correlations above, the uncertainty analysis were performed for the results of experiments, i.e., wet-bulb/dew-point effectiveness, sensible cooling capacity of intake air, EER and water consumption rate by using Engineering Equation Solver (EES) software (Klein 2010). Table 4-5 shows the measured variables and the nominal values gained from the experiments with corresponding relative uncertainties specified by the measurement instruments. Table 4-6-shows the results of uncertainty analysis conducted on the calculated variables.

Table 4-5 Details of the measured variables

No.	Measured variable	Nominal value	Relative uncertainty
	x_n		$\Delta x_n / x_n$
1	$t_{db,1}$	36.36 (°C)	±0.4%
2	$t_{db,2}$	25.67 (°C)	±0.4%
3	$t_{db,3}$	27.29 (°C)	±0.4%
4	RH_1	45%	±1%
5	RH_1	77%	±1%
6	RH_3	82%	±1%
7	u_2	0.54 (m/s)	±5%
8	u_3	0.46 (m/s)	±5%
9	d	0.2 (m)	±0.25%
10	$W_{\mathrm{p}}+W_{\mathrm{w}}+W_{\mathrm{pump}}$	20.2 (W)	±0.05%

A detailed uncertainty analysis was performed to examine the overall uncertainty for all experimental data. It is found that the overall uncertainty was within ±2.0% for

wet-bulb effectiveness, ±5.3% for sensible cooling capacity, ±5.3% for energy efficency and ±5.7% for water consumption rate of dew point cooler.

Table 4-6 Results of uncertainty analysis for the calculated variables

No.	Calculated variable	Nominal value	Absolute uncertainty	Relative uncertainty
	y		Δy	$\Delta y/y$
1	ε_{wb}	1.053	±0.0180	±1.71%
2	ε_{dp}	0.777	±0.0149	±1.92%
3	V_2	61 (m^3/h)	±3.07	±5.03%
4	$Q_{\text{cooling,IA}}$	215.7 (W)	±11.4	±5.29%
5	Energy efficiency	10.6	±1.93	±5.30%
6	V_3	52 (m^3/h)	±2.61	±5.02%
7	w_3	0.03221(kg/kg)	±0.00043	±1.33%
8	w_1	0.01737 (kg/kg)	±0.00021	±1.21%
9	V_w	0.88 (litre/h)	±0.0503	±5.69%

Chapter5.
Discussions of Experiment Results and Validation of Simulations

5.1 Testing results and effects of parameters

5.1.1 Average results for unit performance

Table 5-1 lists the average test results for the performance of the dew point cooling unit working at a constant inlet condition.

Table 5-1 Average results for unit performance

(Inlet dry bulb temperature=36^{o}C, Inlet wet bulb temperature=20^{o}C)

Parameter	High Speed	Low Speed
Outlet airflow (m^3/h)	124	57
Exhaust airflow (m^3/h)	124	57
Working-to-intake air ratio	0.5	0.5
Power consumption (W)	38	30
Wet-bulb effectiveness (%)	79	91
Cooling capacity (W)	546	293
Energy efficiency	14	10

5.1.2 Temperatures versus time

Fig. 5-1 shows the inlet, outlet and exhaust airflow dry-bulb temperature variations process with time during a constant stable period. The outlet air dry-bulb temperature of the unit maintained a constant and the exhaust air dry-bulb temperature was slightly sensitive to the inlet dry-bulb temperature. The slight sensitivity may be partly due to the fact that the outlet air rate is only a partition of the inlet air rate and partly due to the exhaust air, as a partition of inlet air, exchanges mainly latent heat with the inlet

air indirectly. In other words, inlet air dry-bulb temperature have a little effect on the latent heat transfer of dew point cooler.

Fig.5-2 shows the variations of inlet air, outlet air and exhaust air temperatures during a transient state period. There was a slight increase in the outlet and exhaust air temperatures with increasing the inlet air temperature of the cooler, but their sensitivity to the rising inlet temperature was very little, which may be due to the same reasons as in Fig. 5-1.

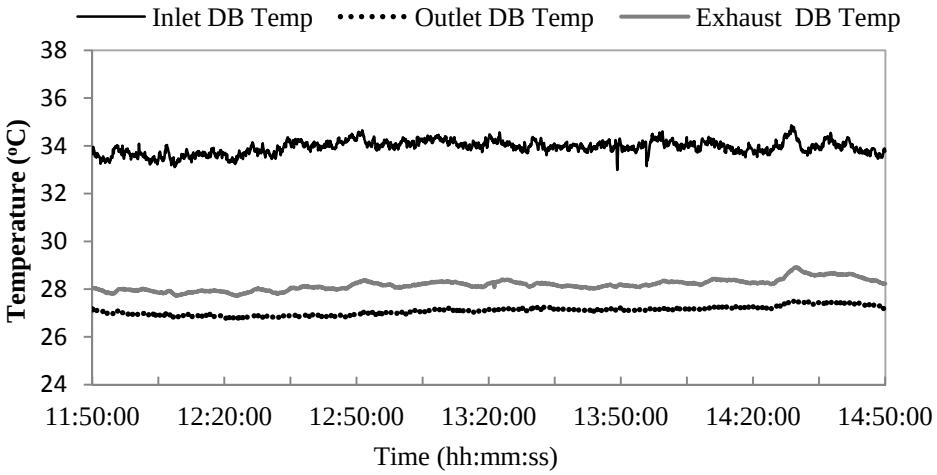

Fig. 5-1 Air temperature variations versus time (outlet airflow rate=116 m^3/h, working-to-intake air ratio=0.5)

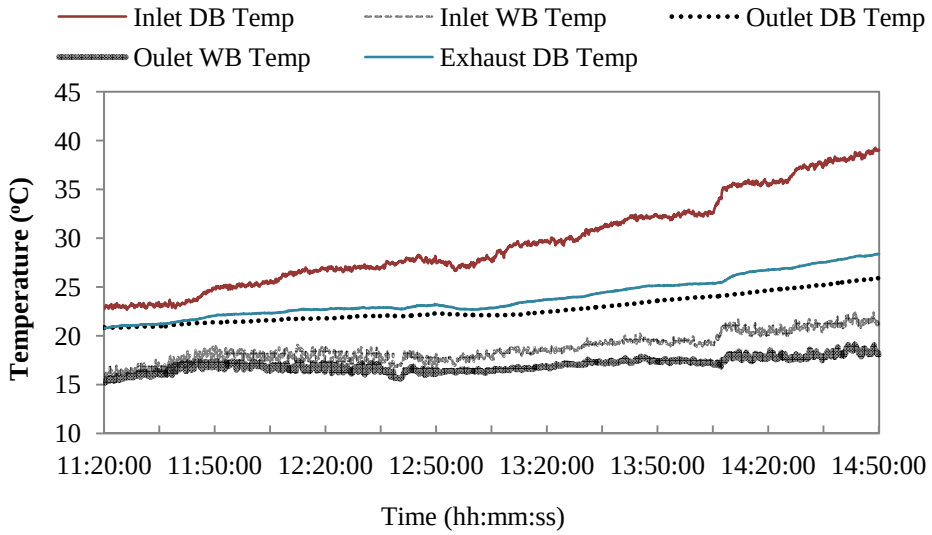

Fig. 5-2 Air temperature variations versus time (outlet airflow rate=116 m^3/h, working-to-intake air ratio=0.5)

5.1.3 Effects of intake air temperature and humidity

Fig. 5-3 shows the effectiveness as a function of temperature difference between inlet air dry-bulb and wet-bulb, which is referred to as inlet wet-bulb depression. Fig. 5-4 shows the effectiveness and inlet temperature variations with time.

Increasing inlet wet bulb depression resulted in the increases in wet-bulb effectiveness and dew-point effectiveness. However, the effectiveness underwent a slight slope when the inlet wet bulb depression was greater than 16.7°C. In other words, the wet-bulb/dew-point effectiveness reached to the peak when the inlet wet-bulb depression was up to 16.7°C. Similarly, Fig. 5-2 shows an increase in wet-bulb effectiveness with increasing inlet wet-bulb depression as well. This may be due to the reduced intake air density as a result of increasing temperature. It contributes to an increased evaporative rate.

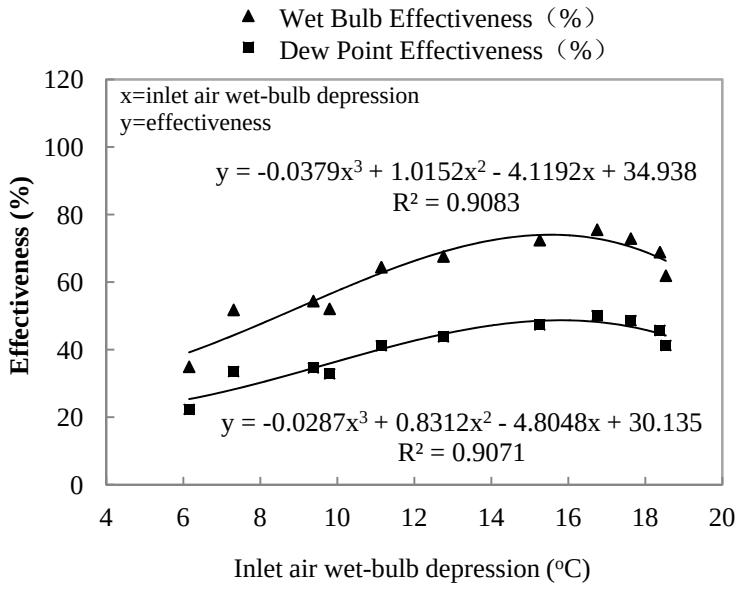

Fig. 5-3 Effectiveness versus inlet air wet-bulb depression (outlet airflow rate=116 m^3/h, working-to-intake air ratio=0.5)

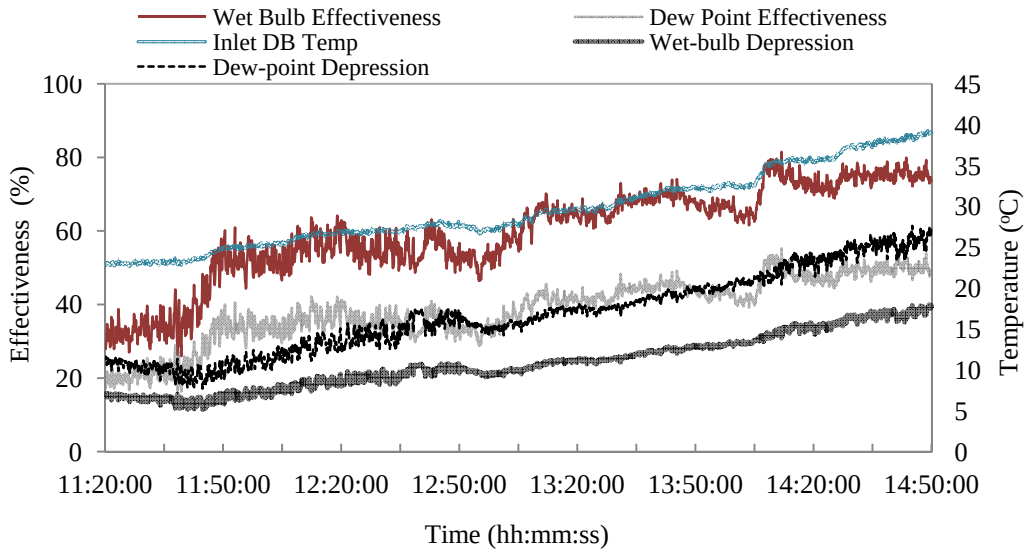

Fig. 5-4 Inlet temperature and effectiveness versus time (outlet airflow rate=116 m^3/h, working-to-intake air ratio=0.5)

Fig. 5-5 shows the cooling output and energy efficiency of the cooler as a function of inlet wet bulb depression. It is noticed that the cooling capacity and energy efficiency gradually increased with the inlet wet bulb depression increasing from 6-16.7°C and then slightly decreased when the inlet wet bulb depression increasing from 16.7-18.5°C. The inlet wet-bulb depression can be regarded as the driven force for indirect evaporative cooling. Thus, indirect evaporative cooling is more suitable for the regions with hot and dry climates.

The slight decrease after the gradual increase, as shown in Fig. 5-5, was due to the fact that condensation may occur at the exhaust air duct when the exhaust air temperature was increased to a degree where the dew-point temperature of exhaust air was higher than the ambient temperature. The occurs of condensation can be verified by analysing state changes of exhaust air with inlet temperature.

The psychrometirc chart of exhaust and ambient air states is shown in Fig. 5-6. State 1 represented the state point of exhaust air when the inlet temperature reached 40°C. When it increased to about 41°C, the exhaust air state changed to state 2 where the condensation may occur. In this situation, the dew-point temperature of exhaust air was increased to 25°C which was higher than the ambient dry-bulb temperature (The ambient dry-bulb temperature was 24.3°C, marked as state 4 on the chart). The state of exhaust air changed to state 3 after being condensed on the surface of extension duct. Therefore, the real temperature and humidity of exhaust air cannot be measured

correctly as the installation positions of humidity and temperature sensors of exhaust air were inside the extension duct.

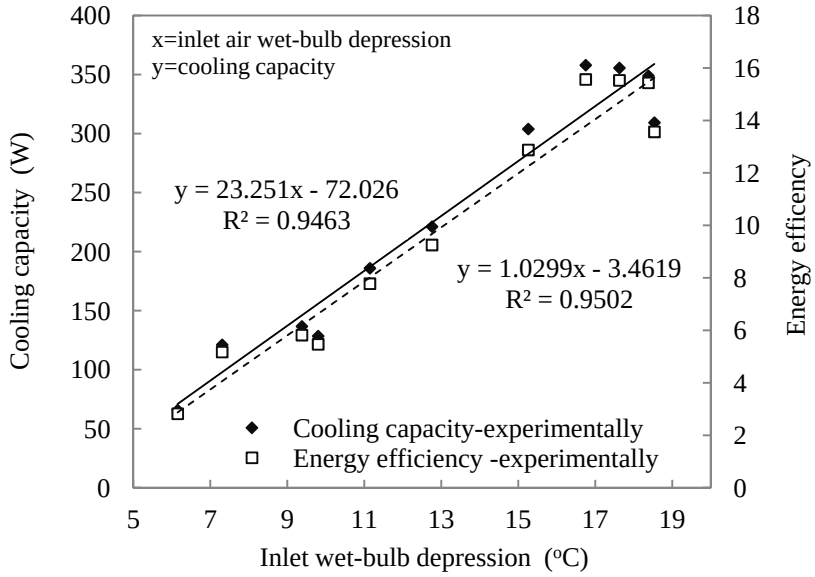

Fig. 5-5 Cooling capacity and energy efficiency versus inlet wet-bulb depression (outlet airflow rate=116 m^3/h, working-to-intake air ratio=0.5)

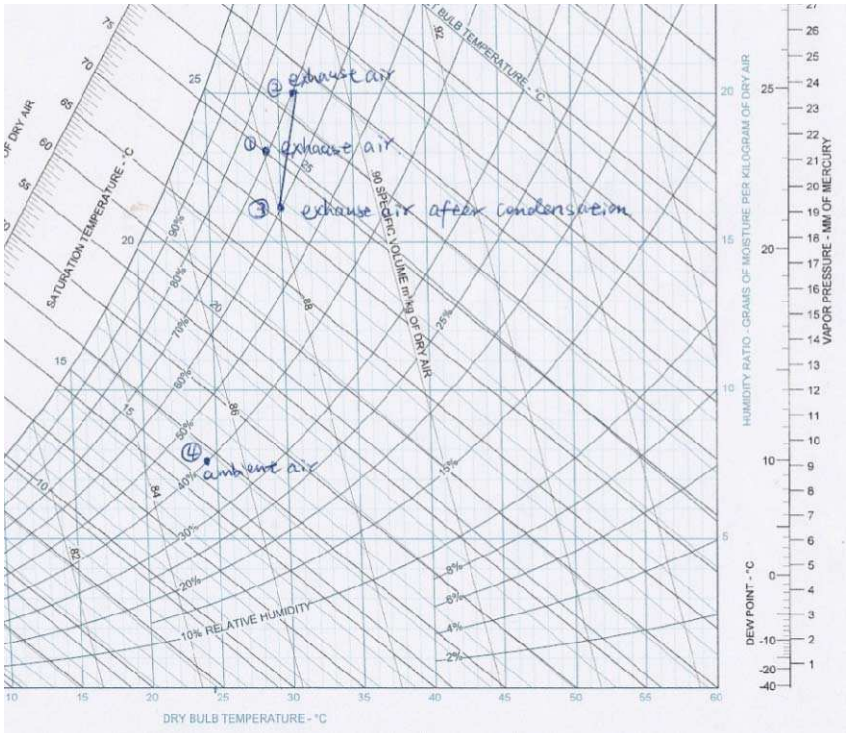

Fig. 5-6 Psychrometric chart illustrating condensation in exhaust air

5.1.4 Effect of intake channel air velocity

Fig. 5-7 shows the wet-bulb/dew-point effectiveness as a function of intake channel air velocity. It is found that the wet-bulb/dew-point effectiveness was decreased gradually with increasing the intake channel air velocity. This may be due to the reduced contact time between working air and wet surfaces which results in a decreased evaporative rate.

Fig. 5-8 shows the cooling capacity and energy efficiency of the cooler as a function of intake channel air velocity. The power consumption and energy efficiency of the cooler were increased with increasing the intake channel air velocity from 0.4 to 1.4 m/s. The increasing energy efficiency may be due to the reason that the increase in cooling capacity was higher than the increase in power consumption. In theory, energy efficiency of the system should decrease with increasing intake air velocity due to a greatly increased pressure drop. However, in this cooler, two fans were connected in parallel to boost the pressure of supply and working air. As a result of connecting in parallel, the overall pressure of the two fans slightly inclined with increasing the airflow rate. Thus, the power consumptions of fans are slightly increased.

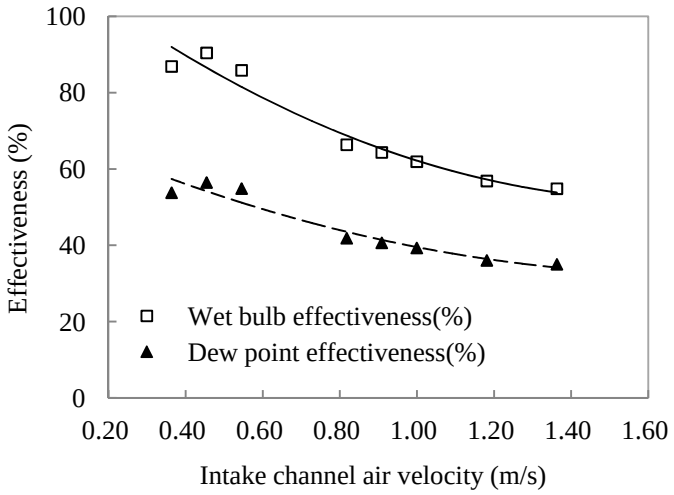

Fig. 5-7 Effectiveness versus intake channel air velocity (dry-bulb temp.=36°C, wet-bulb temp.=20°C, working-to-intake air ratio=0.5)

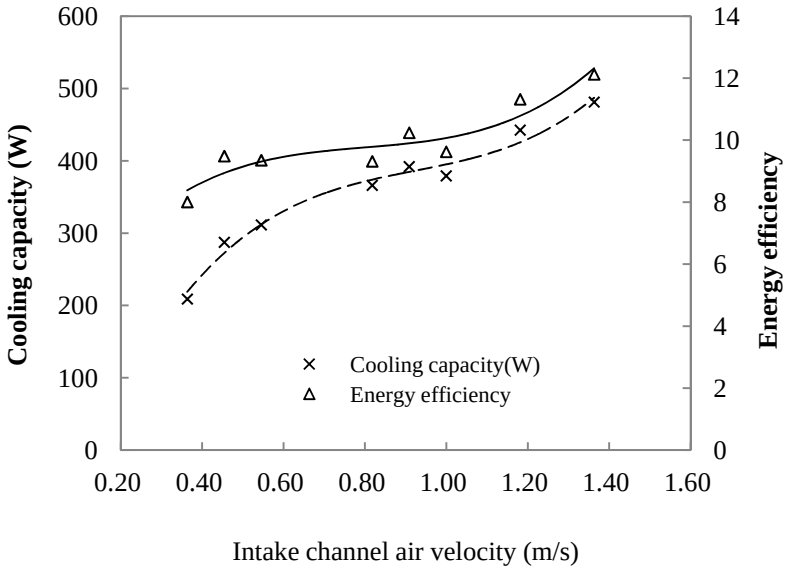

Fig. 5-8 Cooling capacity and energy efficiency versus intake channel air velocity (dry-bulb temp.=36°C, wet-bulb temp.=20°C, working-to-intake air ratio=0.5)

5.1.5 Effect of working-to-intake air ratio

Fig. 5-9 shows the wet-bulb/dew-point effectiveness as a function of working-to-intake air ratio. It can be seen that wet-bulb/dew point effectiveness were increased with increasing the working-to-intake air ratio. This may be due to the increased working air and increased evaporation.

Fig. 5-10 shows the cooling capacity and energy efficiency of the cooler versus working to intake air ratio. It can be found that there is a decrease in cooling capacity and energy efficiency with increasing working-to-intake air ratio. The cooling capacity is reduced owing to the decreased supply air flow rate. The decreased energy efficiency may be due to the increased power consumptions of fans.

From the above analysis, the enhanced effectiveness of cooler is achieved at the lost of cooling capacity. Therefore, a reasonable working-to-intake air ratio should allow the cooler to achieve a compromise between cooling capacity and effectiveness. In the Fig. 5-9, the effectiveness of the cooler increased slightly with increasing the working-to-intake air ratio from 0.5 and 0.7. Thus, taking into account the effects of working-to-intake air ratio on effectiveness and cooling capacity, the appropriate ratio should be in the range of 0.4-0.5.

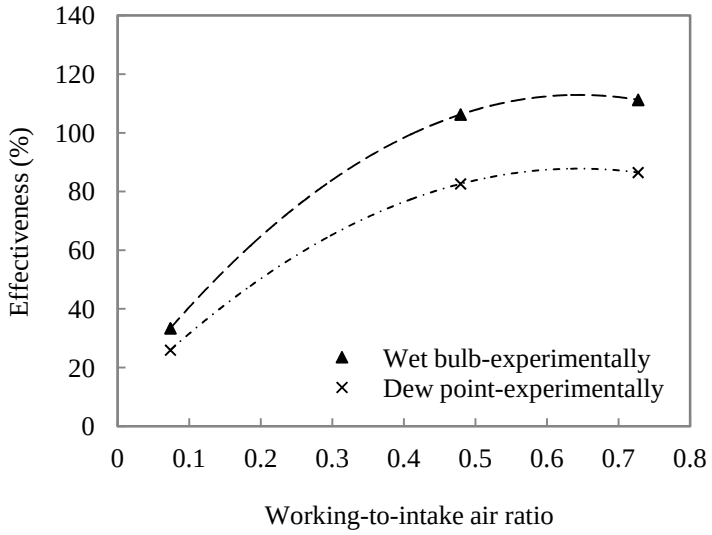

Fig. 5-9 Effectiveness versus working-to-intake air ratio (intake air dry/wet-bulb temp.=36.5/28.5°C, intake channel air velocity=0.4 m/s

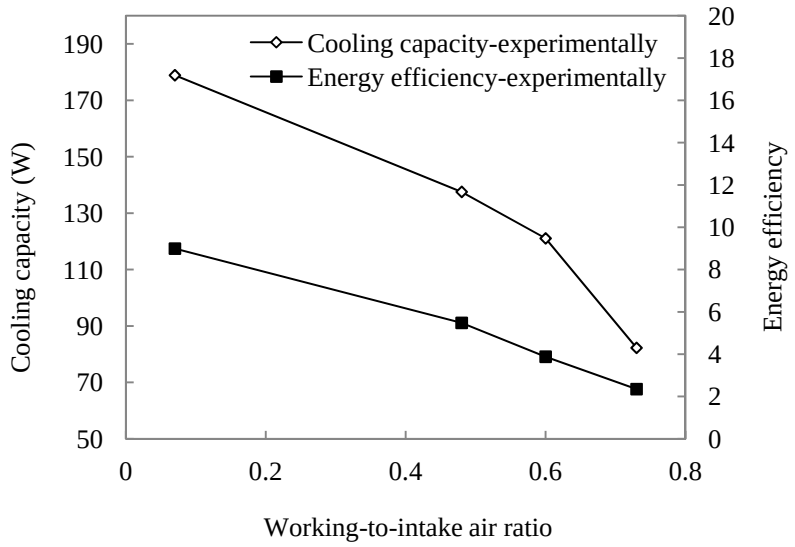

Fig. 5-10 Cooling capacity and energy efficiency versus working-to-intake air ratio (intake air dry/wet-bulb temp.=36.5/28.5°C, intake channel air velocity=0.4 m/s)

5.1.6 Effect of water temperature

The feed water temperature of the cooler was cooled by ice water to study the effect of water temperature on the performance of cooler.

Fig. 5-11 shows the wet-bulb/dew-point effectiveness of the test unit variations with feed water temperature. It is noticed that the wet-bulb/dew-point effectiveness decreased less than 5% when the water temperature increased from 18 to 23^{o}C, which is the normal range of tap water temperature. Therefore, it is concluded that the feed water temperature has insignificant effect on the wet-bulb/dew point effectiveness of the dew point cooler.

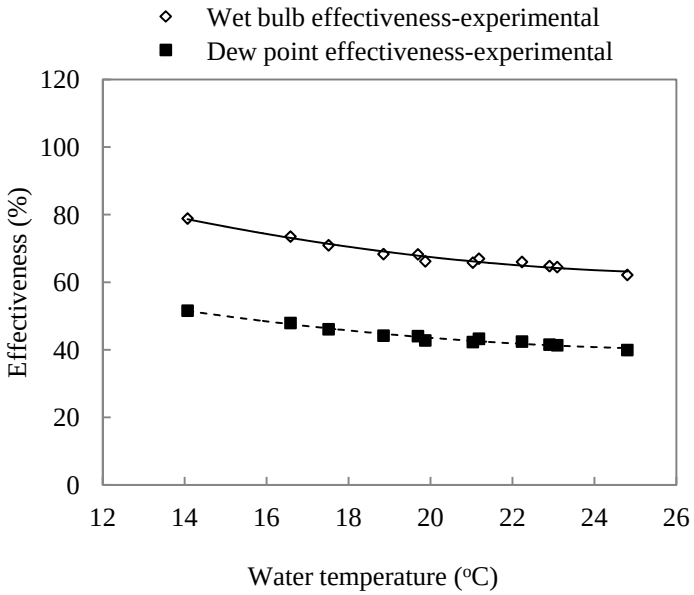

Fig. 5-11 Effectiveness versus water temperature (intake air wet-bulb temperature=20^{o}C, outlet airflow rate=116 m^{3}/h, working-to-intake air ratio=0.5)

5.1.7 Water evaporation rate

Water evaporation rate of the cooling unit is determined by the amount of increase in the humidity ratio of working air multiplying by the working air flow rate during an evaporation process. The calculated water evaporation rates were verified with the measured water consumption rates derived from reading the water level indicators. The difference may lie in the measurement errors, such as inaccurate readings of water level indicators, neglecting of spraying or wasted water, etc.

Fig. 5-12 shows the calculated results of water evaporation rate as a function of inlet wet bulb depression. It is found that the water evaporation rate had a linear relationship with the inlet wet bulb depression when other parameters remained constant. The water evaporation rate was enhanced with increasing the inlet wet bulb depression. The experiment data of water evaporative rate was fitted by a linear function. The fitted linear equation can be useful in the further design to estimate the water evaporative rate of a dew point cooler. For example, if the dry bulb/wet-bulb temperature of inlet air is 34°C and 20°C respectively, the calculated water evaporation rate of the cooler is approximate 0.84 litre per hour. If a dew point cooler continuously operates for 8 hours daily, the daily water evaporation rate is about 6.72 litre, which accounts for 32% volume capacity of the upper water tank. The remaining 68% of water can participate in the water circulation.

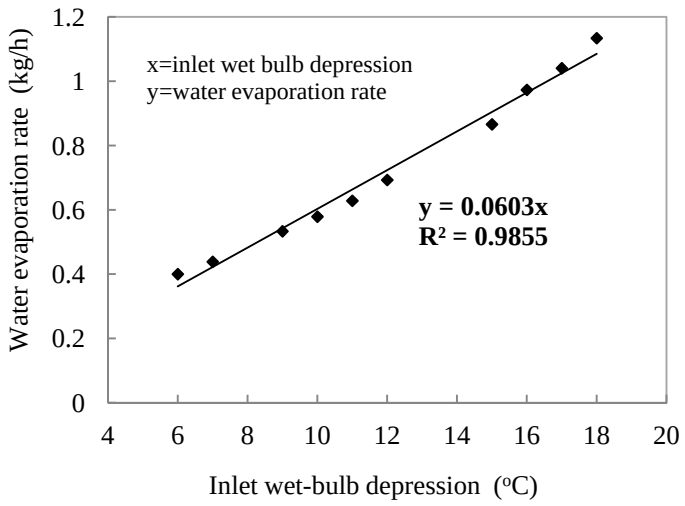

Fig. 5-12 Water evaporation rate versus inlet wet-bulb depression (outlet airflow rate=116 m^3/h, working-to-intake air ratio=0.5)

5.1.8 Performance of cooler in various climate conditions of Europe/China

Testing were conducted to investigate the real performance of the cooler working under various climate conditions of Europe and China. To achieve a high wet-bulb/dew point effectiveness, the dew point cooler was set to operate at 0.4 m/s of intake channel air velocity and 0.5 of the working-to-intake ratio. The intake temperature and humidity of the cooler was controlled by a heater and humidifier to simulate the climate conditions of various cities within Europe and China. The testing

results for the cities of Europe and China with typical climates are shown in Table 5-2 and 5-3 respectively. It is found that the dew point cooler can provide low supply air temperature (from 19 to 24^{o}C) for most cities except for some cities with high humid climate, such as Wuhan, Shanghai, Nanjing and Nanchang of China. Apart from these humid regions, the cooling capacity provided by the dew point cooler can meet the cooling demands of the buildings for most regions of Europe and China.

The wet-bulb effectiveness of the cooler was in the range 0.71 to 1.0, which was slightly lower than the results derived from the computer simulation. The reasons for the difference will be analysed in the next section.

The energy efficiency of the cooler varied from 7.8 to 34.1, depending upon the locations where the cooler is applied. These figures were again lower than the predicted value due to the smaller size of cooler which did not maximise the utilizations of the fans. In other word, the selected fans were larger than the design requirements and they were operated at a lower efficiency than expected. To achieve an ideal energy efficiency as predicted, a larger cooler that is suitable for commercialisation should be further explored, as the part of further work of the research.

Table 5-2 Performance of cooler in various climate conditions of Europe

(Intake channel air velocity=0.4 m/s, working-to-intake air ratio=0.6)

No.	Country	City	Dry-bulb temperature (°C)	Wet-bulb temperature (°C)	Wet-bulb effectiveness	Supply air temperature (°C)	Cooling capacity (kJ/h)	Power (W)	Energy efficiency	Water evaporation rate (litre/h)
1	Denmark	Copenhagen	24	17.3	0.800	18.6	235.48	28.20	2.3	0.18
2	Czech Republic	Prague	27.7	18.6	0.989	18.7	348.60	28.20	3.4	0.22
3	Hungary	Budapest	30.6	19.7	0.906	20.7	485.89	26.5	6.4	0.34
4	Portugal	Lisbon	32.1	19.7	0.852	21.5	347.87	12.25	7.9	0.33
5	Israel	Ben-guion	33.1	22.4	0.849	24.0	160.50	9.12	4.9	0.17
6	Greece	Athens	33.8	20.8	0.839	22.9	615.87	25.10	6.8	0.31
7	Italy	Catania	34.1	21.6	0.891	23.0	441.13	18.80	6.5	0.41
8	Spain	Madrid	35.1	19.5	0.869	21.5	767.77	26.10	8.2	0.40
9	Turkey	Adana	35.1	23	0.995	23.1	529.42	25.90	5.7	0.32
10	Turkey	Izmir	35.5	20.4	0.821	23.1	843.05	27.2	9.5	0.46
11		London	27.4	18.7	0.95	19.1	348.6	28.2	11.6	0.32
12		Birmingham	25.7	17.5	0.84	18.8	290.2	28.2	3.4	0.32
13	UK	Bristol	26.3	18.2	0.83	19.6	281.7	28.2	2.8	0.32
14		Finningley	25.5	17.7	0.79	19.3	260.7	28.2	2.7	0.32
15		Manchester	25.2	17.3	0.71	19.6	235.5	28.2	2.5	0.32

Table 5-3 Performance of cooler in various climate conditions of China

(Intake channel air velocity=0.4 m/s, working-to-intake air ratio=0.6)

No.	City	Dry-bulb temperature (°C)	Wet-bulb temperature (°C)	Wet-bulb effectiveness	Supply air temperature (°C)	Cooling capacity (kJ/h)	Power (W)	Energy efficiency	Water evaporate rate (litre/h)
1	Beijing	34.2	21.9	0.85	23.7	439.1	25.9	4.7	0.33
2	Jinan	34.8	22.9	0.87	24.4	434.8	25.9	4.7	0.32
3	Nanchang	35.7	26.8	0.80	28.6	299.0	26.9	3.1	0.29
4	Nanjing	34.6	27.1	0.79	28.7	248.9	26.9	2.6	0.21
5	Shanghai	34.4	27.4	0.79	28.9	232.3	25.9	2.5	0.23
6	Shijiazhuang	34.9	22.5	0.90	23.7	468.7	25.9	5.0	0.42
7	Wuhan	35.1	27.3	0.78	29.0	255.5	26.9	2.6	0.31
8	Zhangjiakou	31.9	18.4	0.88	20.0	499.0	19.9	7.0	0.23
9	Zhengzhou	34.7	23.6	0.86	25.2	400.9	25.9	4.3	0.32

5.2 Comparison between numerical and experimental results

Upon to completion of the validation of the computer model using several published data, the experimental results of the dew point cooler prototype were compared against the simulation results derived from the verified computer model. The comparison was made on the basis of the identical operating conditions, i.e., the same inlet air condition, same structural and geometrical sizes of heat exchanger. Fig. 5-13 shows the difference between theoretical and experimental wet-bulb effectiveness as a function of inlet wet-bulb depression. A gap of 20 to 30% effectiveness was found. The bigger gap occurred at the smaller wet-bulb depression, and the gap was getting closer when the depression value was higher. The reasons for the gap were given very close examination and below are some critical findings that could explain the situation.

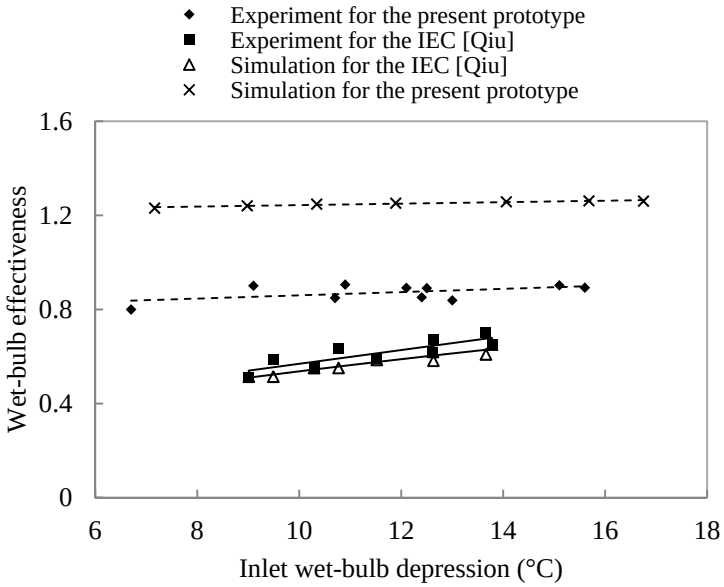

Fig. 5-13 Difference between numerical and experimental wet-bulb effectiveness as a function of inlet wet-bulb depression (outlet airflow rate=116 m^3/h, working-to-intake air ratio=0.5)

First of all, the wet surfaces of heat/mass exchanger were not well distributed with water film as expected. It was caused by the undesirable water distribution(see Fig. 5-14) structure and deteriorated wetting conditions of the fibre sheets. For the water distribution structure in use, the sponge strips in between the wet channels of exchanger may not distribute water uniformly and evenly as expected. In addition, the inserted corrugated sheets may disrupt the water distribution. For the fibre sheets of wet channel, the wetting conditions may be deteriorated after using for several times.

Secondly, across the entrance of the heat exchanger, the intake air channel velocity was not distributed uniformly as assumed in the simulation. The uneven intake air velocity distribution results in the decreased performance of heat/mass exchanger.

Thirdly, the fibre sheets of exchanger were originally coated with a type of thin plastic films, which may be melt into the fibre after coating with aluminum foil by the heating process. This may destroy the fibre structure and lead to a reduced capillary forces. To avoid this, a thermal-grease coating method should be used to replace the current heating method in further work.

Fourthly, the corrugated sheets use as triangular air guiders of channels may be the major barriers affecting the heat transfer between dry and wet air. The situation was that the angle of the corrugated sheets was not absolutely ‘sharp’. Instead, a ‘flat’ angle was in present, as shown in Fig. 5-15 and Fig. 5-16, which blocked a large proportion of heat transfer area and therefore, reduced the effectiveness of the heat exchanger. This situation became even worse during the heat/mass exchanger assembling. As the sheets were stacked together and tighten up using bolts, which heavily squeezed the guider sheets and further widen the contact area between ‘flat’ angle and sheet, see Fig. 5-17. Lesson learnt from this process suggests that the individual rectangular bars should be used in next stage development of the commercial unit. These bars should have 2mm thickness allowing self standing between the channel spacing. The distance between the rectangular bars should be as large as possible, presumably 20 to 30 mm, providing that the supported channels won't collapse

Fifthly, it is found that small quantities of water droplets were spilled over from the wet channels to the dry channels during the operation of cooler. This may be due to the perforations on the aluminum sheets of exchanger were not perfectly drilled in laboratory. It is believed that machinery work will remove this inaccuracy if the cooler is mass produced in factory.

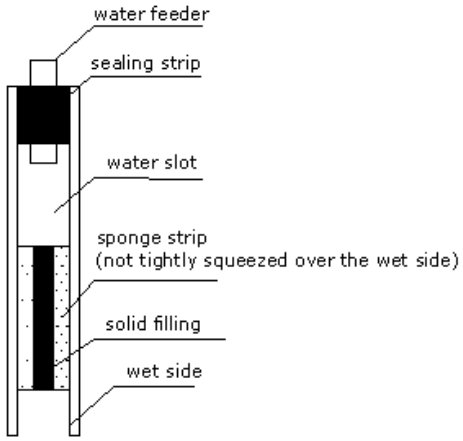

Fig. 5-14 Schematic of water distribution structure

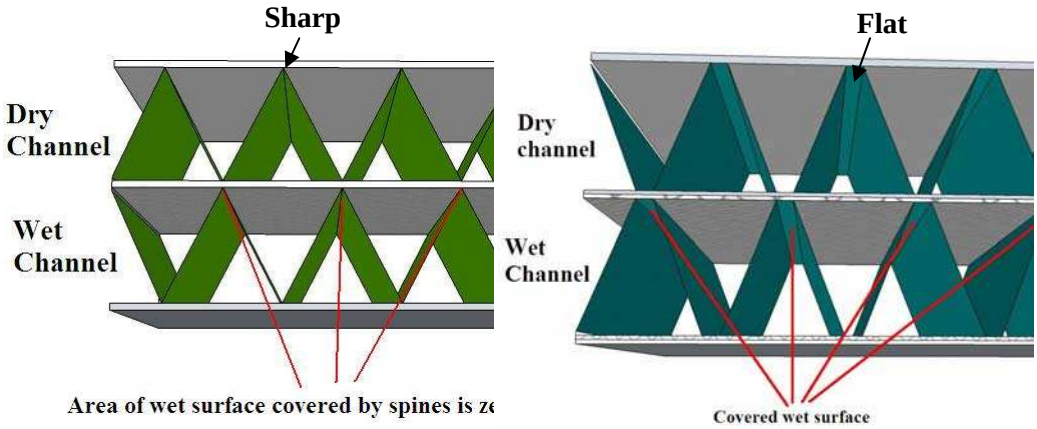

a. theoretical condition b. real condition

Fig. 5-15 The 'angle' illustration of corrugated sheet

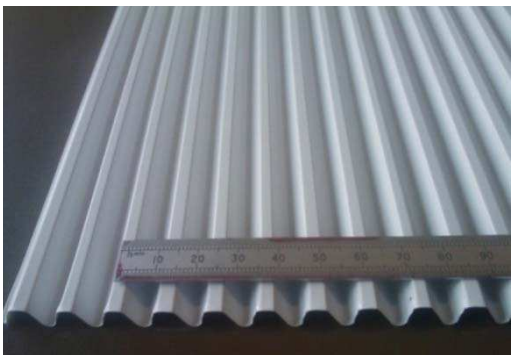

Fig. 5-16 Real guide geometry of corrugated sheet

Fig. 5-17 Bolting up of the exchange sheets stack

Finally, all construction works of the prototype were made manually due to limited manufacturing level in laboratory. This inevitably resulted in the existence of inaccuracy and impreciseness. We expect that factory machinery work will remove these problems.

To summarise, the discrepancy between simulation and experiment may be due to the undesirable wetting condition of fibres, inefficient water distribution structure, uneven intake air distribution, reduced heat transfer area arising from the 'flat-angle' of corrugated sheets.

Other parameters, such as intake air velocity and working-to-intake air ratio, were compared numerically and experimentally as shown in Fig. 5-18 and Fig. 5-19 respectively.

In Fig. 5-18, the rates of decreases in wet-bulb effectiveness with increasing intake air velocity were similar between the simulation and experiment. In Fig. 5-19, the increasing trends of effectiveness with increasing working-to-intake air ratio were very similar between the experimental and numerical results. The gap (20-30%) between them may be due to the same reasons as explained above.

The effects of water temperature on wet-bulb effectiveness of the cooler were compared numerically and experimentally in Fig. 5-20. Either numerical or experimental results suggests that the feed water temperature has an insignificant effect on the effectiveness of heat/mass exchanger.

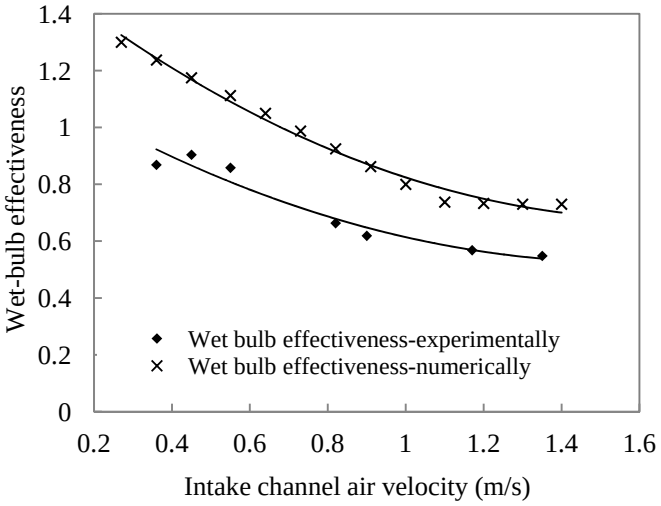

Fig. 5-18 Difference between numerical and experimental wet-bulb/dew-point effectiveness as a function of intake channel air velocity (intake air dry/wet-bulb temperature=36/21°C, working-to-intake air ratio=0.5)

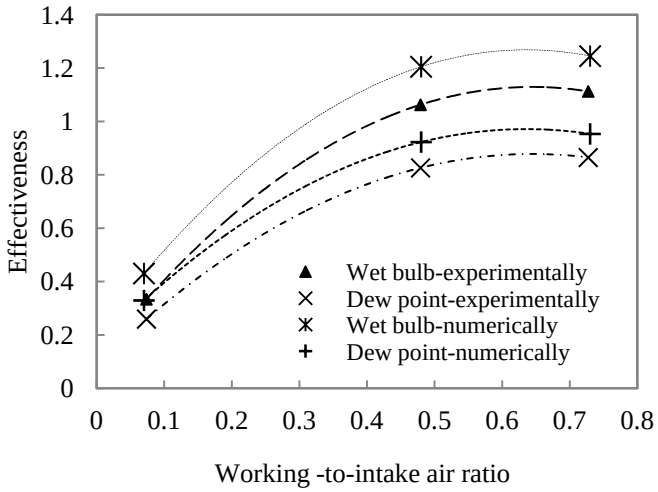

Fig. 5-19 Difference between numerical and experimental effectiveness as a function of working-to-intake air ratio (intake air dry/wet-bulb temperature=36.5/28.5°C, intake channel air velocity=1.0 m/s)

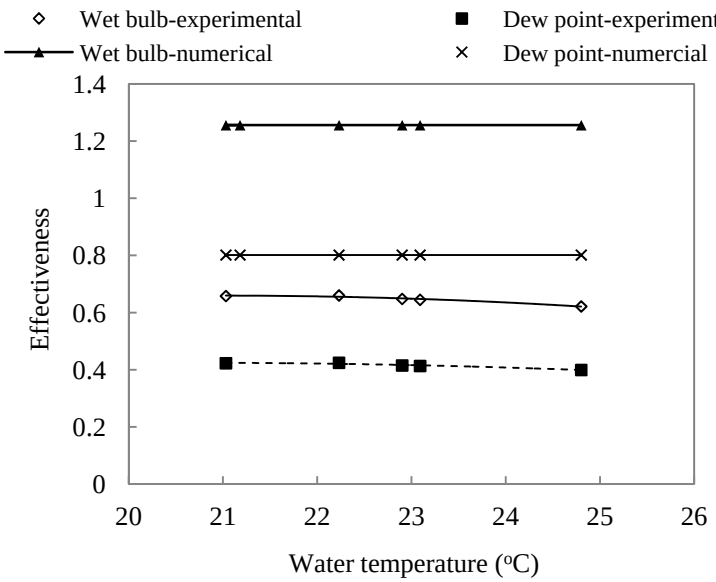

Fig. 5-20 Difference between numerical and experimental wet-bulb/dew-point effectiveness as a function of water temperature (intake wet-bulb temperature=20°C, outlet airflow rate=116 m^3/h, working-to-intake air ratio=0.5)

Chapter6.
Economic, Environmental and Regional Acceptance Analyses

6.1 Research objectives

The objectives of this chapter is to analyses the feasibility of new dew point cooling system to be used in Europe and China and evaluate the economic effect relating to purchase, installation, operation of the system and associated carbon emission reduction. The following results are expected to be achieved from this part of research:

- Acceptance analyses of the new dew point cooling system used in Europe and China areas;
- Estimated capital cost, energy saving and payback period of the system when being operated in the buildings of Europe and China;
- Environmental effect of the system in terms of carbon emission reduction.

6.2 Regional acceptance analyses

6.2.1 Performance evaluation of the dew point cooler

The working principle of the dew point cooling system was illustrated in Chapter 1 – section 1.2.1. According to Fig.1-4 (b), the total cooling capacity of the dew point system can be calculated as follows:

$$Q_{\text{total}} = \frac{\rho_f V_2 (i_1 - i_2)}{3.6} \quad (6\text{-}1)$$

where i_2 can be resolved from the definition of dew-point effectiveness:

$$i_{db,2} = i_{db,1} - \varepsilon_{dp}\left(i_{db,1} - i_{dp,1}\right) \quad (6\text{-}2)$$

where symbol i_1 represents the specific enthalpy of intake air of the dew point cooler. It can be solved using the dry-bulb temperature of intake air and its humidity ratio as shown in Eq.(6-3)(Çengel and Boles 2007). For different regions where the dew point cooler applied to, the transient specific enthalpy of intake air of the cooler can be obtained from regional transient weather data.

$$i_{db,1} = (1.01 + 1.84w_1)t_{db,1} + 2500w_1 \quad (6\text{-}3)$$

The specific enthalpy of saturated air at the intake air temperature ($i_{dp,1}$) could be achieved by the above equation, wherein the corresponding independent variables are replaced by the dew point temperature and constant humidity ratio.

Also, the supply air dry-bulb temperature of dew point cooler can be obtained from the following equation:

$$t_{db,2} = t_{db,1} - \varepsilon_{dp}(t_{db,1} - t_{dp,1}) \quad (6\text{-}4)$$

The air in the dry channels of dew point system experiences a constant humid process, i.e.,$w_2 = w_1$. Thus the wet-bulb temperature of supply air can be decided by the two resolved properties (i.e., $t_{db,2},\ w_2$).

Specific enthalpy of exhaust air can be achieved by law of energy conservation:

$$i_{db,3} = i_{db,2} + \frac{V_1}{V_3}(i_{db,1} - i_{db,2}) \quad (6\text{-}5)$$

In theoretical situations, exhaust air is discharged to outside as saturated moist air (relative humidity$\approx$100%) if being contact with water film thoroughly. Thus the humidity ratio and dry-bulb temperature of exhaust air ($w_3, t_{db,3}$) can be achieved by examining its specific enthalpy, $i_{db,3}$, at the saturation line of psychrometric chart.

If indoor design temperature is given (t_{in}), the effective cooling output of the cooler, a part of cooling capacity, is supplied to remove the internal sensible heat load of the air-conditioned space. The effective cooling output can be expressed as:

$$Q_e = \frac{\rho_f c_{p,f} V_2 \left(t_{in} - t_{db,2}\right)}{3.6} \quad (6\text{-}6)$$

The other part of cooling capacity is used to remove the outdoor fresh air load of the air-conditioned space. It will be referred to as outdoor fresh air cooling output defined as:

$$Q_o = Q_{\text{total}} - Q_e = \frac{\rho_f c_f V_2 \left(t_{db,1} - t_{in}\right)}{3.6} \quad (6\text{-}7)$$

The water consumption per kWh cooling output of the cooler is calculated by:

$$V_w = 3600 \frac{w_3 - w_2}{\rho_w (i_{db,1} - i_{db,2})} \quad (6\text{-}8)$$

Some assumptions were made to simplify the calculations of feasibility study: (1) the density/specific heat of air and water were regarded as constants, i.e., $\rho_f = 1.2$ kg/m^3, $c_{p,f} = 1.0$ kJ/(kg · K), $\rho_w = 1000$ kg/m^3, $c_{p,w} = 4.2$ kJ/(kg · K) (2) the dew-point effectiveness is assumed as a constant in the calculation process, i.e., $\varepsilon_{dp} = 0.85$; (3) The ratio of working to intake air volume rate is 0.5, i.e., $2V_3 = V_1$, $2V_2 = V_1$; (4) specific enthalpy of air is in a linear relationship with temperature.

6.2.2 Analyses of the Europe/China weather data

Weather data for a typical design year relevant to various locations of the Europe and China countries were extracted from CIBSE guide book A (CIBSE 2001) and analysed accordingly. The cooling design temperatures, including the dry-bulb, wet-bulb and dew point temperatures of the outdoor air, are the major parameters to be considered. The design conditions are based on wet-bulb temperatures which represent extremes of the total sensible (temperature-related) plus latent (moisture-related) heat of outdoor air (0.4% un-guaranteed frequency) (CIBSE 2001), as shown in Table 6-1. These data are commonly used in the design of cooling towers, evaporative coolers and fresh air ventilation systems.

It is found that a lower value of relative humidity results in a higher value of temperature difference between the dry bulb and dew point temperatures, which is what the users most want in terms of good use of the benefit of dew point cooling. The relationship between the relative humidity and the difference between the dry-bulb to dew-point temperatures is presented in Fig. 6-1.

If the relative humidity is 70%, the temperature difference between dry bulb and dew point is around 6^{o}C. Assuming the dew-point effectiveness is 0.85, a 5.1^{o}C temperature difference between supply air and room space can be achieved. This difference is good enough to cool the common types of buildings within Europe.

For most geographic regions of Europe and China, the air's relative humidity is below 70%, and therefore dew point cooling is suitable for use in cooling of buildings. The drier the air in the region, the better the performance of the dew point cooling system. The ideal regions for this application are Portugal, Spain, France, German, Hungary, Poland, Romania, UK and China where the climates remain dry and hot in summer seasons. Other countries including Denmark, Norway, Netherlands, Switzerland, Sweden and UK, are also suitable for this application, but the performance of the dew point system is reduced due to the relatively lower temperature difference between the

dry-bulb and the dew-point. In some regions of Italy (e.g. Venice and Rome), dew point cooling is unsuitable as the outdoor air's relative humilities are as high as 76 to 82%, which leave very little room for utilizing the benefit of dew point cooling, i.e. temperature difference between the dry-bulb and dew-point.

Table 6-1 Cooling design temperatures for different regions in the Europe/China

Country	City	DBT, °C	WBT, °C	DPT, °C	Relative humidity ,%	Difference between DBTand DPT, °C	Difference between DBT and WBT, °C
Denmark	Copenhagen	23.2	18.2	15.0	60	8.2	5.0
France	Bordeaux	29.6	23.0	20.0	56	9.6	6.6
	Lyon	29.1	22.2	19.0	53	10.1	6.9
	Toulouse	30.2	23.0	20.0	53	10.2	7.2
German	Berlin	27.0	20.1	16.2	52	10.8	6.9
	Frankfurt	27.8	20.5	16.7	51	11.1	7.3
	Dresden	27.4	20.1	17.0	52	10.4	7.3
Hungary	Budapest	30.5	21.4	17.0	45	13.5	9.1
Italy	Bologna	31.6	24.9	22.4	57	9.2	6.7
	Rome	28.6	26.1	25.1	82	3.5	2.5
	Milan	29.7	24.2	22.0	63	7.7	5.5
	Venice	28.4	25.1	23.8	76	4.6	3.3
Netherlands	Groningen	25.2	20.6	18.2	66	7.0	4.6
	Eindhoven	26.5	20.3	17.2	57	9.3	6.2
Norway	Oslo	22.7	16.6	13.2	53	9.5	6.1
	Trondheim	21.3	17.4	15.0	67	6.3	3.9
Poland	Krakow	27.9	21.2	18.0	54	9.9	6.7
	Warsaw	27.6	21.0	17.8	54	9.8	6.6
Portugal	Lisbon	30.8	22.7	19.2	48	11.6	8.1
	Porto	27.2	20.8	17.8	55	9.4	6.4
Romania	Bucarest	30.5	23.6	20.8	56	9.7	6.9
Spain	Sevilla	36.4	24.6	19.8	36	16.6	11.8
	Madrid	34.4	21.9	16.0	33	18.4	12.5
Switzerland	Lugano	27.9	22.6	20.3	63	7.6	5.3
	Zurich	26.5	19.7	16.6	52	9.9	6.8
Sweden	Goteborg	23.5	17.7	14.5	55	9.0	5.8
	Ostersund	21.7	15.9	12.2	53	9.5	5.8
	Stockholm	23.6	18.4	15.6	62	8.0	5.2
UK	London	26.0	19.6	16.2	55	9.8	6.4
	Birmingham	23.8	18.5	15.5	59	8.3	5.3
	Edinburgh	20.8	17.2	14.8	70	6.0	3.6
	Manchester	23.2	18.3	15.5	62	7.7	4.9
China	Beijing	34.4	21.7	15.6	33	18.8	12.7
	Xi'an	35.0	22.8	17.4	36	17.6	12.2
	Shanghai	34.4	27.2	24.9	58	9.5	7.2
	Guangzhou	35.6	27.2	24.5	53	11.1	8.4

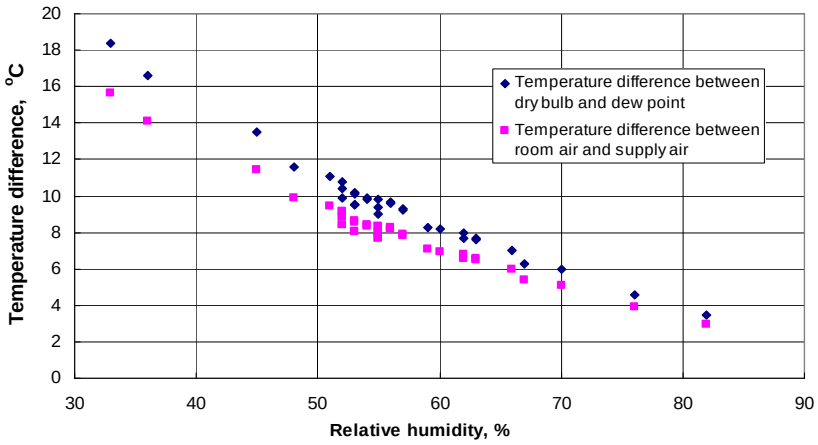

Fig. 6-1 Cooling potential of the dew point system vs. air relative humidity

6.2.3 Availability of water source, temperature level and volume consumption

Owing to its instantaneous supply and ease of connection, tap water is the most convenient medium used for the dew point system. To assess its availability, tap water temperature and volume consumption rate are critical parameters, which need to be taken into careful consideration.

Ideally, tap water temperature should be lower than dew point of the atmosphere, which allows an effective cooling to be achieved when system is in operation. Since tap water is delivered from the water source through the pipe services, and the pipes are embedded at the level of 50 to 100 cm below the ground, the water temperature will eventually reach the soil temperature at the same depth level. The data of soil temperature under 100 cm below the ground are shown in Table 6-2 (EnergyPlus 2010).

It is seen that tap water temperature is about the same or slightly lower than the dew point of the atmosphere above the earth. This allows dew point cooling to be carried out in an effective way. In most regions of Europe, water consumption rates are in the range 2 to 2.5 litre/kWh. However, Norway has less need for water (from 1.28 to 1.5 litre/kWh). The reason for this is due to Norway's relatively lower temperatures, including dry-bulb, wet-bulb and dew point, which lead to reduced cooling requirements (and thus less water need).

Taking a 100 m^2 building space with average cooling load of 30 W/m^2 as an example, if the system operates only at day time, i.e., from 9:00 am to 5:00 pm, Total required daily cooling energy for the system would be:

$$100(\mathrm{m}^2) \times 30(\mathrm{W/m}^2) \times 8\ (\mathrm{hour}) = 24\ \mathrm{kWh} \quad (6\text{-}9)$$

Thus the daily water consumption for the building would be:

$$V_{\mathrm{daily}} = 24V_w \quad (6\text{-}10)$$

The specific enthalpy of exhaust air can be calculated using the following equation, which should be solved before calculating the humidity ratio of exhaust air.

$$i_{db,3} = 1.01t_{db,3} + w_3(2501 + 1.85t_{db,3}) \quad (6\text{-}11)$$

(To be continued, please see the next page)

Table 6-2 Water temperature/consumption and supply air flow rate in different regions of Europe/China

Country	City	Water consumption rate, litre/kWh	Tap water temp.,^{o}C	Supply airflow rate for 100 m^2 building, m^3/h	Daily water consumption for 100 m^2 building, litre
Denmark	Copenhagen	2.05	15.0	1278	49.22
France	Bordeaux	2.19	18.9	1092	52.67
	Lyon	2.19	19.1	1038	52.67
	Toulouse	2.19	19.4	1028	52.67
German	Berlin	2.43	15.4	971	58.25
	Frankfurt	2.31	16.1	944	55.44
	Dresden	2.12	13.6	1008	50.82
Hungary	Budapest	2.22	15.6	777	53.36
Italy	Bologna	2.36	20.6	1140	56.71
	Rome	2.54	21	2995	60.99
	Milan	2.22	20.6	1361	53.30
	Venice	2.31	19.3	2279	55.44
Netherlands	Groningen	2.22	13.7	1498	53.30
	Eindhoven	2.27	14.5	1127	54.56
Norway	Oslo	1.47	8.6	1104	35.27
	Trondheim	1.28	8.2	1664	30.76
Poland	Krakow	2.12	13.3	1059	50.82
	Warsaw	2.28	13.9	1070	54.66
Portugal	Lisbon	2.27	20.7	904	54.54
	Porto	2.14	17.9	1115	51.31
Romania	Bucarest	2.32	17.3	1081	55.71
Spain	Sevilla	2.37	20.6	632	56.80
	Madrid	2.18	15.8	570	52.43
Switzerland	Lugano	2.19	18.8	1379	52.62
	Zurich	2.31	17.1	1059	55.44
Sweden	Goteborg	2.08	10.4	1165	49.81
	Ostersund	2.10	8.1	1104	50.33
	Stockholm	2.12	10.8	1310	50.82
UK	London	2.20	13.9	573	70.31
	Belfast	2.23	9.8	545	60.24
	Birmingham	2.21	10.6	556	59.01
China	Beijing	2.25	23.6	835	64.22
	Shanghai	2.2	20.7	1385	66.34
	Guangzhou	2.14	24.5	1873	64.21

6.2.4 Cooling potential and airflow rate scale of the dew point cooling system

The cooling potential of the dew point system can be calculated by Eqs .6-1 to 6-6, which provides the cooling outputs of the system in various regions of the Europe and China. The calculations also yield the amount of cooling energy used for removing internal load and fresh air load. All calculations are based on 1 m^3/h air volume flow rate, and the calculation results are shown in Fig. 6-2. It is found that the cooling output varies with the region where the system is applied and is in the range of 1.8 to 5.2 W per m^3/h air-flow-rate. In mild climate regions like UK, Norway and Denmark, or humid regions like Venice and Rome, the cooling output of the system is relatively low, and is mainly used to remove internal sensible load. However, in hot and dry climate regions like Spain, Romania, Portugal and Germany, the cooling output is much higher and a large percentage of the output is used to remove fresh air load.

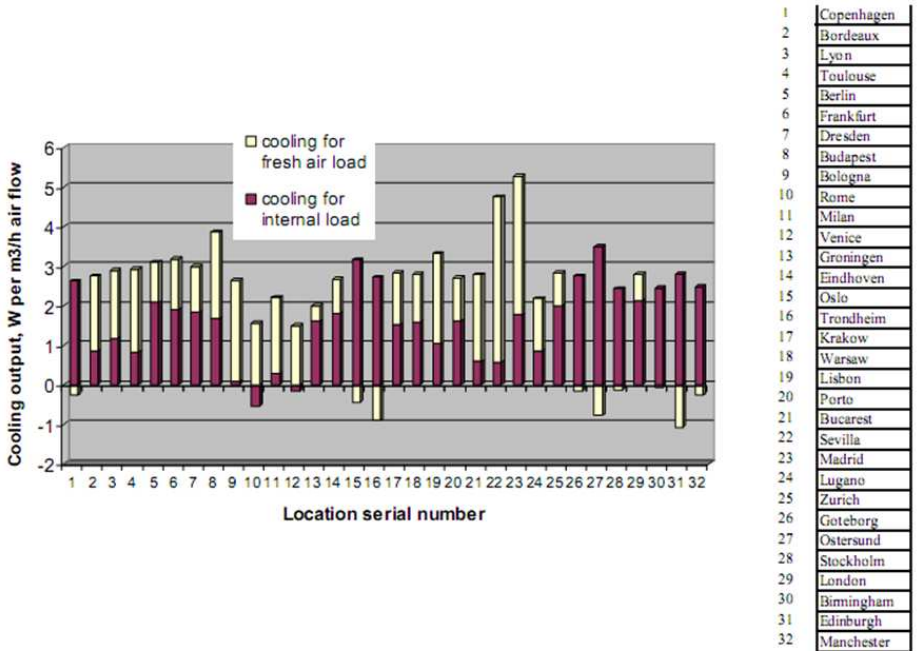

Fig. 6-2 Cooling potential of dew point system in different regions of Europe

Table 6-2 also presents the required volume flow rate for 100 m^2 of building with 30 W/m^2 cooling load. For mild or humid climate regions, the required volume flow rate is relatively higher, which reaches a value up to 1400 to 1900 m^3/h. However, in dry and hot climate regions, the volume flow rate is smaller, in the range 700 to 1200 m^3/h. If the building is in operation for 8 hours a day, the water consumption of the dew

point system will be in the range 50 to 60 litres per day. A summary of average cooling capacities for the representative cities in UK and China in the summer seasons is given in Table 6-3.

Table 6-3 Cooling capacity and air flow rate in the selected cities of UK and China

Country	City	Cooling capacity, W per m^3/h	Air flow rate for 2 kW effective cooling output, m^3/h
China	Harbin	4.23	540
	Beijing	2.98	840
	Shijiazhuang	3.02	802
	Xi'an	2.96	771
	Shanghai	1.72	1400
	Kunming	3.74	568
	Guangzhou	1.14	1870
UK	London	3.7	570
	Aberdeen	4.1	507
	Aughton	3.8	550
	Belfast	3.8	560
	Birmingham	3.8	568
	Finningley	4.14	518

6.3 Economic Analysis

A preliminary economic analysis of the prototype dew point air conditioner was carried out in order to understand its commercial viability within the Europe and China. The analyses were based on the recommended commercial unit, which was derived from the further work section. The technical parameters of the unit are outlined in Table 6-4.

Table 6-4 Technical parameters of 8 kW commercial dew point unit

Inlet DBT/ WBT	Supply air flow rate	Working-to-intake air ratio	WB effectiv-eness	Supply air temp.	Cooling capacity	Input power	Energy efficiency	Water evaporation rate
^oC	m^3/h		%	^oC	W	W		L/h
37.8/ 21.1	1530	0.44	97.7	17.1	8303	450	18.5	10.02

6.3.1 Estimated capital cost

The capital cost of the unit was calculated by summing up the prices of the components contained in the unit, taking into account an appropriate rate of labour cost and sale profit. It should be stressed that the prices of the components were quoted from the selected product catalogue and the labour cost was estimated on the basis of mass production premise. The sale profit was considered to be 30% of the capital cost. Details of the calculation are presented in Table 6-5.

Table 6-5 Capital cost calculation

Component	Unit Price (euro)	Quantity	Cost (euro)
Tangible fan	89	1 [piece]	89
Axial fan	76	1[piece]	76
Water pump	82	1 [piece]	82
Air filter	2.8	1[piece]	2.8
Upper water tank	6.5	1[piece]	6.5
Lower water tank	7.6	1[piece]	7.6
Water pipe	3.2	3.6 [m]	11.6
Fan speed controller	43	1[piece]	43
Intake air grill	0.8	1[piece]	0.8
Supply air grill	1.9	1[piece]	1.9
Float switch	4	1[piece]	4
Casing galvanised steel sheet 1005 mm x 605 mm x 0.6 mm	24	6[piece]	144
Heat exchanger aluminium sheet 0.3 mm	380	1[piece]	380
Heat exchanger glass fibre	100	1[piece]	100
Labour cost	10	72	720
Sum of the individual cost			1669.2
Profit (30% × Sum)			500
Total			2169.2

6.3.2 Operating cost

The unit will provide cooling to the target building at cost of small amount of electricity used for driving the fan unit and certain volume of tap water used for taking the heat away from the product air. The operating cost was estimated on the basis of the above mentioned 8 kW rating unit when being used in a typical London office building. It has been known that the peak cooling load of an office environment at London weather condition is around 80 W/m^2, and its average load is about 30 W/m^2 (IP and G 2002). To meet the cooling demand of the space at most time of its operation, this 8.0 kW rating unit was considered to take around 100 m^2 of office space. It was assumed that the unit will be in operation at the office working hours, i.e., from 9:00 am to 5:00 pm during a summer season from July to September. In that case, the overall cooling energy demand for the office space will theoretically be 3 months x 30 days x 8 hours x 30 W/m^2 x 100 m^2/1000 = 2160 kWh.

It has been indicated from the previous tasks that the unit will be able to achieve an average energy efficiency (or COP) of 18 at cooling operation. To deliver 2160 kWh of cooling energy, the electricity power consumption will be 120 kWh (2160/18). Considering the average electricity price of 16 cent per kWh within the Europe region (2011) the total cost of the electricity use will be 19.2 euro (120 x 0.16) per annum.

The water consumption will be 2.1 litre/kWh x 2160 kWh=4,536 litre, considering the average water price of 160 cent per cubic meter (2011), the total water cost will be 4.536 x 1.6 = 7.26 euro per annum. Summing up the two parts costs yields a total operating cost of 26.46 euro.

Similarly, cost for operation at other selected Europe cities including Bern, Cyprus, Lisbonand Athens will be calculated based on their average cooling load ranging from 40 (Olesen 2002), 45(Florides, Kalogirou et al. 2000), 50 (Silva 2005) to 55 W/m^2. (Mihalakakou, Santamouris et al. 2007) and Beijing of China has the 65 W/m^2 average cooling load for office buildings (Lu 2008). The results are summarised in Table 6-6.

Table 6-6 Operating cost of the cooling systems at several cities in Europe and China

City	London	Bern	Cyprus	Lisbon	Athens	Beijing
Average cooling load, W/m^2	30	40	45	50	55	65
Operating cost – dew point system, euro	26.46	36.8	41.4	46.0	50.6	59.8
Operating cost – mechanical compression system, euro	115.2	153.6	172.8	192.0	211.2	249.6

6.3.3 Economic benefits relative to mechanical compression cooling systems

Owing to the inherent feature of the dew point system, i.e., removing use of the energy (power) intensive compressor, it has achieved significantly higher energy efficiency (or COP) (i.e., 18) than the conventional mechanical compression cooling system (i.e., 3) and consequently, its operating cost will be greatly reduced.

The initial purchase cost of the mechanical compression system of 8 kW cooling capacity is currently around 2000 euro (Aircon247.com), which is a figure slightly lower than the initial cost of the dew point system (2170 euro). This is due to the extensive sale volume and mature technology established in association with the mechanical system. The increase in the capital investment will be rapidly repaid by significant saving of the operating cost of the dew point system. The payback period of the dew point system relative to conventional mechanical compression system can be calculated using the following equation:

$$\mathrm{PP_{dew}} = \frac{\mathrm{C_{cp,dew}} - \mathrm{C_{cp,con}}}{(\mathrm{C_{opt,con}} - \mathrm{C_{opt,dew}}) + (\mathrm{C_{m,con}} - \mathrm{C_{m,dew}})} \quad (6\text{-}12)$$

In the calculation, maintenance cost of both dew point and conventional systems was considered to be 1.5 % of their capital cost (Guerra 1994), owing to their simplicity in operation and little maintenance requirement. The results derived from the above calculation is summarised in Table 6-7. It is noted the cost increase in capital investment will be repaid in about 0.91 – 1.88 years.

Considering 30-year life cycle of both dew point and conventional systems (Palmer, P.E. et al. 2002), the net saving in energy bills during this period by using the dew point system in Europe and China will be calculated using the following equation:

$$C_{net,bill,sav} = (30 - PP_{dew})\{(C_{opt,con} - C_{opt,dew}) + (C_{m,con} - C_{m,dew})\}. \quad (6\text{-}13)$$

It is seen that for 100 m^2 building space using a 8 kW rating dew point cooing unit, the life cycle energy bill saving will be in the range 2534.7 to 5447.1 euro.

Table 6-7 Economic benefit of the dew point systems relative to the conventional mechanical compression system

City	London	Bern	Cyprus	Lisbon	Athens	Beijing
Payback period, year	1.88	1.42	1.26	1.14	1.05	0.91
Life cycle net energy bill saving, euro	2534.7	3410.7	3849.4	4286.8	4722.8	5447.1

6.4 Environmental effect

Section 6.3 has worked out the annual electricity power saving of the dew point system over the conventional mechanical compression cooling system, in terms of kWh per annum. These figures could be easily converted into carbon emissions reduction by using the following equation:

$$Em_{co2} = f_{c,c} En_a / 1000 \quad (6\text{-}14)$$

The results derived from the calculation are presented in Table 6-8. As to 100 m^2 building space, using a 8 kW rating dew point cooling unit, its annual CO_2 emission reduction will be in the range 0.323 to 0.7 tons. Considering that each year there will be 5 million m^2 of European building using this technology, the estimated annual carbon emissions reduction will be as high as 35,000 tons.

Additional environmental benefit by using the dew point cooing system is to offer an opportunity giving up use of CFCs and HCHCs refrigerants, which have been proven to be the direct reason forming the earth's ozone layer and causing global warming.

Table 6-8 Environmental benefits of dew point system relative to conventional mechanical compression system

City	London	Bern	Cyprus	Lisbon	Athens	Beijing
Carbon emissions reduction for 100 m^2 building space, tons,	0.323	0.430	0.484	0.538	0.591	0.700
Carbon emissions reduction for 5 million m^2 building space, tons,	16,150	21,500	24,200	26,900	29,550	34,991

Chapter7.
Conclusions

This study has developed a new dew point indirect evaporative cooler for buildings. The performance of the heat/mass exchanger has been investigated using an optimal design, computer modelling and experiments. For this type of dew point cooler to be used in European countries and in China, an economic, environmental and acceptance analysis has been performed.

Some key findings are summarised in the following statements:

1. The wet-bulb/dew point effectiveness of the new dew point cooler depends mainly on the intake air velocity, the geometrical sizes of channels, and the working-to-intake air ratio but depends less on the feed water temperature. The energy efficiency of the dew point cooler is affected by the intake air velocity, the working-to-intake air ratio, as well as its effectiveness. An optimised design of the exchanger in the dew point cooler is a compromise between effectiveness and energy efficiency.

2. Decreasing the channel height of heat/mass exchanger in dew point cooler will result in an increase of both effectiveness and flow resistance. As a result, the energy efficiency will be reduced slightly. To achieve an acceptable effectiveness and energy efficiency, the channel height could be controlled to a value between 3-6 mm, and the channel length would be designed to 1-1.2 m.

3. It has been found that the wet-bulb/dew point effectiveness and energy efficiency decrease with increasing the intake air velocity. A low velocity improves the performance of dew point cooler, but also may increase cost due to the demand for an increasing exchanger size. Reducing air velocity by 50% will lead to a 100% increase in the cost of exchanger material. In an air conditioning application, the intake air velocity of channel (intake channel air velocity) should be controlled to the value between 0.5 and 1m/s.

4. The effectiveness of the dew point heat/mass exchanger increases with an increasing working-to-intake-air ratio. However, the increased ratio leads to an increase in flow resistance, which may offset the benefit of the enhanced

effectiveness. A working-to-intake-air ratio between 0.4 and 0.5 is a recommended as it leads to the highest level of compromise between effectiveness and energy efficiency.

5. For the experiment prototype, its wet-bulb effectiveness varied from 55% to 110%, with a dew- point effectiveness ranging from 40%-85% under all test conditions. Although the wet-bulb effectiveness derived from experiment was less than that predicted by numerical simulation which was as high as 130%, its effectiveness was still higher than the majority of typical indirect evaporative coolers (with air-to-air heat exchanger) could achieve (40-80%).

6. The supply temperatures provided by the experiment prototype ranged from 19 to 29^{o}C under all test conditions. The effectives of the cooler improved with increasing intake dry-bulb temperature or intake wet-bulb depressions (difference between dry- bulb and wet- bulb temperature).

7. The energy efficiency (or COP) of the experiment prototype varied from 3 to 12, with an average of 8.8 under all test conditions. The energy efficiency of the dew point cooler is much higher than that of the best conventional air conditioner (the energy efficiency is 3.8). Compared to the energy efficiency (over 11.7) of indirect evaporative coolers based on the M-cycle principle, the energy efficiency of the dew point cooler in this study is slightly lower because the M-cycle heat/mass exchanger follows a cross-flow pattern which has a lower flow resistance than that in the counter flow heat/mass exchanger under the same conditions. For the dew point cooler, a larger energy efficiency could be achieved through selecting the most favourite fan which is able to work more efficiently under most operating conditions.

8. The feed water temperature has a negligible impact on the performance of the dew point cooler. For the experiment prototype, it is found that there was less than 5% decrease in wet-bulb effectiveness with an increasing water temperature from 18^{o}C to 23^{o}C. The water evaporative rate of the prototype varied from 0.2-1.3 litre/h under all tested conditions.

9. Through conducting a feasibility analysis on the dynamic performance of the dew point cooler in various climate conditions in different areas in Europe and China, it is concluded that the dew point cooler is suitable for most regions with

dry, mild and hot climate conditions. For some regions with a humid climate, the performance of the dew point cooler would be too low to be used alone. A pre-dehumidifier should be incorporated to enhance its performance for a wider application. It is also concluded that a lower value of relative humidity can result in a higher value of temperature difference between the dry-bulb and dew-point temperatures, and a higher cooling performance of the dew point cooler.

10. Tap water can easily be used to support cooling of the dew point system. Its temperature is about the same or slightly lower than the dew point of the ambient air, which can ensure effective cooling. The water consumption rate varies with the region where the system is used, but generally it ranges from 2 to 2.5 litre/kWh output. Dry and hot climate regions need more water supplies but mild or humid climate regions require less.

11. The cooling output of the dew point system varies according to the region where the system is employed, but is usually in the range 1.0 to 5.2 W per m^3/h airflow. In regions with a mild or humid climate, the cooling output is relatively low, and is mainly used to remove internal sensible load. In hot and dry climate regions, the cooling output is much higher and a large percentage of the output is used to remove fresh air load.

12. A case study suggests that for a 100 m^2 building space with 30 W/m^2 cooling load, the required air volume flow rate of the dew point cooler is in the range 700 to 1900 m^3/h, depending upon the region where the building is located. The daily water consumption of the cooler is in the range of 50 to 70 litre/8 h.

13. For a 100 m^2 building space, a dew point cooler with 8 kW rating cooling capacity is found to be a suitable choice to meet its peak cooling load. The capital cost of such a unit is 2170 euro, slightly higher than that of a conventional mechanical compression unit with the same cooling capacity. An 8 kW rating dew point cooler consumes electricity and water which costs 28 to 60 euro each year, while a mechanical compression system of the same cooling capacity will have a consumption of 115 to 250 euro of electricity annually, depending upon the location the system. The payback period of the dew point system will be 0.91 to 1.8 years. Over a lifecycle of 30 years, a 8 kW rating unit being used in a 100 m^2 of building space will harvest significant savings in

energy bills in the range 2500 to 5400 euro, depending upon the location of the cooler.

14. For the 8 kW rating dew point cooler, its annual carbon emissions could be reduced in the range 0.3 to 0.7 tons, depending upon the location of the system. Considering a 5 million m^2 of building space that the system is potentially applied within Europe and China, the estimated carbon emissions reduction could be as high as 35,000 tons per annum.

Chapter8.
Further work

The research works have led to successful transfer of the patent technology into a Chinese company, and an 8 kW commercial dew point cooler is currently under development.

The required technical performance of dew point cooler is detailed in Table 8-1. To achieve the specific technical targets, the optimal study has been undertaken to allow:

- Optimisation of the performance of heat/mass exchanger, i.e. increasing effectiveness, cooling capacity, and energy efficiency ratio;
- Determination of the size of cooling unit;
- Minimisation of the system cost;
- Simplification of the fabrication and assembly process.

Table 8-1 Performance design standards of 8 kW dew point evaporative cooling unit

Working-to-intake air ratio	Product airflow rate (m^3/h)	Intake airflow rate (m^3/h)	WB effectiveness (%)	Intake DBT/WBT (^oC)	Cooling capacity (W)	Product air DBT (^oC)	Max input power (W)	Energy efficiency
0.44	1530	2737	97.65	37.78/ 21.11	8303	21.5	450	18.5

The major work lied in the optimisation of heat/mass exchanger, which is the most important component in the unit. Based on the proposed concept, a new structure enabling decreased pressure drop and enhanced effectiveness was designed. The simulation was undertaken to examine the performance of the new structure. Further, the new cooler configuration has also been developed including selection of fans and pump et al.

8.1 Heat/mass exchanger configuration

A new exchanger stacked with corrugation sheets was designed to maximum heat transfer area and reduce pressure drop. The structure of the new exchanger is shown in

Fig. 8-1. The corrugation sheets are formed by moulding process using a type of paper made of cellulous fibre. After moulding into corrugations shape, the cellulous paper is well strengthened. One surface of the corrugation sheet is coated with water-proof material, such as wax or aluminium film, to avoid water permeation. The other surface is the fibre material with great water absorbing capability. Water-proof material is used to form dry channel, whereas the fibre material is to form adjacent wet channel. The new design makes the fabrication process much easier than the previous design.

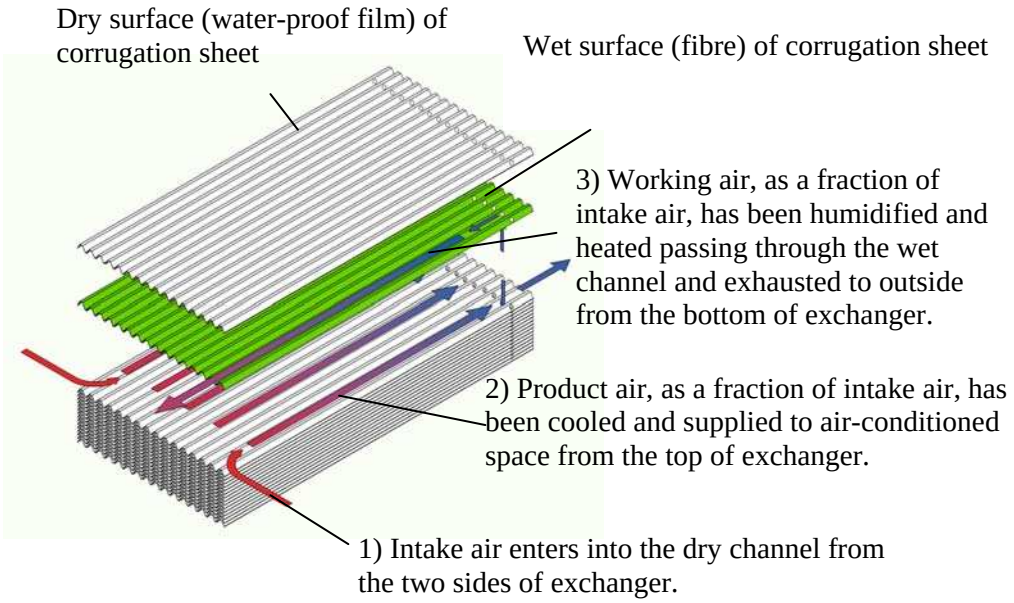

Fig. 8-1 New heat/mass exchanger structure stacked with corrugation sheets

8.2 Dew point cooling unit configuration

The 8 kW dew-point cooler is equipped with the corrugation sheets stacked heat /mass exchanger. The configuration of the cooling system is given in Fig. 8-2. The main electric components in the 8 kW cooling system include supply and exhaust air fans and water pump. The supply air fan equipped on the top of system is used to provide pressure for the supply air. Whereas, the exhaust air fan equipped on the bottom of system is used to provide pressure for working air. The individual pressure drop of supply air and working air were calculated to choose the suitable supply/exhaust air fan product. The water consumption rate and recirculation water flow rate of the system were calculated to choose the suitable water pump product and design the size of water tanks.

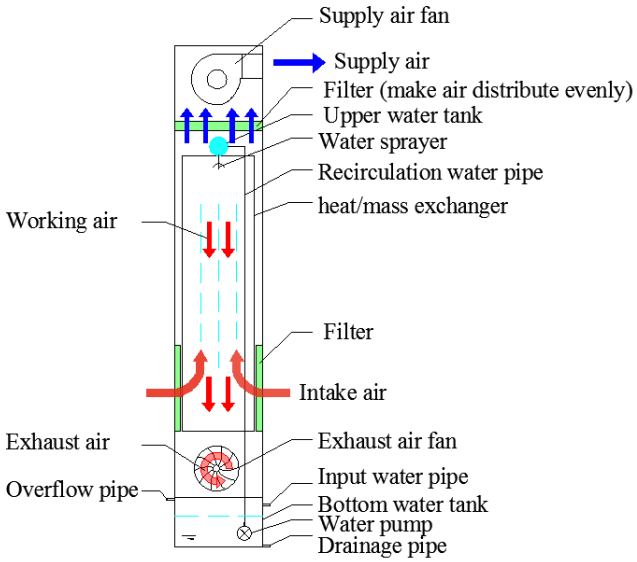

Fig. 8-2 Schematic of 8 kW dew-point indirect evaporative cooling system

8.3 Simulation results of heat/mass exchanger

Design calculations of the heat/mass exchanger should be based on the required per-set condition, i.e. intake airflow rate, 2737 m^3/h, Intake air dry/wet bulb temperature, 37.78/21.11^oC, working-to-intake air ratio, 0.44, as shown in Table 8-2.

Table 8-2 Pre-set simulation conditions for the 8 kW heat/mass exchanger

Intake air DBT (^oC)	Intake air WBT (^oC)	Intake air channel velocity (m/s)	Working –to-intake air ratio	Dry channel spacing (mm)	Wet channel spacing (mm)	Thickness of sheets (mm)
37.78	21.11	3.0	0.44	4.0	4.0	0.25

Simulation was undertaken to determine the optimal channel length by using the developed computer model in the Chapter 3. The results of simulation are shown in Fig. 8-3 and 8-4. It is suggested that the channel length should be sized to 0.9 m in order to achieve the desired cooling performance. At this geometrical setting, the predicted pressure drops along the product and working air channels are approximate 25 Pa and 48 Pa respectively. The predicted performance of the optimal heat/mass exchanger are summarised in Table 8-3.

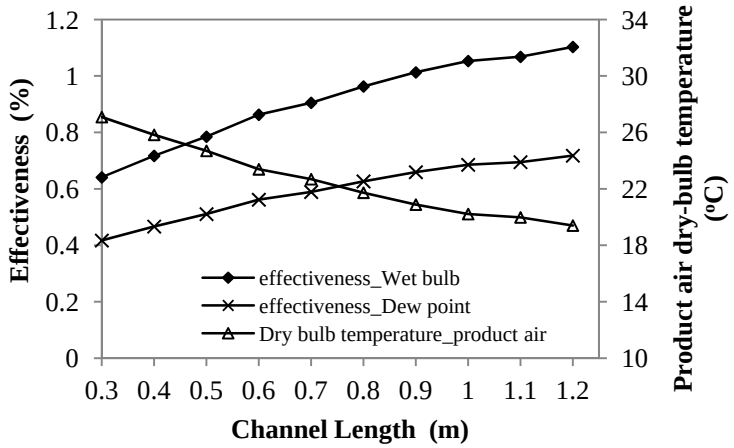

Fig. 8-3 Effectiveness and product air dry-bulb temperature of the model as a function of channel length

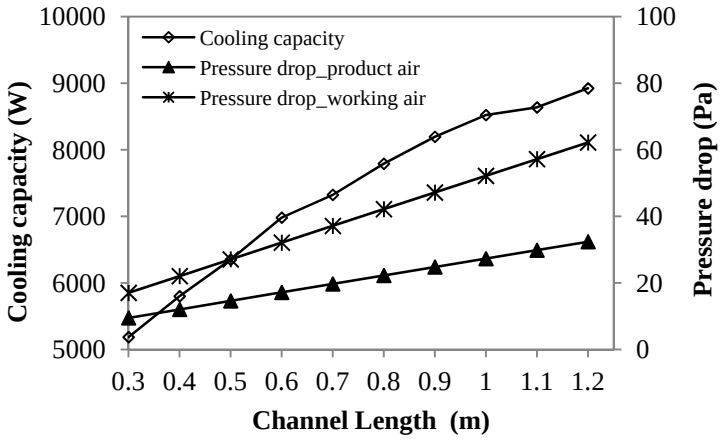

Fig. 8-4 Cooling capacity and pressure drop of the model as a function of channel length

Table 8-3 Predicted performance of the 8 kW heat/mass exchanger

Length of exchanger (m)	Width of exchanger (m)	Height of exchanger (m)	WB effective-ness	Cooling capacity (kW)	product air pressure drop (Pa)	working air pressure drop (Pa)
1.32	0.415	0.913	1.02	8.3	25.09	47.78

8.4 Unit performance predictions

This commercial unit is currently under construction. Due to commercial sensitivity, the detailed information of the unit design is restricted to public. However, the overall design performance of the unit is publishable and is summarised in Table 8-4. It is expected to achieve a cooling output of 8kW at the specified operating condition, with the effectiveness of 1.02 at 1530 m^3/h of supply air flow and 1200 m^3/h of discharge air flow; whereas the power input of the unit is approximate 450 W and the calculated energy efficiency is 18.5.

Table 8-4 The overall design performance of the 8 kW dew point cooling unit

Working –to-intake air ratio	Product airflow rate (m^3/h)	Working airflow rate (m^3/h)	Intake airflow rate (m^3/h)	WB effectiveness	Intake air DBT/WBT (^oC)	Cooling capacity (W)	Product air DBT (^oC)	Input power (W)	Energy efficiency
0.44	1530	1207	2737	1.02	37.8/21.1	8303	20.9	300	18.5

Appendix

Appendix A Thickness of heat/mass exchanger material samples

Samples	Thickness(mm)
pure textile fibre	0.259
pure kraft paper	0.180
pure non-woven fabric	0.180
aluminium foil	0.153
gluing film	0.100
aluminium coating textile fibre(coating by heat)	0.370
aluminium coating kraft paper(coating by heat)	0.200
waxing kraft paper	0.209
aluminium coating non-woven fabric	0.280
aluminium coating textile fibre(coating by glue)	0.410
aluminium coating kraft paper(coating by glue)	0.470

Appendix B Simulation programme of the counter-flow heat and mass exchanger (EES)

```
function h_local(K, H0, L, LENGTH, N, A, RE, PR, DE,MU_F, MU_W, LAM)
    IF  (K*LENGTH/N<L) THEN

    nuss1:=1.86*(RE*PR*DE/(K*LENGTH/N))^(1/3)*(MU_F/MU_W)^0.14;
        h1:=LAM*nuss1/DE;
            IF (K=1) THEN
                h2:=0
                GOTO 10
            endif
            nuss2:=1.86*(RE*PR*DE/((K-
1)*LENGTH/N))^(1/3)*(MU_F/MU_W)^0.14;
        h2:=LAM*nuss2/DE;
10:     h:=h1*K-h2*(K-1);
    ELSE
            IF ((K-1)*LENGTH/N>L) THEN
            h:=H0
            ELSE
            nuss1:=1.86*(RE*PR*DE/(L))^(1/3)*(MU_F/MU_W)^0.14;
                h1:=LAM*nuss1/DE;
                IF (K=1) THEN
                    h2:=0
                    GOTO 20
                endif
                nuss2:=1.86*(RE*PR*DE/((K-
1)*LENGTH/N))^(1/3)*(MU_F/MU_W)^0.14;
            h2:=LAM*nuss2/DE;
```

```
20:                    h3:=(h1*L-h2*(K-1)*LENGTH/N)/(L-(K-1)*LENGTH/N)

                       h:=(h3*(L-(K-1)*LENGTH/N)+H0*(K*LENGTH/N-
L))*N/LENGTH;



                ENDIF

        ENDIF

h_local:=h;



END



function Q_local(TF, TW, K, H0, L, LENGTH, N, A, RE, PR, DE,MU_F, MU_W,
LAM)

        Q_local:=h_local(K, H0, L,LENGTH, N, A, RE, PR, DE, MU_F, MU_W,
LAM)*(LENGTH/N)*A*(TF-TW)

end



function en_air(airtemp, hum)

        en_air:=1.005*airtemp+(2500+1.84*airtemp)*hum

end



function en_water(watertemp)

        en_water:=2500+1.84*watertemp

end



function la_laminar(Re)

        la_laminar:=53.3/Re

end
```

```
function resistance_onway(l,d,v,Rou,Re)

        resistance_onway:=la_laminar(Re)*(l/d)*v^2*Rou/(2*9.8)

end


function keci(air_fraction)

        keci:=0.2536*air_fraction^3+0.7981*air_fraction^2-
1.4305*air_fraction+0.8041

end


function resistance_local(air_fraction,v,Rou)

        resistance_local:=keci(air_fraction)*v^2*Rou/(2*9.8)

end


"construction geometry"

height=0.01

a=2*Height/1.732;

S=Height*a/2;

De=4*S/(3*a);

length=number_channel*a;

thickness=0.00025;

lam_material=0.6;

"air inlet boundary condition"

t_enviroment=28

tb_enviroment=20

td_enviroment=DEWPOINT(AirH2O,T=t_enviroment,P=p0,B=tb_enviroment);

hum_enviroment=HUMRAT(AirH2O,T=t_enviroment,P=p0,d=td_enviroment);

Rou_enviroment=DENSITY(AirH2O,T=t_enviroment,P=p0,w=hum_enviroment);
```

```
Qm_enviroment=Rou_enviroment*U*S;

U=1;

p0=101.325;


"water zone boundary condition"

twater_supply=16.05;


"common parameters"

nuss0=2.47;

D0=0.000022;

cp_water=4.183;

workingair_fraction=0.5;

t0=273;

n=13;

number_channel=13;


Duplicate j=1,n

        tw[0,j]=twater_supply

        tw[number_channel+1,j]=tw[number_channel,j]

end

Duplicate i=1,number_channel

"CHANNEL i "

"air inlet parameter in dry channel"

t_dryin[i]=t_enviroment;

hum_dry[i]=hum_enviroment;

Rou0[i]=Rou_enviroment;
```

```
qm[i]=Qm_enviroment;

"fluid properties in the DRY channel"
tf_dry[i]=(t_dryin[i]+t_dryout[i])/2;
Rou[i]=DENSITY(AirH2O,T=tf_dry[i],P=p0,w=hum_dry[i]);
Cp[i]=CP(AirH2O,T=tf_dry[i],P=p0,w=hum_dry[i]);
Lam[i]=CONDUCTIVITY(AirH2O,T=tf_dry[i],P=p0,w=hum_dry[i]);
mu_dry[i]=VISCOSITY(AirH2O,T=tf_dry[i],P=p0,w=hum_dry[i]);
pr[i]=PRANDTL(Air,T=tf_dry[i]);

"flow parameters in the DRY channel"
Re[i]=U*De*Rou[i]/mu_dry[i];
l[i]=0.05*De*Re[i]*Pr[i];
h0[i]=Lam[i]*nuss0/De;

"air inlet parameter in WET channel"
twet_in[i]=t_dryout[i];
hum_in[i]=hum_dry[i];
Rou0_wet[i]=DENSITY(AirH2O,T=twet_in[i],P=p0,W=hum_in[i]);
qm_wet[i]=qm[i]*workingair_fraction;
U_wet[i]=qm_wet[i]/Rou0_wet[i]/S;

"FLUID and wall PROPERTIES in WET channel"
tf_wet[i]=(twet_in[i]+twet_out[i])/2;
hum_f[i]=(hum_in[i]+hum_out[i])/2;
Rou_wet[i]=DENSITY(AirH2O,T=tf_wet[i],P=p0,W=hum_f[i]);
```

Cp_wet[i]=CP(AirH2O,T=tf_wet[i],P=p0,W=hum_f[i]);

Lam_wet[i]=CONDUCTIVITY(AirH2O,T=tf_wet[i],P=p0,W=hum_f[i]);

mu_wet[i]=VISCOSITY(AirH2O,T=tf_wet[i],P=p0,W=hum_f[i]);

pr_wet[i]=PRANDTL(Air,T=tf_wet[i]);

"flow parameters in the WET channel"

Re_wet[i]=U_wet[i]*De*Rou_wet[i]/mu_wet[i];

l_wet[i]=0.05*De*Re_wet[i]*Pr_wet[i];

h0_wet[i]=Lam_wet[i]*nuss0/De;

"Resistance calculation"

Resistance[i]=(resistance_onway(length,de,U,Rou[i],Re[i])+resistance_local(workingair_fraction,U,DENSITY(AirH2O,T=t_dryout[i],P=p0,w=hum_dry[i]))+resistance_onway(length,de,U_wet[i],Rou_wet[i],Re_wet[i]))*9.8

"boundary condition at the inlet and outlet position in dry channel and wet channel"

tf[i,n+1]=t_dryin[i]

tf[i,1]=t_dryout[i]

tf2[i,1]=twet_in[i]

tf2[i,n+1]=twet_out[i]

hum[i,1]=hum_in[i]

hum[i,n+1]=hum_out[i]

tw[i,0]=tw[i,1]

tw[i,n+1]=tw[i,n]

Duplicate j=1,n

"FLUID and wall PROPERTIES in basic cell"

mu_w[i,j]=VISCOSITY(AirH2O,T=tw[i,j],P=p0,D=tw[i,j]);

t_average[i,j]=((tf2[i,j]+tf2[i,j+1])/2+tw[i,j])/2;

d[i,j]=D0*((t_average[i,j]+t0)/t0)^1.5;

le[i,j]=Lam_wet[i]/Rou_wet_local[i,j]/(1000*Cp_wet[i])/d[i,j];

hum_wall[i,j]=HUMRAT(AirH2O,T=tw[i,j],P=p0,D=tw[i,j]);

Rou_wall[i,j]=DENSITY(AirH2O,T=tw[i,j],P=p0,D=tw[i,j]);

Lam_water[i,j]=CONDUCTIVITY(Water,T=tw[i,j],P=p0)

Rou_wet_local[i,j]=DENSITY(AirH2O,T=(tf2[i,j]+tf2[i,j+1])/2,P=p0,W=(hum[i,j]+hum[i,j+1])/2)

"heat tranfer in dry channel"

Q_dry[i,j]=Q_local((tf[i,j]+tf[i,j+1])/2, tw[i,j], -j+1+n, h0[i], l[i], LENGTH, N, A, Re[i], pr[i], De, mu_dry[i], mu_w[i,j], Lam[i]);

"energy balance in the dry channel"

Q_dry[i,j]=qm[i]*1000*Cp[i]*(tf[i,j+1]-tf[i,j]);

"mass tranfer in wet channel"

hm_local[i,j]=h_local(j, h0_wet[i], l_wet[i], LENGTH, N, A, Re_wet[i], pr_wet[i], De, mu_wet[i], mu_w[i,j], Lam_wet[i])*le[i,j]^(-2/3)/Rou_wet_local[i,j]/(1000*Cp_wet[i]);

m[i,j]=hm_local[i,j]*(LENGTH/N)*a*(Rou_wet_local[i,j]*hum_wall[i,j]-Rou_wet_local[i,j]*(hum[i,j+1]+hum[i,j])/2)

"mass tranfer balance in the wet channel"

m[i,j]=qm_wet[i]*(hum[i,j+1]-hum[i,j])

"heat tranfer in wet channel"

Q_wet[i,j]=Q_local((tf2[i,j]+tf2[i,j+1])/2, tw[i,j], j, h0_wet[i], l_wet[i], LENGTH, N, A, Re_wet[i], pr_wet[i], De, mu_wet[i], mu_w[i,j], Lam_wet[i])

dert[i,j]=qm_wet[i]*1000*(en_air(tf2[i,j+1],hum[i,j+1])-en_air(tf2[i,j],hum[i,j]));

Cooling_vaporation[i,j]=1000*m[i,j]*en_water(tw[i,j])

"energy balance in the wet channel"

Cooling_vaporation[i,j]=Q_wet[i,j]+dert[i,j]

"total energy balance in the combined channel"

water_volume[i,j]=SUM(m[k,j], k=i,number_channel)

Q_dry[i,j]=dert[i,j]-Lam_water[i,j]*thickness*(tw[i,j+1]+tw[i,j-1]-2*tw[i,j])*a/(length/n)-Lam_water[i,j]*thickness*(tw[i+1,j]+tw[i-1,j]-2*tw[i,j])*(length/n)/a-1000*cp_water*water_volume[i,j]*(tw[i-1,j]-tw[i,j])

END

END

tp_aver=Average(t_dryout[1..number_channel])

resis_average=Average(Resistance[1..number_channel])

effectiveness_Wetbulb=(t_enviroment-tp_aver)/(t_enviroment-tb_enviroment)

effectiveness_Dewpoint=(t_enviroment-tp_aver)/(t_enviroment-td_enviroment)

"effectiveness_Dewpoint=0.75"

effectiveness_energy=1005*(t_enviroment-tp_aver)*(1-workingair_fraction)*Rou_enviroment*U*S/(resis_average*U*S);

Q_cooling=1005*(t_enviroment-tp_aver)*(1-workingair_fraction)*Rou_enviroment*U*S

Appendix C Test data of the dew point cooling unit

No.	1	2	3	4	5	6	7	8
Intake air dry-bulb temp. (^{o}C)	36.0	36.0	36.0	36.0	36.0	36.0	36.0	36.0
Intake air wet-bulb temp. (^{o}C)	20.0	20.0	20.0	20.0	20.0	20.0	20.0	20.0
Supply air dry-bulb temp. (^{o}C)	21.0	21.0	22.3	25.1	25.5	26.1	26.6	27.0
Outlet air channel velocity (m/s)	0.18	0.23	0.27	0.41	0.45	0.50	0.59	0.68
Intake air channel velocity (m/s)	0.36	0.45	0.55	0.82	0.91	1.00	1.18	1.36
Working to intake air ratio	0.50	0.50	0.50	0.50	0.50	0.50	0.50	0.50
Feed water temperature (^{o}C)	19.1	19.3	19.5	19.2	19.1	19.2	19.1	19.2
Wet bulb effectiveness (%)	86.9	90.4	85.8	66.4	64.3	61.9	56.8	54.8
Dew point effectiveness (%)	53.8	56.4	54.9	41.8	40.6	39.3	36.0	35.0
Power consumption (W)	26.1	30.3	33.3	39.3	38.3	39.4	39.1	39.7
Cooling capacity (W)	209	288	312	366	392	379	443	481
Energy efficiency (or COP)	8.0	9.5	9.4	9.3	10.2	9.6	11.3	12.1

Appendix C (Continued)

No.	9	10	11	12	13	14	15	16	17	18	19	20
Intake air dry-bulb temp. (^{o}C)	37.7	37.8	38.1	38.0	38.1	38.2	38.3	38.5	38.9	36.5	36.5	36.5
Intake air wet-bulb temp. (^{o}C)	20.7	20.9	20.8	20.5	20.6	20.6	20.7	20.6	20.6	28.5	28.5	28.5
Supply air dry-bulb temp. (^{o}C)	24.5	25.4	25.8	26.0	26.2	26.4	26.6	26.7	26.8	33.8	28.0	27.6
Outlet air channel velocity (m/s)	0.46	0.46	0.46	0.46	0.46	0.46	0.46	0.46	0.46	0.31	0.21	0.11
Intake air channel velocity (m/s)	0.92	0.92	0.92	0.92	0.92	0.92	0.92	0.92	0.92	0.40	0.40	0.40
Working to intake air ratio	0.5	0.5	0.5	0.5	0.5	0.5	0.5	0.5	0.5	0.07	0.48	0.73
Feed water temperature (^{o}C)	14.1	16.6	17.5	18.9	19.7	21.2	19.9	21.0	22.2	25.7	25.8	25.4
Wet bulb effectiveness (%)	78.9	73.5	71.0	68.3	68.3	67.0	66.2	65.8	66.0	33.0	106.1	111.2
Dew point effectiveness (%)	51.6	48.0	46.1	44.2	44.0	43.3	42.8	42.3	42.5	26.3	83.3	86.2
Power consumption (W)	38.3	32.3	36.9	38.4	39.1	35.1	34.0	36.1	38.2	19.9	25.1	35.0
Cooling capacity (W)	546	463	457	446	445	439	435	439	449	72	128	70
Energy efficiency (or COP)	14.3	14.3	12.4	11.6	11.4	12.5	12.8	12.2	14.0	9.0	5.5	2.3

Appendix C (Continued)

No.	21	22	23	24	25	26	27	28	29	30
Intake air dry-bulb temp. (^{o}C)	23.1	25.2	27.1	27.4	29.6	32.2	35.7	37.9	39.3	40.1
Intake air wet-bulb temp. (^{o}C)	17.0	18.1	18.0	17.6	18.5	19.5	20.5	21.3	21.9	21.8
Supply air dry-bulb temp. (^{o}C)	21.1	21.5	22.0	22.2	22.4	23.5	24.5	25.4	26.5	27.4
Outlet air channel velocity (m/s)	0.46	0.46	0.46	0.46	0.46	0.46	0.46	0.46	0.46	0.46
Intake air channel velocity (m/s)	0.92	0.92	0.92	0.92	0.92	0.92	0.92	0.92	0.92	0.92
Working to intake air ratio	0.5	0.5	0.5	0.5	0.5	0.5	0.5	0.5	0.5	0.5
Feed water temperature (^{o}C)	20.2	20.4	20.6	21.8	20.6	21.3	20.8	21.1	20.3	20.3
Wet bulb effectiveness (%)	34.0	52.2	55.1	52.5	64.9	68.4	73.5	75.4	73.6	69.6
Dew point effectiveness (%)	21.4	33.5	34.9	32.8	41.2	44.2	48.0	49.7	49.0	46.1
Power consumption (W)	23.4	23.5	23.5	23.9	23.6	23	22.9	22.6	23.4	23.5
Cooling capacity (W)	80	144	195	199	277	335	430	485	497	492
Energy efficiency (or COP)	14.3	14.3	3.4	6.1	8.3	8.3	11.8	14.5	18.8	21.5

References

Afonso, C. F. A. (2006), *Recent advances in building air conditioning systems*, Applied Thermal Engineering, vol. 26, pp. 1961-1971.

Aircon247.com (2011), *Fujitsu ASYA30 8 kW 30,000 Btu High Wall Split Inverter Air Conditioning System*, from http://www.aircon247.com/p/1059791/fujitsu-asya30-8kw-30000btu-high-wall-split-inverter-air-conditioning-system-.html.

Alonso, J. F. S., F. J. R. Martínez, et al. (1998), *Simulation model of an indirect evaporative cooler*, Energy and Buildings, vol. 29, pp. 23-27.

Anderson, W. M. (1986). *Three-stage evaporative air conditioning versus conventional mechanical refrigeration*, ASHRAE Transactions, vol. 92, pp. 358-370.

ARI (2003), ARI Standard 210/240, *Standard for unitary air-conditioning and air-source heat pump equipment*, Air-conditioning and Refrigeration Institute, VA 22203.

ASHRAE (1996), *Ashrae handbook heating, ventilating, and air-conditioning systems and equipment: inch-pound edition*, American Society of Heating, Refrigerating and Air-Conditioning Engineers.

ASHRAE (2000), ANSI/ASHRAE Standard 143-2000, *Method of test for rating indirect evaporative coolers*, American Society of Heating, Refrigerating and Air-Conditioning Engineers, Inc. GA 30329.

Beijing Fenglong Agriculture Technology Co., L. (2006). *Evaporative Cooling Pad*, from

http://beijing-fenglong-agriculture-technology.tradenote.net/product/536186-Evaporative-Cooling-Pad.html.

Brooks, B. R. and D. L. Field (2003), *Indirect evaporative cooling apparatus*, U. S. Patent. U.S. US6523604B1: 12.

California Energy Commission (2008), *Division 2: State energy resources conservation and development commission*, California code of regulations Title 20 Public utilities and energy, California.

Çengel, Y. A. and M. A. Boles (2007), *Thermodynamics: an engineering approach*, New York, McGraw-Hill Higher Education.

Chen, P. and X. Yue (1999), *Handbook of air condtioning and refrigeration*, Shanghai, TongJi University Press (in Chinese).

CIBSE (2001), *CIBSE Guide A: Environmental design*, London, Chartered Institution of Building Services Engineers.

Coleman, H. W. and W. G. Steele (1989), *Experimentation and uncertainty analysis for engineers*, New York, John Wiley & Sons.

Coolerado (2006), *Coolerado HMX (Heat and Mass Exchanger) brochure*, C. Corporation. Arvada, Colorado, USA.

Delfani, S., J. Esmaeelian, et al. (2010), *Energy saving potential of an indirect evaporative cooler as a pre-cooling unit for mechanical cooling systems in Iran*, Energy and Buildings, vol. 42, pp. 2169-2176.

Elberling, L. (2006), *Laboratory evaluation of the Coolerado cooler-indirect evaporative cooling unit*, Pacific Gas and Electric Company.

Erens, P. J. and A. A. Dreyer (1993), *Modelling of indirect evaporative air coolers*, International Journal of Heat and Mass Transfer, vol. 36, pp. 17-26.

EnergyPlus (2010), *EnergyPlus Energy Simulation Software*: *Weather Data*, from http://apps1.eere.energy.gov/buildings/energyplus/cfm/weather_data.cfm.

Florides, G. A., S. A. Kalogirou, et al. (2000), *Energy consumption analysis of a typical house in Cyprus*, 10th Mediterranean Electrotechnical Conference, Melecon. vol. 3, pp. 1165-1168.

Gillan, L. E., V. Maisotsenko, et al. (2010), *Fabrication materials and techniques for plate heat and mass exchangers for indirect evaporative coolers*, U. S. P. A. Publication. Unit States, Idalex Technologies, Inc.

Guerra, Z. (1994), *Evaporative air conditioner for automotive application*, Massachusetts Institute of Technology.

Guo, X. C. and T. S. Zhao (1998), *A parametric study of an indirect evaporative air cooler*, International Communications in Heat and Mass Transfer, vol. 25, pp. 217-226.

Halasz, B. (1998), *A general mathematical model of evaporative cooling devices*, Revue Générale de Thermique, vol. 37, pp. 245-255.

Heidarinejad, G., M. Bozorgmehr, et al. (2009), *Experimental investigation of two-stage indirect/direct evaporative cooling system in various climatic conditions*, Building and Environment, vol. 44, pp. 2073-2079.

Hettiarachchi, H. D. M., M. Golubovic, et al. (2007), *The effect of longitudinal heat conduction in cross flow indirect evaporative air coolers*, Applied Thermal Engineering. vol. 27, pp. 1841-1848.

Higgins, C. and H. Reichmuth (2007), *Desert CoolAire™ package unit technical assessment: Field performance of a prototype hybrid indirect evaporative air-conditioner*, New Buildings Institute.

Idalex Technologies, I. (2003), *The Maisotsenko cycle – conceptual*: *A technical concept view of the Maisotsenko cycle*, from

http://www.idalex.com/technology/how_it_works_-_engineering_perspective.htm.

Incropera P. F., D.P. DeWitt, et al. (2007), *Fundamentals of heat and mass transfer*,6th edition, New York: John Wiley & Sons.

IP, K. and D. G (2002), *A/C Energy Efficiency in UK Office Environments*, International Conference on Electricity Efficiency in Commercial Buildings (IEECB), Nice, France.

ISAW (2005), *Natural Air Conditioner (Heat and Mass Exchanger) Catalogues*, ISAW Corporation Ltd., Hangzhou, China.

Jaber, S. and S. Ajib (2011), Evaporative cooling as an efficient system in Mediterranean region, Applied Thermal Engineering, vol. 31, pp. 2590-2596.

Jiang, Y. (2008), *Chinese building energy consumption situation and energy efficiency strategy*, New Architecture (in Chinese).

Jiang, Y. and X. Xie (2010), Theoretical and testing performance of an innovative indirect evaporative chiller, Solar Energy, vol. 84, pp. 2041-2055.

Klein, S. A. (2010). Engineering Equation Solver (EES).

Kozuba, E. and S. Slayzak (2009), *Coolerado 5 Ton RTU performance: western cooling challenge results, Technical report NREL/TP-550-46524*, National Renewable Energy Laboratory.

Kulkarni, R. K. and S. P. S. Rajput (2011), *Performance evaluation of two stage indirect/direct evaporative cooler with alternative shapes and cooling media in direct stage*, International Journal of Applied Engineering Research, vol. 1, pp.800-812.

Lilly, P. and P. Misemer (1996), *Evaporative cooling: An assessment of california market potential and estimated impacts of key deployment barriers*, Renewable Energy, vol. 8, pp. 165-168.

Lu, Y. (2008), *Practical heating HVAC design manual second edition*, China Building Industry Press (In Chinese).

Maclainecross, I. L. and P. J. Banks (1981), *A general-theory of wet surface heat-exchangers and its application to regenerative evaporative cooling*, Journal of Heat Transfer-Transactions of the Asme. vol. 103, pp. 579-585.

Maheshwari, G. P., F. Al-Ragom, et al. (2001). *Energy-saving potential of an indirect evaporative cooler*, Applied Energy, vol. 69, pp. 69-76.

Maisotsenko, V., L. E. Gillan, et al. (2004), *Method and apparatus for dew point evaporative product cooling*. U. S. Patent. United States, Idalex Technologies, Inc., 6776001.

Maisotsenko, V. and I. Reyzin (2005), *The Maisotsenko cycle for electronics cooling*, Proceedings of the ASME/Pacific Rim Technical Conference and Exhibition on Integration and Packaging of MEMS, NEMS, and Electronic Systems: Advances in Electronic Packaging, San Francisco, CA, U.S., pp. 415–424.

Mihalakakou, M., K. Santamouris, et al. (2007), *Estimating the ecological footprint of the heat island effect over Athens, Greece*, Climatic Change, vol. 80, pp. 265-276.

Munters (2011), CELdek, from http://www.munters.us/en/us/Products--Services/HumiCool-Division/HVAC/Evaporative-Cooling-Pads/?Product=4C2CD751-F93C-4F84-9546-80C2DC97F973.

Navon, R. and H. Arkin (1993), *Economic comparison of an air conditioner and a desert cooler for residences in arid areas*, Construction Management and Economics, vol. 11, pp. 62-70

Navon, R. and H. Arkin (1994), *Feasibility of direct-indirect evaporative cooling for residences, based on studies with a desert cooler,* Building and Environment, vol. 29, pp. 393-399.

Olesen, B. W. (2002), *Control of slab heating and cooling systems studied by dynamic computer simulations*, AICARR conference, Milan.

Palmer, J. D. (2002), *Evaporative cooling design guidelines manual-for new mexico schools and commercial buildings*, New Mexico, Energy Conservation and Management Division.

Pérez-Lombard, L., J. Ortiz, et al. (2008), *A review on buildings energy consumption information*, Energy and Buildings, vol. 40, pp. 394-398.

Pescod, D. (1979), *A heat exchanger for energy saving in an air conditioning plant*, ASHRAE Trans., vol. 85, pp. 238-251.

Petroleum, B. (2009), *BP statistical review of world energy June 2009*, London, UK.

Qiu, G. (2007), *A novel evaporative/desiccant cooling system*, PhD thesis, The University of Nottingham.

Ren, C. and H. Yang (2006), *An analytical model for the heat and mass transfer processes in indirect evaporative cooling with parallel /counter flow configurations*, International Journal of Heat and Mass Transfer, vol. 49, pp. 617-627.

Riangvilaikul, B. and S. Kumar (2010), *An experimental study of a novel dew point evaporative cooling system*, Energy and Buildings, vol. 42, pp. 637-644.

Ruegg, T. R. and H. E. Marshall (1990), Building Economics: Theory and practice. 1st edition, New York: Van Nostrand Reinhold.

Silva, M. M. d. (2005), *Solar air conditioning potential for offices in Lisbon*. Master dissertation, University of Strathclyde.

Source, E. (2009), *HVAC: Evaporative Cooling*, from http://www.esource.com/BEA/hosted/Xcel/PA_42.html.

Steeman, M., A. Janssens, et al. (2009), *Performance evaluation of indirect evaporative cooling using whole-building hygrothermal simulations*, Applied Thermal Engineering, vol. 29, pp. 2870-2875.

Stoitchkov, N. J. and G. I. Dimitrov (1998), *Effectiveness of crossflow plate heat exchanger for indirect evaporative cooling: Efficacité des échangeurs thermiques à plaques, à courants croises pour refroidissement indirect évaporatif*, International Journal of Refrigeration, vol. 21, pp. 463-471.

Tulsidasani, T. R., R. L. Sawhney, et al. (1997), *Recent research on an indirect evaproative cooler (IEC) part 1: optimization of the COP*, Int.J.Energy Res., vol. 21, pp. 1099–1108.

Tulsidasani, T. R., R. L. Sawhney, et al. (1997), *Recent research on an indirect evaporative cooler (IEC) part 2: thermal performance of a non-conditioned building coupled with an IEC*, Int.J.Energy Res., vol. 21, pp. 1203-1214.

UK Power (2011), *Electricity Running Costs Calculator*, from http://www.ukpower.co.uk/tools/running_costs_electricity/.

Velasco Gómez, E., F. J. Rey Martínez, et al. (2005), *Description and experimental results of a semi-indirect ceramic evaporative cooler*, International Journal of Refrigeration, vol. 28, pp. 654-662.

Wang, Y., X. Huang, et al. (2005), *Theoretical and experimental study of absorbing water materials wrapped on ellipse tube type indirect evaporative cooler*, Fluid Machinery, vol. 33, pp. 46-49 (in Chinese).

Watt, J. R. (1988), *Power cost comparison: evaporative vs refrigerative cooling, in energy-saving heating and cooling systems*, ASHRAE Annual Meeting, Ottawa, Ontario, pp. 41-47.

White, F. M. (1979), *Fluid mechanics*, New York ; London (etc.): McGraw-Hill.

Wuebbles, D. J. (1994), *The role of refrigerants in climate change*, International Journal of Refrigeration, vol. 17, pp. 7-17.

Xia, A. (2010), *Marketing review: 2010 air conditioning market characteristics*, from http://www.marketingreview.biz/marketing/2010-air-conditioning-market-characteristics/.

Zhan, C., X. Zhao, et al. (2011), *Numerical study of a M-cycle cross-flow heat exchanger for indirect evaporative cooling*, Building and Environment, vol. 46, pp. 657-668.

Zhao, X., Li, J.M., Riffat, S.B. (2008), *Numerical study of a novel counter-flow heat and mass exchanger for dew point evaporative cooling*, Applied Thermal Engineering, vol. 28, pp. 1942-1951.

Zhao, X., S. Liu, et al. (2008), *Comparative study of heat and mass exchanging materials for indirect evaporative cooling systems*, Building and Environment, vol. 43, pp. 1902-1911.